LC GC north america
solutions for separation scientists
Volume 37 Number 7 July 2019
www.chromatographyonline.com

A Revolutionary Technology for Macromolecular Characterization

A New Paradigm in Light Scattering Technology

LENS 3™
Multi-Angle Laser Light Scattering

- **Direct Molecular Weight by Low Angle**
- **R_g Below 10 nm for the First Time**
- **HPLC/UHPLC Compatibility**
- **Powerful and Intuitive Software**

LenS3 in UHPLC Mode: Herceptin® Biosimilar (150 KDa)

TSKgel UP-SW3000, 2 µm, 4.6 mm ID x 30 cm

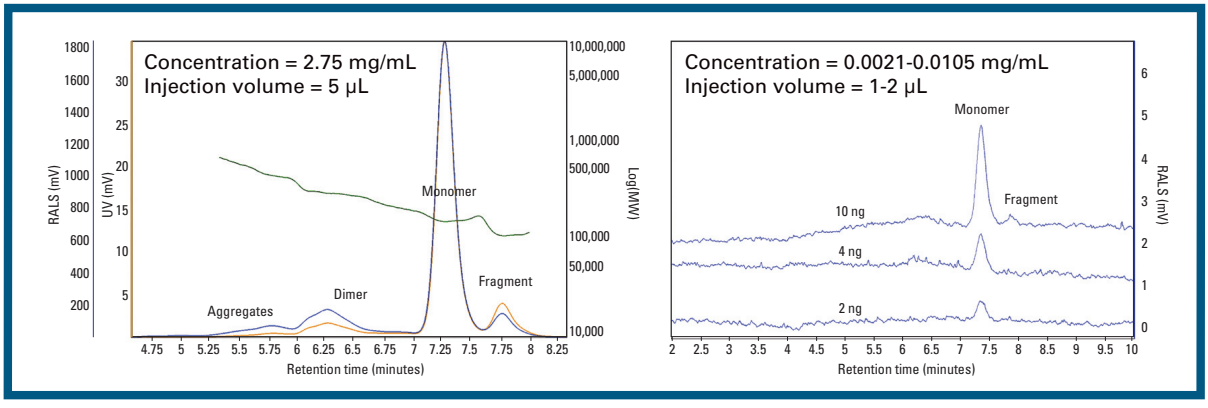

mAb monomer, fragment, oligomers and aggregate detection with sensitivity down to only 2 ng!

TOSOH BIOSCIENCE
www.tosohbioscience.com

TOSOH

See Your Molecule in a Whole New Light

A Winning Combination for Your Polymer Analysis

LenS™ 3 Multi-Angle Laser Light Scattering + EcoSEC® Elite HLC-8420GPC

Delivering greater stability and reproducibility than ever before. Supported by team of GPC experts.

Driven by SECview Software

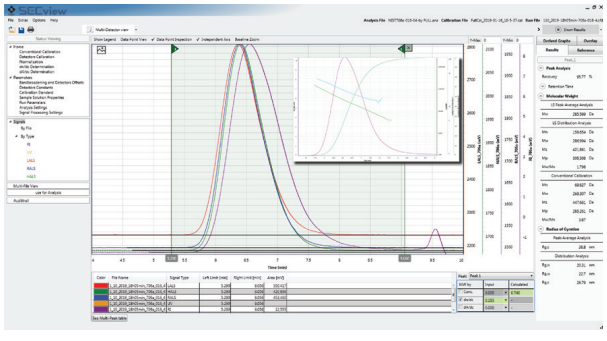

SECview™ Advanced Multi-Detector SEC Software

Actualization, *not* Extrapolation of Your Data

For more information visit tosohbioscience.com

TOSOH BIOSCIENCE
www.tosohbioscience.com

TOSOH

LC GC
north america
solutions for separation scientists
Volume 37 Number 7 July 2019
www.chromatographyonline.com

Temperature-Programmed GC: Why Are Those Peaks All So Sharp?

ENVIRONMENTAL METHOD DEVELOPMENT: KEY CHALLENGES

How Buffer Preparation Affects LC Retention Repeatability

Supelco® titration products.

Exquisite accuracy. Every time.

Maintaining your high standards requires analytical products you can rely on, along with the right documentation and expertise.

That's why our titration reagents, solvents, reference materials and indicators are exquisitely crafted to ensure you reliably achieve your analytical goals and comply with guidelines and regulations. So for flawless performance, time after time, choose Supelco® titration products.

For more information, please visit:
SigmaAldrich.com/SuccessReplicated

The Life Science Business of Merck KGaA, Darmstadt, Germany operates as MilliporeSigma in the US and Canada.

Supelco®
Analytical Products

HPLC Polymers 101

The power of polymeric columns

Polymer HPLC columns have a lot of benefits. They don't require any functionalization for reversed-phase separations, and rigid polymeric supports intrinsically resist chemical and pH degradation, a fundamental problem with silica columns. Plus, polymer's inertness to most chemical environments makes it a robust and economical solution.

Hamilton offers a line of pH stable polymer HPLC columns for reversed phase, anion exchange, cation exchange, and ion exclusion separations perfect for pharmaceuticals, small molecules, proteins, peptides, DNA, organic, and inorganic ions, and more.

Advantages of polymer over silica

- ✓ pH range of 1 – 13
- ✓ Widest chemical compatibility
- ✓ Temperatures higher than 60 °C
- ✓ Maximum sample recovery
- ✓ Longest average life span

To learn more about how polymer columns can perform for you, visit
www.hamiltoncompany.com/polymers-101
or call toll free **1-888-525-2123**

HAMILTON®

LC GC
north america

MANUSCRIPTS: For manuscript preparation guidelines, see chromatographyonline.com/lcgc-author-guidelines, or call The Editor, (732) 596-0276. *LCGC* welcomes unsolicited articles, manuscripts, photographs, illustrations, and other materials but cannot be held responsible for their safekeeping or return. Every precaution is taken to ensure accuracy, but *LCGC* cannot accept responsibility for the accuracy of information supplied herein or for any opinion expressed.

SUBSCRIPTIONS: For subscription and circulation information: *LCGC*, P.O. Box 6168, Duluth, MN 55806-6168, or call (888) 527-7008 (7:00 a.m.–6:00 p.m. central time). International customers should call +1-218-740-6477. Delivery of *LCGC* outside the United States is 14 days after printing. For single and back issues, call (800) 598-6008 or (218) 740-6480. (*LCGC Europe* and *LCGC Asia Pacific* are available free of charge to users and specifiers of chromatographic equipment in Western Europe and Asia and Australia, respectively.)

CHANGE OF ADDRESS: Send change of address to *LCGC*, P.O. Box 6168, Duluth, MN 55806-6168; alternately, send change via e-mail to fulfill@hcl.com or go to the following URLs:
• Print: http://ubmsubs.ubm.com/?pubid=LCGC
• Digital: http://ubmsubs.ubm.com/?pubid=LCGC&V=DIGI
Allow four to six weeks for change. PUBLICATIONS MAIL AGREEMENT No. 40612608. Return all undeliverable Canadian addresses to: IMEX Global Solutions, P.O. Box 25542, London, ON, N6C 6B2, CANADA. Canadian GST number: R-124213133RT001.

C.A.S.T. DATA AND LIST INFORMATION: Contact Melissa Stillwell, tel. (218) 740-6831, e-mail MStillwell@mmhgroup.com.
REPRINTS: Reprints of all articles in this issue and past issues of this publication are available (500 minimum). Licensing and Reuse of Content: Contact our official partner, Wright's Media, about available usages, license fees, and award seal artwork at Advanstar@wrightsmedia.com for more information. Please note that Wright's Media is the only authorized company that we've partnered with for MultiMedia Healthcare materials.
INTERNATIONAL LICENSING: Contact Jillyn Frommer, tel. (732) 346-3007, fax 732-647-1104, or e-mail JFrommer@mmhgroup.com.

Alliance for Audited Media

50% Recycled Paper 10-20% Post Consumer Waste

485F US Highway One South, Suite 210
Iselin, NJ 08830
(732) 596-0276 • Fax: (732) 647-1235

Decade Elite

Electrochemical detector for any (U)HPLC system with the software of your choice

DataApex Clarity™

CHROMELEON 7.2

Agilent OpenLAB CDS

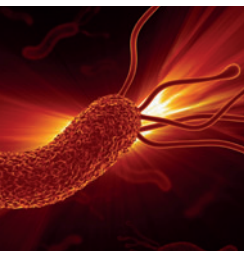

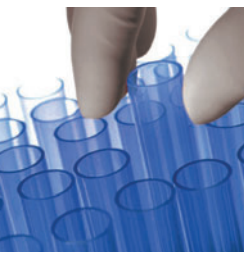

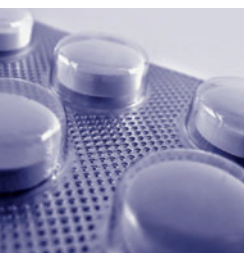

www.AntecScientific.com

CONTENTS

LC GC north america

COVER DESIGN BY
DAN WARD

Cover image courtesy of Konstiantyn/stock.adobe.com

DEPARTMENTS

LCGC North America (ISSN 1527-5949 print) (ISSN 1939-1889 digital) is published monthly by MultiMedia Healthcare LLC, 325 West First Street STE 300 Duluth, MN 55802, and is distributed free of charge to users and specifiers of chromatographic equipment in the United States and Canada. Single copies (prepaid only, including postage and handling): $15.50 in the United States, $17.50 in all other countries; back issues: $23 in the United States, $27 in all other countries. LCGC is available on a paid subscription basis to nonqualified readers in the United States and its possessions at the rate of: 1 year (13 issues), $74.95; 2 years (26 issues), $134.50; in Canada and Mexico: 1 year (13 issues), $95; 2 years (26 issues), $150; in all other countries: 1 year (13 issues), $140; 2 years (26 issues), $250. Periodicals postage paid at Duluth, MN 55806 and at additional mailing offices. POSTMASTER: Please send address changes to LCGC, P.O. Box 6168, Duluth, MN 55806-6168. PUBLICATIONS MAIL AGREEMENT NO. 40612608, Return Undeliverable Canadian Addresses to: IMEX Global Solutions, P. O. Box 25542, London, ON N6C 6B2, CANADA Canadian GST number: R-124213133RT001. Printed in the USA.

Optimize your UHPLC instrumentation

Cheminert UHPLC injectors, switching valves, and selectors make it easy. Internal volume is minimized and dead volume is virtually eliminated. A proprietary rotor material and stator coating on some models achieve pressures to 20,000 psi, suitable for the most demanding analytical techniques. All models are compatible with any VICI actuation option.

- For high speed, high throughput, micro or nano flow UHPLC
- Pressures available in 10k, 15k, and 20k psi
- Bore sizes from 100-250 µm
- Fitting sizes available in 360 µm to 1/16"
- Zero dead volume

VICI

www.vici.com

For more information: tech@vici.com

Editorial Advisory Board


MilliporeSigma
Unleash the impossible
Whatever projects you're working on, from a simple test to life-sustaining medical breakthroughs, you can count on the unparalleled Sigma-Aldrich® portfolio along the way. With proven, reliable, cutting-edge lab and production materials, we are always expanding and perfecting our global portfolio. So we'll be with you from day one to the day your impossible dream suddenly doesn't seem so impossible.
To find out more, visit:
SigmaAldrich.com/UnleashTheImpossible
122
MilliporeSigma, the vibrant M and Sigma-Aldrich are trademarks of Merck KGaA, Darmstadt, Germany or its affiliates. All other trademarks are the property of their respective owners. Detailed information on trademarks is available via publicly accessible resources.
© 2019 Merck KGaA, Darmstadt, Germany and/or its affiliates. All Rights Reserved.
The Life Science Business of Merck KGaA, Darmstadt, Germany operates as MilliporeSigma in the US and Canada.
Sigma-Aldrich®
Lab & Production Materials

PEAKS of Interest

John B. Fenn Award Presented to John R. Yates III at ASMS Conference

John R. Yates III, a professor in the Department of Molecular Medicine at The Scripps Research Institute (La Jolla, California), received the John B. Fenn Award for a Distinguished Contribution in Mass Spectrometry at the American Society for Mass Spectrometry (ASMS) conference on June 3, in Atlanta, Georgia. The award recognizes Yates for his development of automated, large-scale interpretation of peptide tandem mass spectral data. His SEQUEST algorithm laid a critical foundation for the field of proteomics and has enhanced the accuracy and effectiveness of mass spectrometry for understanding important biological and clinical questions.

Subsequent software developments that have followed from Yates's work have continued to facilitate molecular and cellular biology research, in areas such as peptide and protein quantitation, identification of posttranslational modifications, and the use of DNA sequences to enable proteogenomic methods. Yates also enabled large-scale studies to identify the components of protein complexes in single-celled organisms and mammalian cells.

This award honors the memory of John B. Fenn, who shared the 2002 Nobel Prize for the development of electrospray ionization. Fenn joined ASMS in 1986 and remained an active member until his passing in 2010. The award is conferred at the ASMS Annual Conference with the presentation of a $10,000 cash award, a recognition plaque, and the award lecture.

ASMS Research Awards Recognize Young Academics

The winners of the 2019 Research awards from ASMS are James F. Davies of the University of California, Riverside; Nicolas L. Young of Baylor College of Medicine (Houston, Texas); and Eleanor Browne, of the University of Colorado, Boulder. The awards were presented on June 4, in Atlanta, Georgia.

The awards promote the research of academic scientists within the first four years of joining the tenure track or research faculty of a North American university at the time the award is conferred. These awards, in the amount of $35,000 for each winner, are fully supported by Bruker, Thermo Fisher Scientific, and Waters Corporation.

Callie Cole of Fort Lewis College (Durango, Colorado) is the winner of the 2019 Primarily Undergraduate Institution Research Award, presented on June 4. The $20,000 award, sponsored by Agilent, promotes academic research in mass spectrometry by faculty members and their students at primarily undergraduate institutions. It is given to the recipient's institution on behalf of the recipient's research. ■

CHROMATOGRAPHY MARKET PROFILE

LC and LC–MS in Food and Beverage Laboratories

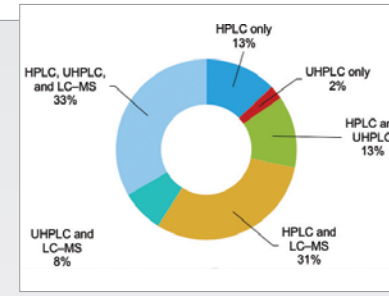

Chromatography installations for food and beverage laboratories in China

Rising consumer awareness for foodborne illness, food allergies, and food adulteration has led to increased scrutiny of the global food supply chain. Beyond food safety and microbial testing, regulators are actively defining acceptable levels of chemical additives, residues, and contaminants in food products, leading to increased testing and the demand for liquid chromatography and mass spectrometry instruments.

While gas chromatography–mass spectrometry (GC–MS) remains the workhorse for routine food testing applications, high performance liquid chromatography (HPLC) methods have become increasingly popular and are typically preferred for thermally labile, nonvolatile, and highly polar compounds. Applications for HPLC include the analysis of preservatives, lipids and oils, vitamins, fatty acids, carbohydrates, and peptides.

Most food and beverage laboratories use HPLC, but as in most other industrial segments, laboratories have been adopting UHPLC methods and replacing their HPLC instruments with UHPLC systems. And, with increased regulations, the use of mass spectrometry has become more prevalent, particularly for residue analysis, authenticity, and food safety. In fact, in a recent survey of Chinese testing laboratories, approximately three-quarters of food and beverage laboratories were using LC–MS technologies. Moreover, the use of UHPLC instruments was found in over half of the laboratories surveyed.

In China, the market for LC and LC–MS systems in the food and beverage market was estimated at about $125 million in 2017. The Chinese market for LC–MS instruments is expected to be robust, increasing by double digits for the next five years, fueled by solid growth for high-end mass spectrometers, including tandem MS instruments. Although indigenous HPLC suppliers are making modest inroads into the testing market, Waters and Shimadzu are the leading LC instrument vendors in China. Agilent and Thermo Fisher are also key manufacturers in this market segment.

Market size and growth estimates were adopted from *TDA's Industry Data*, a database of technology market profiles and benchmarks covering laboratory and process analytical instrumentation that are updated quarterly. This market profile also includes data from the *2019 Instrument Industry Outlook* report from independent market research firm Top-Down Analytics (TDA). For more information, contact Glenn Cudiamat, general manager, at (310) 871-3768 or glenn.cudiamat@tdaresearch.com. Glenn is a market research expert who has been covering the analytical instrumentation industry for more than two decades.

THEIRS COMES WITH A MANUAL.
OURS, A TEAM.

ION CHROMATOGRAPHY BY

Metrohm

Get the support your lab deserves.
Learn more at LeaveTheFamiliar.com

COLUMN WATCH

Hybrid Particle Columns: The First Twenty Years

June 2019 marked the twentieth anniversary of the introduction of the first high performance liquid chromatography (HPLC) columns containing hybrid organic–inorganic particles. In this article, we review the chemistry and key attributes of hybrid particle columns, and show examples demonstrating how these columns have been used for separations of a variety of analytes.

Thomas H. Walter

Since their introduction twenty years ago, hybrid particle columns have become widely used in an ever-expanding range of applications. By combining the desirable features of organic and inorganic materials, hybrid particles offer benefits over both silica and organic polymer stationary phases. Compared to silica, hybrid particles exhibit improved stability to basic mobile phases and reduced silanol acidity. Compared to organic polymers, hybrid particles offer higher column efficiencies and improved mechanical strength. In this article, we examine the history and evolution of hybrid particle columns, highlighting examples of separations enabled by hybrid particle technology for analytes ranging from small molecules to biopolymers.

Hybrid Particles

Hybrid organic–inorganic materials contain both organic (organosiloxane) and inorganic (silica) components. Although extensively studied by the materials science community (1), there were few reports of the use of hybrid particles in HPLC prior to 1999 (2). One notable early publication by Unger, Becker, and Roumeliotis demonstrated that organic functional groups such as benzyl and 1,2-diol-3-propoxypropyl could be incorporated into both the internal and surface structure of chromatographic particles by co-hydrolysis and co-condensation of an organotriethoxysilane and tetraethoxysilane (TEOS) (3). In a modification of this approach, a team at Waters synthesized particles from TEOS and methyltriethoxysilane (Figure 1), then derivatized these particles with silanes to yield C_{18}-bonded hybrid particles (4). These particles showed significantly improved stability to alkaline mobile phases versus similarly bonded silica particles. A family of HPLC columns based on these hybrid particles was introduced in June 1999.

Chromatographic Performance of Methyl Hybrid Columns

Compared to silica-based columns, the main distinguishing feature of methyl hybrid columns is improved resistance to alkaline mobile phases. Typical C_{18}-silica columns are only recommended for use up to pH 8, due to the onset of particle dissolution and bonded phase hydrolysis in higher pH mobile phases, leading to losses of efficiency and retention (5). The presence of methyl groups throughout the hybrid particle slows the rate of hydrolysis compared to similarly bonded C_{18}-silica particles, resulting in longer column lifetimes when using alkaline mobile phases (6–8). A trifunctional C_{18} bonded phase based on these methyl hybrid particles was also shown to be stable to strongly acidic mobile phases, where bonded phase hydrolysis can result in a loss of retention (6,8). Indeed, the unbonded methyl hybrid particles are remarkably stable to acidic solutions, with no loss of carbon found after exposure to 1 M HCl at 100 °C for 16 h (6).

Another benefit demonstrated for methyl hybrid columns is improved peak shape for basic analytes, particularly when using neutral pH mobile phases (6,7). Peak tailing for bases at neutral pH is primarily caused by the ion-exchange interaction of protonated bases with ionized silanol groups. Methyl hybrid stationary phases exhibit greatly reduced silanol acidity, as measured by the retention of lithium ion (Li^+) with a 60:40 methanol–water mobile phase buffered to different pH values (9). A similar conclusion was reached based on studies of the retention of the quaternary ammonium ion bretylium (10). The lower silanol acidity of methyl hybrid columns results in symmetric peaks for basic analytes over a wide range of mobile phase pH values (7).

One key benefit of using a column that has an extended upper pH limit is that it can be used to investigate the

Imtakt USA

LC-MS: Amino acids in human serum (SSA)

血清中遊離アミノ酸のLC–MS分析（スルホサリチル酸処理）

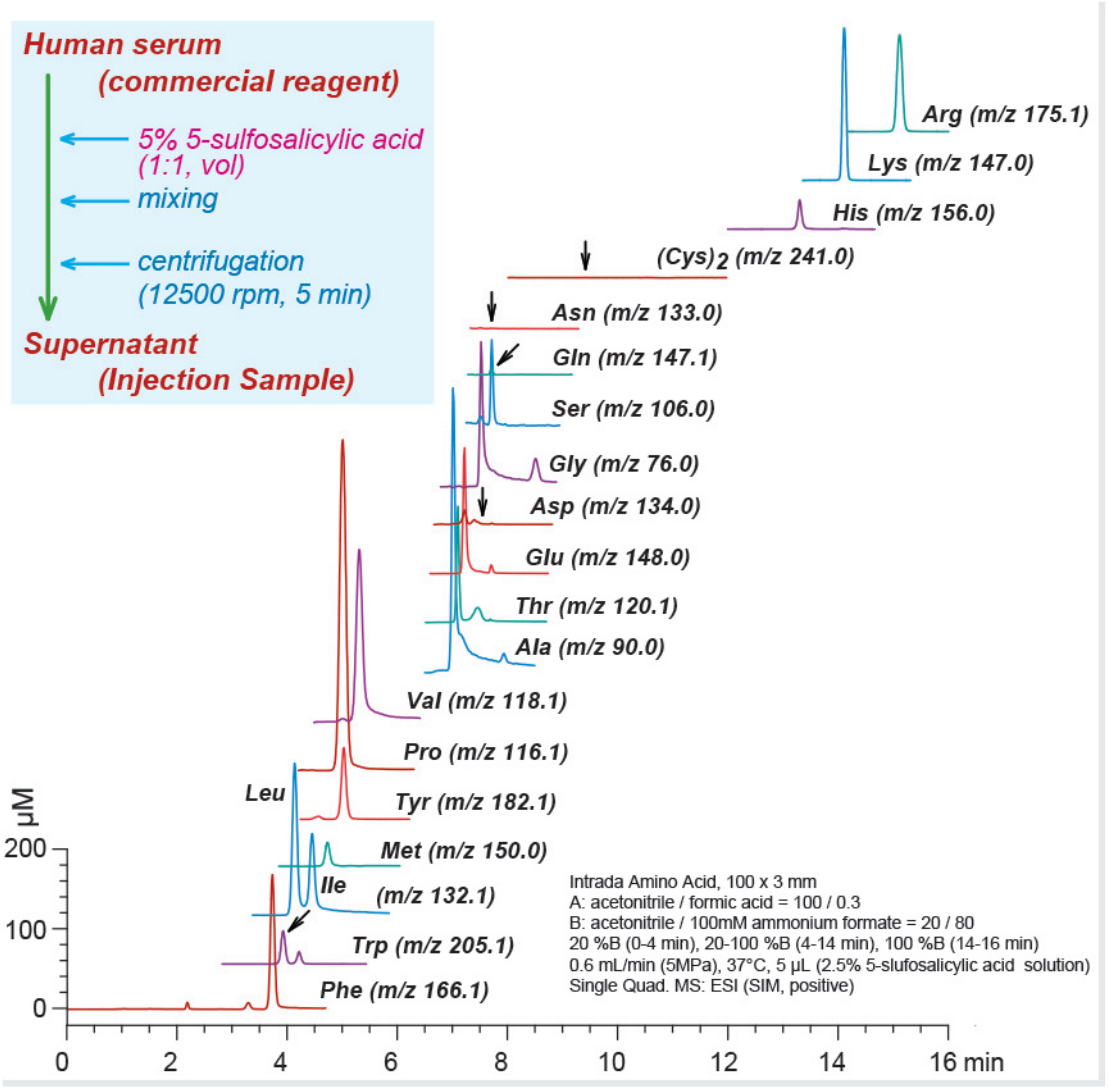

Here we show a simple sample preparation procedure and a non-derivatized LC-MS method for high throughput amino acid analysis. We have developed the world's first amino acid column designed to separate amino acids without any derivatization called ***Intrada Amino Acid***. This unique multi-mode column is designed with both normal phase and ion-exchange ligands developed specifically to retain and separate amino acids. In this example, we started with a human serum sample which was processed to remove the proteins from the sample with SSA. Once the proteins were removed, the sample was directly injected onto the ***Intrada Amino Acid*** column, without a dry-down or reconstitution steps. This is a turn-key solution for high throughput amino acid analysis of biological samples. To learn more please visit *www.imtaktusa.com.*

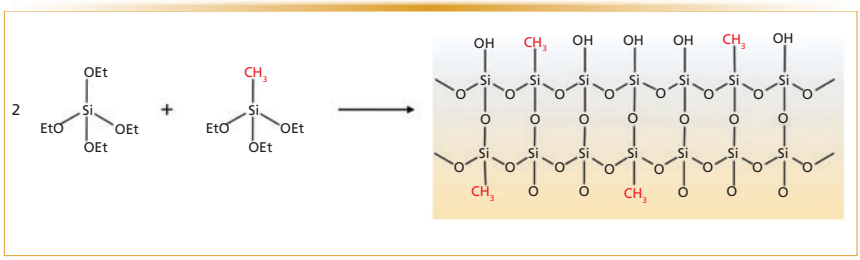

FIGURE 1: Synthesis of methyl hybrid particles from tetraethoxysilane and methyltriethoxysilane. In the schematic on the right, the top layer represents the surface, and the bottom layer represents the internal structure of the particle.

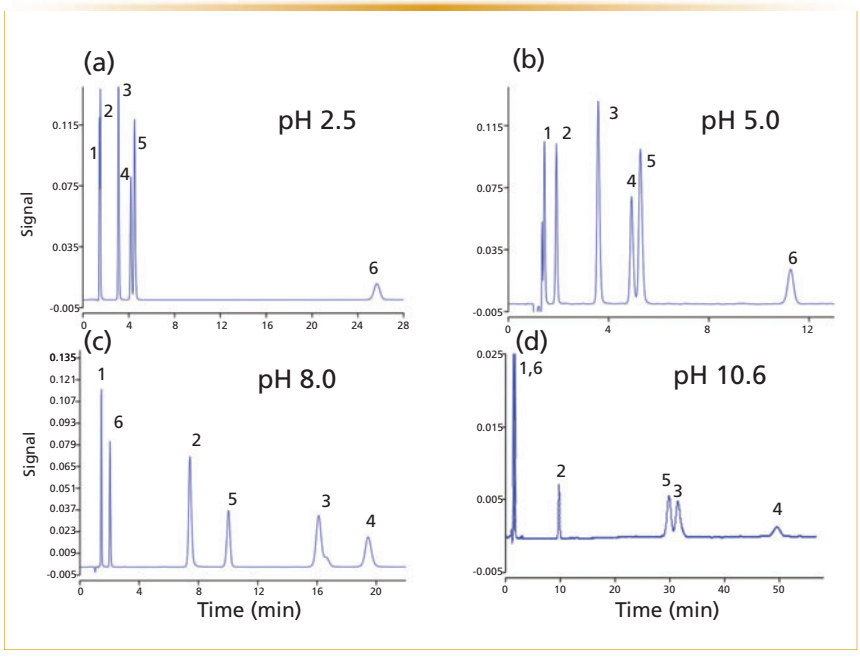

FIGURE 2: Chromatograms showing the isocratic separation of a mixture of acidic and basic analytes using an XTerra RP18 5-µm, 3.9 mm x 150 mm column and mobile phases containing 65:35 (*v/v*) 20 mM buffer–acetonitrile with four different pH values. The flow rate was 1.0 mL/min and ultraviolet (UV) detection was used at 210 nm for (a) pH 2.5, (b) pH 5.0, (c) pH 8.0, and at 230 nm for (d) pH 10.6. Peaks: 1 = acetaminophen, 2 = lidocaine, 3 = doxepin, 4 = imipramine, 5 = nortriptyline, 6 = ibuprofen.

optimum mobile phase pH for mixtures containing ionizable analytes with pK_a values greater than approximately 8 (7,8). Compared to other parameters that influence selectivity, such as the stationary phase chemistry and the organic component of the mobile phase, mobile phase pH has been shown to have a significantly greater impact for ionizable analytes (11). An example illustrating the effect of mobile phase pH on the separation of six ionizable analytes is shown in Figure 2 (7). Large changes in selectivity are observed as the pH is varied, with the retention of the basic analytes lidocaine (pK_a 7.7), doxepin (pK_a 9.0), imipramine (pK_a 9.4), and nortriptyline (pK_a 10.5) increasing as the pH is increased, converting them from their protonated to their neutral forms. In contrast, the retention of the acidic analyte ibuprofen (pK_a 4.4) decreases as the pH is increased, converting it from its neutral to its deprotonated form. Although acetaminophen is neutral from pH 2 to 8, the phenol group (pK_a 9.5) is ionized at pH 10.6, resulting in decreased retention. The best separation was achieved using a pH of 8. Investigating low and high pH mobile phases has been shown to be a valuable strategy for method development (12). A related idea involves two-dimensional HPLC separations using a pH 10 mobile phase with a C_{18}-methyl hybrid column for the first dimension and a pH 2.6 mobile phase with a C_{18}-silica column for the second dimension (13). Separations using a pH gradient from 10.5 to 3.0 have also been demonstrated using a C_{18}-methyl hybrid column for mixtures of ionizable analytes (14).

A second benefit afforded by using a column that is stable over a wide pH range is that the loading capacity of basic analytes with pK_a values greater than approximately 8 may be increased by using a mobile phase in which they are neutral, that is one with a pH higher than their pK_a values (15,16). Capacity increases of a factor of 20 or more were reported for several bases when changing the mobile phase aqueous buffer from pH 3.75 to pH 10.0 (15). At the lower pH, where the analytes are protonated, mutual ionic repulsion affects their adsorption on the stationary phase. The greater loading capacities for bases when using high-pH mobile phases is particularly beneficial for preparative applications.

When the methyl hybrid columns were introduced, the family included short columns packed with 2.5 µm particles for use in fast separations. The benefits of using small particles to achieve higher speed separations had been well established (17), and columns containing particles as small as 1.5 µm were available in 1995 (18). Limited by the roughly 6000 psi pressure ceiling of the HPLC systems available at that time, these small particles could only be used in short (≤50 mm) columns. Ultrafast separations (<1 min) were demonstrated using 2.1 mm x 20 mm columns packed with 2.5-µm C_{18}–methyl hybrid columns (19). Spurred by reports from Jim Jorgenson's group on the use of much longer capillary columns packed with 1.5-µm particles at ultrahigh pressures (20), studies were carried out to investigate the use of longer columns packed with 2.5-µm C_{18}–methyl hybrid particles on a prototype ultra-

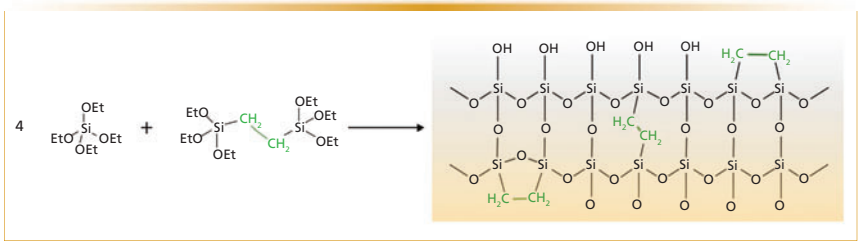

FIGURE 3: Synthesis of second-generation hybrid particles from tetraethoxysilane and 1,2-bis(triethoxysilyl)ethane. In the schematic on the right, the top layer represents the surface and the bottom layer the internal structure of the particle.

high-pressure liquid chromatography (UHPLC) system. Although these experiments demonstrated that 2.1 mm x 150 mm columns packed with methyl hybrid particles could produce the predicted high efficiencies, the columns were not mechanically stable enough to give acceptable lifetimes at the pressures generated when operating at or above the optimum flow rate (21). The methyl hybrid particles are not strong enough to tolerate the column packing pressures needed to obtain stable columns for use at pressures greater than 6000 psi.

Second-Generation Hybrid Particle Columns: Bridged-Ethylene Hybrid (BEH) Technology

The need for higher strength hybrid particles led to the development of a second-generation hybrid particle composition. Hybrid materials prepared using organic groups bridging two or more silicon atoms had been reported in 1995 (22). In contrast to the methylsiloxane groups in methyl hybrid particles, such bridging organic groups do not reduce the number of cross-link sites when co-condensed with TEOS to form particles. Hybrid particles containing bridged-ethylene groups (Figure 3) exhibit superior strength, as well as a significant increase in high-pH stability (23,24). When the first UHPLC system was introduced in 2004, with a pressure limit of 15,000 psi, the columns designed for it contained these second-generation hybrid particles in a 1.7-µm particle size (25). A family of columns containing 2.5-, 3.5- and 5-µm second-generation hybrid particles was introduced in 2005 (24).

These second-generation hybrid particle columns have been found to be useful in a wide range of applications, including separations of

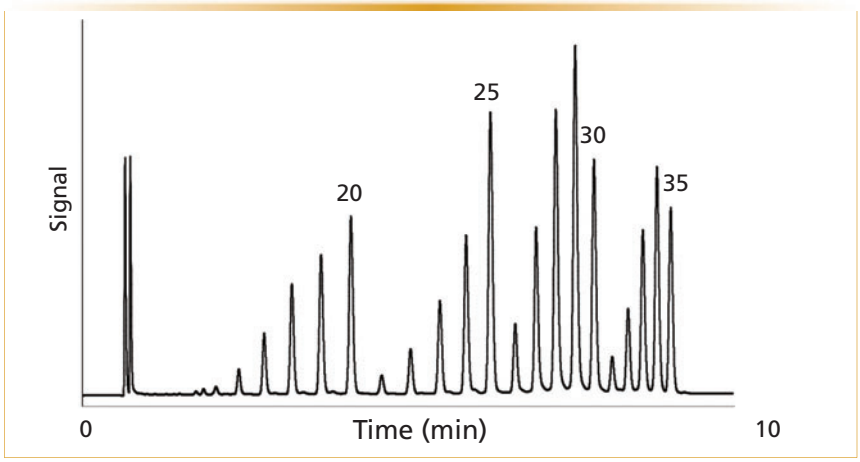

FIGURE 4: Chromatogram showing the gradient separation of a 15-to 35-mer oligothymidine ladder using an Acquity BEH C_{18} 1.7-µm, 2.1 mm x 50 mm column. Mobile phase A contained 15 mM triethylamine and 400 mM hexafluoroisopropanol in water and mobile phase B contained 50:50 mobile phase A:methanol. The gradient started at 19% methanol and the methanol concentration was increased linearly at 0.5%/min. The flow rate was 0.2 mL/min and the column temperature was 60 °C.

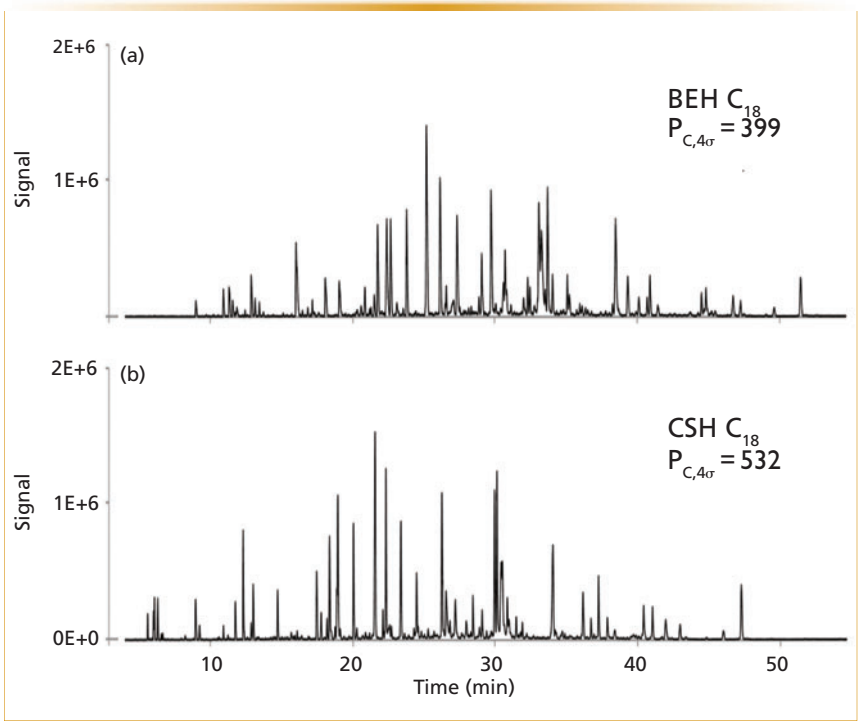

FIGURE 5: Total ion chromatograms showing gradient separations of a tryptic digest of enolase using (a) Acquity BEH C_{18} and (b) Acquity CSH C_{18} columns, both 1.7-µm, 2.1 mm x 150 mm. Mobile phase A contained 0.1% formic acid in water and mobile phase B was 0.1% formic acid in acetonitrile. The concentration of mobile phase B was increased linearly from 2 to 50% over 60 min. The flow rate was 0.3 mL/min and the column temperature was 40 °C. The 4-sigma peak capacities determined using twelve peptides spanning the separations are indicated.

both low and high molecular weight analytes (26). A Scopus search for articles containing the terms "BEH" or "XBridge" and "columns" found 2,142 documents as of June 10, 2019. One application that benefits from both the extended upper pH limit and the speed benefit of 1.7-µm second-generation hybrid particles is the reversed-phase separation of oligonucleotides. As shown in Figure 4, a 2.1 mm x 50 mm 1.7-µm second-generation hybrid C_{18} column provides baseline separation of a 15- to 35-mer oligodeoxythymidine ladder in less than 10 min (27). The aqueous mobile phase used for this ion-pairing reversed-phase separation contains triethylamine and has a pH of approximately 8. The column temperature used was 60 °C. The combination of the alkaline mobile phase and the elevated temperature results in short lifetimes for conventional C_{18}-silica columns. However, with the extended high-pH stability of the second-generation hybrid particles, good column lifetimes may be achieved under these conditions.

The extended high-pH stability of second-generation hybrid particles is also beneficial in hydrophilic interaction liquid chromatography (HILIC). An example of a high pH HILIC application is the separation of food sugars using second-generation hybrid amide columns. Although amino columns are commonly used for this separation, using an unbuffered acetonitrile–water mobile phase, the amino groups on the stationary phase may react with reducing sugars, leading to inaccurate peak areas (28). Poor retention time stability is also an issue with many amino columns. Lacking amino groups, amide stationary phase are non-reactive with reducing sugars. To produce single peaks for the reducing sugars, instead of resolving the anomers, a base such as triethylamine is added to the mobile phase and an elevated column temperature is used. Even under high temperature (90 °C) alkaline conditions (pH 10.3), a 1.7-µm second-generation hybrid amide column showed excellent retention stability over 2000 injections of samples prepared from food matrices (28).

A number of second-generation hybrid variants have been created to

address the needs of different applications. Wide pore (300-Å) versions were developed for reversed-phase separations of peptides and proteins (26,29) and HILIC separations of glycoproteins (30). Higher pore volume materials in a range of pore sizes were developed for use in size-exclusion chromatography (SEC) of proteins and synthetic polymers (31,32). In addition, specialized bonded phases on second-generation hybrid particles have been developed for use in supercritical fluid chromatography (SFC) (33).

Charged-Surface Hybrid (CSH) Technology Columns

A recent direction in hybrid particle columns involves introducing a low concentration of positively charged groups into the surface of second-generation hybrid particles (34). The benefits of this approach include modified selectivity for ionized analytes and improved loading capacity and peak shape for basic analytes when using acidic mobile phases containing low concentrations of ions (0.1% formic acid) (35). The improved peak shape of bases in 0.1% formic acid is important in LC–MS methods using electrospray ionization, where the use of this mobile phase modifier is preferred to maximize detection sensitivity. One important application benefitting from charge-modified hybrid columns is the separation of basic peptides, such as those produced by digesting proteins with trypsin or lys-C (36). Charge-modified hybrid C_{18} columns were found to give higher peak capacities for basic peptides compared to second-generation hybrid C_{18} columns, particularly when using relatively high mass loads and mobile phases containing 0.1% formic acid. This enables the use of a single high-resolution peptide mapping method with both ultraviolet (UV) and mass spectrometry (MS) detection. The separation of a tryptic digest of enolase using 2.1 mm x 150 mm 1.7-µm charge-modified hybrid C_{18} and 1.7-µm second-generation hybrid C_{18} columns with mobile phases containing 0.1% formic acid is shown in Figure 5 (37). The peptides were detected using a quadrupole time-of-flight (QTOF) mass spectrometer. The separation conditions were identical for the two columns. Twelve peptides spanning the separation were selected to calculate the peak capacity. The results show that the charge-modified hybrid C_{18} column produced a peak capacity that is 33% higher than that achieved using a second-generation hybrid C_{18} column.

The presence of the positively charged groups in charge-modified hybrid stationary phases enables them to retain polar anionic compounds that are poorly retained on conventional reversed-phase materials. For example, a charge-modified hybrid C_{18} column was found to provide improved retention and separation of glucosinolates extracted from *Arabidopsis thaliana* leaves (38). Glucosinolates are secondary metabolites that contain a sulfonated oxime group, along with a thioglucose moiety and a side chain derived from an amino acid. The mobile phase contained 0.05% formic acid, chosen to minimize ion suppression for this UHPLC–TOF-MS method. The method was used to identify and quantify 21 glucosinolates with a total run time of 11 min. As a second example, a charge-modified hybrid phenyl-hexyl column was shown to separate 10 citric acid cycle metabolites using 0.1% formic acid as the mobile phase additive (39). The analytes were detected using tandem mass spectrometry (MS/MS) in the negative ion mode. Excellent separations were achieved for the isobaric compounds citric acid and isocitric acid and for malic acid and fumaric acid. Separation of the latter pair is important because malic acid may undergo in-source fragmentation followed by decomposition in the collision cell to give the same MS/MS transition as fumaric acid.

Conclusions

The combination of improved high- pH stability, low silanol acidity, and high efficiency have made hybrid particle columns valuable tools for HPLC separations of a wide range of analytes. By expanding the accessible mobile phase pH range beyond that of silica-based columns, hybrid particle columns have allowed a wider range of mobile-phase conditions to be explored during method development. This

expansion has enabled a broader selectivity space to be accessed, particularly for mixtures containing ionizable analytes with pK_a values greater than approximately 8. It has also provided dramatically higher loading capacities for basic analytes. With the first UHPLC columns leveraging the mechanical strength of second-generation hybrid particles, hybrid particle columns became inextricably linked with UHPLC, fueling the rapid growth in applications for these columns. These applications include reversed-phase, HILIC, and size-exclusion separations. In the related area of SFC, hybrid particle columns have also proved to be valuable. With the availability of new selectivity options such as those in the charge-modified hybrid family, the range of applications for hybrid particle columns will continue to expand. As observed thirteen years ago, and still true today, "a vast number of organic–inorganic combinations remain unexplored at the molecular building block level. This fact hints (if not exclaims) that hybrid technology will continue to contribute to the advancement of the separation sciences" (2).

References

(1) R.M. Laine, C. Sanchez, C.J. Brinker and E. Giannelis, Organic/Inorganic Hybrid Materials, (Material Research Society, Symposium Proceedings Vol. 519, 1998).

(2) J.E. O'Gara and K.D. Wyndham, *J. Liq. Chromatogr. Relat. Tech.* **29**, 1025–1045 (2006).

(3) K.K. Unger, N. Becker, and P. Roumeliatis, *J. Chromatogr.* **125**, 115–127 (1976).

(4) U. S. patents 6,686,035; 7,223,473; 7,919,177 and 8,778,453.

(5) J.J. Kirkland, M.A. van Straten, and H.A. Claessens, *J. Chromatogr. A* **691**, 3–19 (1995).

(6) T.H. Walter, Waters White Paper 990858, (1999).

(7) Y.-F. Cheng, T.H. Walter, Z. Lu, P. Iraneta, B.A. Alden, C. Gendreau, U.D. Neue, J. M. Grassi, J.L. Carmody, J.E. O'Gara, and R.P. Fisk, *LCGC NA* **18**, 1162-1172 (2000).

(8) U.D. Neue, T.H. Walter, B.A. Alden, Z. Jiang, R.P. Fisk, J.T. Cook, K.H. Glose, J.L. Carmody, J.M. Grassi, Y.-F. Cheng, Z. Lu, and R.J. Crowley, *Amer. Labor.* **31** (22), 36–39 (1999).

(9) A. Mendez, E. Bosch, M. Roses, and U.D. Neue, *J. Chromatogr. A* **986**, 33–44 (2003).

(10) U.D. Neue, C.H. Phoebe, K. Tran, Y.-F. Cheng, and Z. Lu, *J. Chromatogr. A* 925, 49–67 (2001).

(11) U.D. Neue and A. Mendez, *J. Sep. Sci.* **30**, 949–963 (2007).

(12) U.D. Neue, E. . Grumbach, J.R. Mazzeo, K. Tran, and D.M. Wagrowski-Diehl, Handbook of Analytical Separations, Vol. 4 (Elsevier Science: Amsterdam, 2003), pp. 185–214.

(13) M. Gilar, P. Olivova, A.E. Daly, and J.C. Gebler, *J. Sep. Sci.* **28**, 1694–1703 (2005).

(14) R. Kaliszan, P. Wiczling, and M.J. Murkuszewski, *Anal. Chem.* **76**, 749–760 (2004).

(15) U.D. Neue, T.E. Wheat, J.R. Mazzeo, C.B. Mazza, J.Y. Cavanaugh, F. Xia, and D.M. Diehl, *J. Chromatogr. A* **1030**, 123–134 (2004).

(16) N.H. Davies, M.R. Euerby, and D.V. McCalley, *J. Chromatogr. A* **1119**, 11–19 (2006).

(17) J.H. Knox and M. Saleem, *J. Chromatogr. Sci.* **7**, 614–622 (1969).

(18) T. Issaeva, A. Kourganov, and K. Unger, *J. Chromatogr. A* **846**, 13–23 (1999).

(19) Y.-F. Cheng, Z. Lu, and U. Neue, *Rapid Commun. Mass Spectrom.* **15**, 141–151 (2001).

(20) J.E. McNair, K.C. Lewis, and J. W. Jorgenson, *Anal. Chem.* **69**, 983-989 (1997).

(21) E.S.P. Bouvier and B. Mathews, unpublished results.

(22) D.A. Loy and K.J. Shea, *Chem. Rev.* **95**, 1431–1442 (1995).

(23) K.D. Wyndham, J.E. O'Gara, T.H. Walter, K.H. Glose, N.L. Lawrence, B.A. Alden, G.S. Izzo, C.J. Hudalla, and P.C. Iraneta, *Anal. Chem.* **75**, 6781–6788 (2003).

(24) K.D. Wyndham, T.H. Walter, P.C. Iraneta, U.D. Neue, P.D. McDonald, D. Morrison, and M. Baynham, Waters White Paper 720001159EN (2005).

(25) J.R. Mazzeo, U.D. Neue, M. Kele, and R.S. Plumb, *Anal. Chem.* **77**, 460A–467A (2005).

(26) U.D. Neue, M. Kele, B. Bunner, A, Kromidas, T. Dourdeville, J.R. Mazzeo, E.S. Grumbach, S. Serpa, T.E. Wheat, P. Hong, and M. Gilar, *Adv. Chromatogr.* **48**, 99–143 (2009).

(27) M. Gilar and U.D. Neue, *J. Chromatogr. A* **1169**, 139–150 (2007).

(28) C. Hudalla, J. Cook, M. Dion, P. Iraneta, P. Smith, D. Walsh and K. Wyndham, Waters Poster PSTR10126471 (2009).

(29) A. Staub, D. Zurlino, S. Rudaz, J.-L. Veuthey, and D. Guillarme, *J. Chromatogr. A* **1218**, 8903-8914 (2011).

(30) A. Periat, S. Fekete, A. Cusumano, J.-L. Veuthey, A. Beck, M. Lauber, and D. Guillarme, *J. Chromatogr. A* **1448**, 81–92 (2016).

(31) M. Janco, J.N. Alexander IV, E.S.P. Bouvier, and D. Morrison, *J. Sep. Sci.* **36**, 2718-2727 (2013).

(32) E.S.P. Bouvier and S.M. Koza, *Trends Analyt. Chem.* **63**, 85–94 (2014).

(33) S. Khater, C. West, and E. Lesellier, *J. Chromatogr. A* **1319**, 148–159 (2013).

(34) P.C. Iraneta, K.D. Wyndham, D.R. McCabe, and T.H. Walter, Waters White Paper 720003929EN (2011).

(35) N. Lucie, V. Hana, and P. Solich, *Talanta* **93**, 99–105 (2012).

(36) M.A. Lauber, S.M. Koza, S.A. McCall, B.A. Alden, P.C. Iraneta, and K.J. Fountain, *Anal. Chem.* **85**, 6936–6944 (2013).

(37) M.A. Lauber, S.M. Koza, and K.J. Fountain, Waters Application Note 720004571EN (2013).

(38) G. Glauser, F. Schweizer, T.C.J. Turlings, and P. Reymond, *Phytochem. Anal.*, **23**, 520–528 (2012).

(39) K.M. Smith, R.S. Plumb, and P.D. Rainville, Waters Technology Brief 720006463EN (2019).

ABOUT THE AUTHOR

Thomas H. Walter is a Corporate Fellow at Waters Corporation, and works in Milford, Massachusetts.

ABOUT THE COLUMN EDITOR

David S. Bell is a director of Research and Development at Restek. He also serves on the Editorial Advisory Board for *LCGC* and is the Editor for "Column Watch." Over the past 20 years, he has worked directly in the chromatography industry, focusing his efforts on the design, development, and application of chromatographic stationary phases to advance gas chromatography, liquid chromatography, and related hyphenated techniques. His undergraduate studies in chemistry were completed at the State University of New York at Plattsburgh (SUNY Plattsburgh). He received his PhD in analytical chemistry from The Pennsylvania State University and spent the first decade of his career in the pharmaceutical industry performing analytical method development and validation using various forms of chromatography and electrophoresis. His main objectives have been to create and promote novel separation technologies and to conduct research on molecular interactions that contribute to retention and selectivity in an array of chromatographic processes. His research results have been presented in symposia worldwide, and have resulted in numerous peer-reviewed journal and trade magazine articles. Direct correspondence to: LCGCedit@ubm.com

CONNECT WITH LCGC ON SOCIAL MEDIA

Join your colleagues in conversation, respond to hot topic questions, and stay up-to-date on breaking news. "Like" and follow us on Twitter, LinkedIn, Facebook, and YouTube today!

LCGC

www.chromatographyonline.com/LCGCSocialMedia

LC TROUBLESHOOTING

Mobile Phase Buffers in LC: Effect of Buffer Preparation Method on Retention Repeatability

For liquid chromatography (LC) methods where the buffer pH and composition have an influence on retention, which buffer preparation method will provide the most repeatable results?

Dwight R. Stoll and Devin M. Makey

The measurement of pH, one of the most common of all analytical measurements, plays a major role in many chemical processes, affecting everything from the productivity of bioreactors in the biopharmaceutical industry, to the performance of separation methods in liquid chromatography (LC) and electrophoresis. Given that pH measurement is so common, I think we can be lulled into the perception that it is also simple, and that the pH reported by any benchtop pH meter can be accepted at face value under all circumstances. In my interactions working with people at a variety of experience levels over the years, I have often felt that people preparing buffers for use in LC are a little too trusting of the pH values reported by pH meters under ordinary circumstances. In preparation for this month's "LC Troubleshooting" column, my student Devin Makey and I performed some experiments to see if we could move in the direction of getting answers to questions around the topic of the "best" way to prepare buffers for use in LC. What follows here is a description of those experiments, and the data we observed. I believe that the results are interesting, and can support best practices for improving the reliability of LC methods. I know they are certainly affecting the way we operate in my laboratory, and I hope you will find them useful as well.

Dwight Stoll

Introduction

The Role of Eluent pH in LC

The pH of the eluent has a significant impact on retention and peak shape in several modes of LC separations. This is well understood in reversed-phase separations, where retention is strongly dependent on the solubility of the analyte in the organic–aqueous eluent. The pH of the eluent affects the charge state of various functional groups (COOH, NH_2, and so forth), and the charge state of these functional groups has a major impact on the solubility of the analyte in water; this is the origin of the primary influence of pH on retention. For example, a simple weak organic acid like benzoic acid will be neutral (uncharged) in eluents buffered well below the pK_a (~4.1), because the carboxylic acid functional group will be protonated. However, in eluents buffered well above the pK_a, the carboxylic acid functional group will be deprotonated, and carry a negative charge. The strong interactions between the negatively charged carboxylate group and the highly dipolar water molecules result in a much higher water solubility of the benzoic acid in the high pH eluent, and thus lower reversed-phase retention under these conditions. This is exemplified by the experimental retention data shown in Figure 1 for benzoic acid on a C18 reversed-phase column, where the eluent was buffered at different pH levels.

The same chemistry is relevant in hydrophilic interaction (HILIC) separations, though the dependence of retention on pH is often more complicated than it is in reversed-phase separations because of the more influential role of electrostatic interactions between the analyte and the stationary phase in HILIC. The influence of pH on other LC modes such as ion-exchange is even more evident because the magnitude of electrostatic interactions between the analyte and stationary phase is the dominant factor influencing retention. Thinking through these examples, it is clear that pH adjustment of buffered eluents is a topic with broad implications in LC.

Current Perspectives on Buffer Preparation

We also recognize that buffer preparation and pH adjustment is a pretty controversial topic in the LC community. This topic has been covered on multiple occasions in this column, focusing on aspects including buffer selection (1), preparation methods (2,3), and the idea of solution pH when an organic solvent is added to the mix (4). In a recent article of our own, we discussed the effects of different methods of buffer preparation on results from HILIC separations (5). In our preparation for this installment, we have found, through discussions with a variety of people, that they often have strongly held beliefs about what is

It's the DAWN of a new day.

Learn more at wyatt.com/NextGen

WYATT TECHNOLOGY

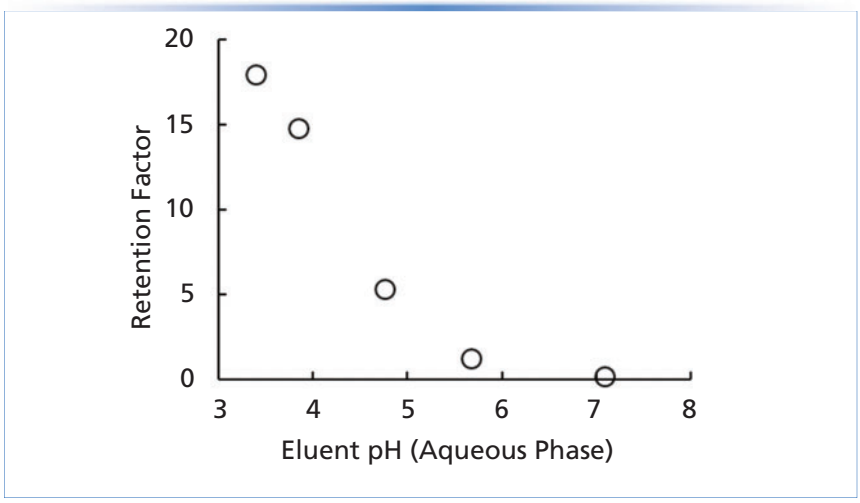

FIGURE 1: Effect of eluent pH on the retention of benzoic acid under reversed-phase conditions. Chromatographic conditions: column, SB-C18; eluent, 10:90 acetonitrile–phosphate buffer; temperature, 40 °C.

TABLE I: Reagents added to make 0.5 L potassium phosphate buffers solutions in the range of pH 2.8 to 3.2[a].

Mass KH_2PO_4 (g)	Mass 85% H_3PO_4 (g)	Expected PH	Measured pH
4.083	0.75	2.80	2.84
4.083	0.67	2.85	2.84
4.083	0.60	2.90	2.92
4.083	0.54	2.95	2.97
4.083	0.47	3.00	2.94
4.083	0.43	3.05	3.04
4.083	0.37	3.10	3.12
4.083	0.33	3.15	3.17
4.083	0.30	3.20	3.12

a) The pH levels of all solutions used in this work were measured using a low sodium error glass electrode (Orion 8101BNWP ROSS Half-Cell Electrode, from Thermo Scientific (Waltham, MA), calibrated using pH 1.68 and 4.00 standards from VWR (West Chester, PA).

right and wrong when it comes to buffer preparation, but also that these positions are not always clearly supported by experimental evidence. With this as a backdrop, we set out to make some of our own measurements with the hope that they would add to understanding in this area.

The most commonly used approach to buffer preparation for use in LC involves adding a salt of a buffering agent to water, then adding a small volume of relatively concentrated acid or base solution until a target pH is reached (as indicated by a pH electrode), and finally diluting to a specified volume. For example, suppose we are interested in a making 1 L of phosphate buffer at pH 6. Although there are many ways to prepare this buffer, a commonly used approach would be to first add sodium hydrogen phosphate (Na_2HPO_4) to about 900 mL of water. The pH of this initial solution will be about 9. Then, we could add phosphoric or hydrochloric acid to the solution slowly and watch the pH meter, stopping the addition of acid when the meter reads 6.00. We could then transfer the solution to a 1 L volumetric flask, and fill it to the mark with water. The focus of this article is really trying to answer the question, "If we make this buffer ten times, will we have added exactly the same amount of acid when we have stopped at pH 6.00, according to the pH meter?" If the answer is "yes," then

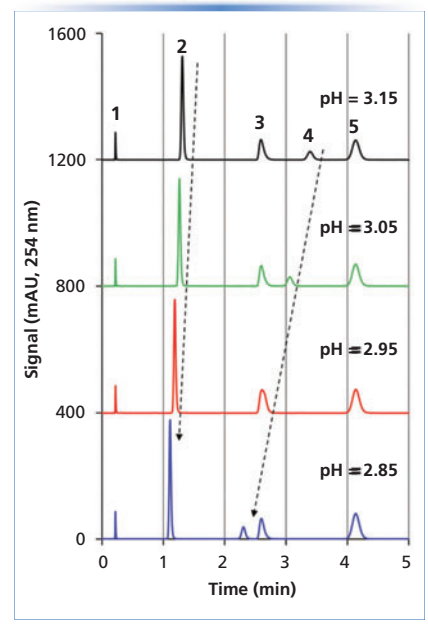

FIGURE 2: Effect of eluent pH on the retention of probe compounds (2) 4-aminobiphenyl, (3) n-butylbenzoic acid, (4) 4-hexylaniline, and (5) ethylbenzene. Uracil (1) was used as a dead time marker. Chromatographic conditions: column, StableBond C18 (50 mm x 4.6 mm i.d., 3.5-µm); flow rate, 2.0 mL/min.; eluent, 40:60 acetonitrile–buffer; temperature, 40 °C.

all is well, and we should expect similar results from LC separations involving these ten buffers. We will show that more often than not the answer is "no," and that the extent of variation of the acid added from one buffer to the next is enough to cause measurable variability in retention in some cases. At this point you may be asking yourself, "How can the answer possibly be 'no'?" That in itself is a good question, and one that requires many more words than we can fit in this short article. We'll come back to this question at the end of our discussion, and suggest some reading material for those interested in really digging into this more. For now, on to the data.

Experiments, Results, and Discussion

Dependence of Retention on pH for Some Probe Molecules

As a first step in this work, we set out to identify some simple probe molecules to use under reversed-phase

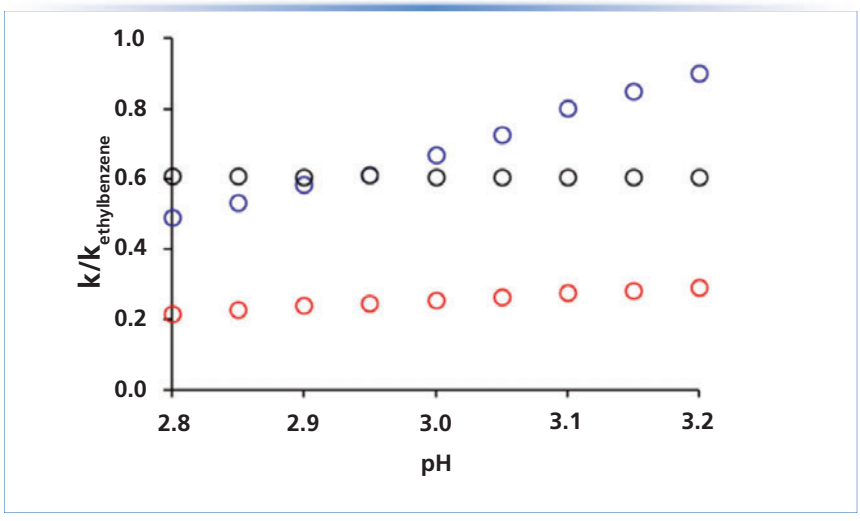

FIGURE 3: Retention of the three ionizable probes relative to the retention of ethylbenzene. Conditions are as in Figure 2. Key: O hexylaniline, O butylbenzoic acid, O aminobiphenyl.

conditions, and measure the dependence of their retentions on eluent pH. We chose one neutral molecule (ethylbenzene), one weak acid (butylbenzoic acid, pK_a ~4.2), and two weak bases (4-hexylaniline, pK_a ~4.8; and 4-aminobiphenyl, pK_a ~4.3), and used uracil in our test mixture as a column dead time marker. We then prepared about 500 mL each of nine potassium phosphate buffers with expected aqueous pH values between 2.80 and 3.20, in increments of 0.05 units. The approach was to first add potassium phosphate (the same amount in each case, 30 millimoles), then add different amounts of phosphoric acid as needed to reach the target solution pH, and finally add enough water to reach a total mass of 500.0 g. These amounts are shown in Table I, and were calculated by solving the charge balance equation for this system for the number of moles of phosphoric acid that was required at each pH level. Activity coefficients were calculated using the extended Debye-Hückel equation (6).

Using each of these buffers as the aqueous component of the eluent, we measured the retention times of the four probe compounds on a C18 col-

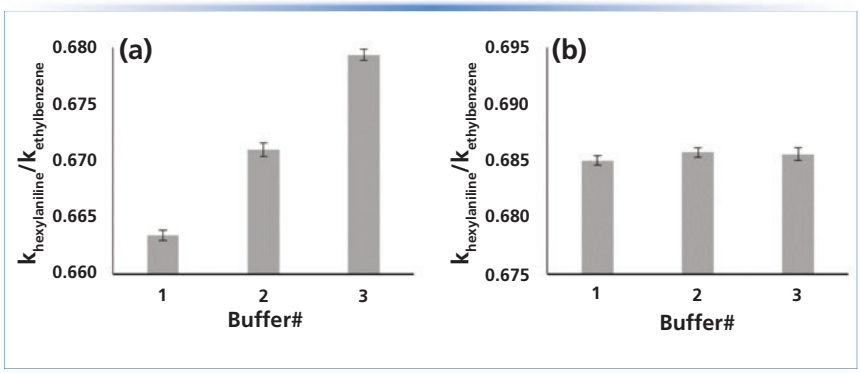

FIGURE 4: Relative retention of hexylaniline (normalized to ethylbenzene) for six buffers prepared by the same analyst; (a) for pH meter-directed approach, and (b) for gravimetric approach. Chromatographic conditions are as in Figure 2. Details of the buffer preparations are given in Table II. Error bars represent one standard deviation for ten replicate injections of the probe compound with a given buffer.

TABLE II: Buffer preparation steps and amounts of reagents added for three different replicate buffers made using the pH meter-directed and gravimetric approaches.

Step	pH Meter-Directed Approach	Buffer Number 1	2	3
1	Weighed 4.0827 g KH_2PO_4 in a weighing boat	4.0827 g	4.0827 g	4.0827 g
2	Transferred salt to 500 mL beaker			
3	Rinsed weighing vessel 4x with H_2O			
4	Added 450 g H_2O			
5	Titrated to pH 3.00 with 0.85% H_3PO_4	29.3 mL	26.9 mL	24.9 mL
6	Transferred solution to 500 mL volumetric flask and filled to line with H_2O			
Step	**Gravimetric Approach**	**Buffer Number 1**	**2**	**3**
1	Weighed 4.0827 g KH_2PO_4 in a weighing boat	4.0827 g	4.0828 g	4.0827 g
2	Weighed 28.179 g 0.85% H_3PO_4 in a beaker	28.1727 g	28.1788 g	28.1734 g
3	Transferred salt and acid to solvent bottle			
4	Rinsed weighing vessels 4x with H_2O			
5	Diluted up to 500 g with H_2O	500.03 g	500.02 g	500.00 g
Measured pH		**2.98**	**2.97**	**2.96**

umn. The resulting chromatograms for five of the buffers are shown in Figure 2, and a plot of the retention factors of the three ionizable probes relative to the retention factor of ethylbenzene is shown in Figure 3. At this point we make two observations. First, Figure 2 shows that the retention of ethylbenzene is nominally independent of pH, as expected, allowing us to normalize the retention of the other three probe compounds to the retention of ethylbenzene to minimize the effects of other variables such as temperature and organic to water ratio in the eluent on these measurements. On the other hand, the retention of the other three probes all exhibit some dependence of retention on pH, with the hexylaniline being the most sensitive of the three by far. Second, Figure 3 shows that the observed retention of each of the three ionizable probes is a smooth function of the calculated pH. Although the exact dependence of retention on pH is unknown for these conditions, we would at least expect it to be a smooth relationship.

TABLE III: Percent relative standard deviation (% RSD) of relative retention of hexylaniline measured using buffers (n = 3 in each case) prepared by four different analysts and two different methods.

Analyst	Approach	
	pH Meter-Directed	Gravimetric
1	2.72	0.06
2	2.23	0.10
3	2.34	0.02
4	1.25	0.003

Comparison of pH Meter-Directed and Gravimetric Methods of Buffer Preparation

Now, let's return to our question above: "If we make this buffer ten times, will we have added exactly the same amount of acid when we have stopped at pH 6.00, according to the pH meter?" We prepared three replicates of a nominal pH 3 buffer as described in Table I by using two different methods:

A) pH meter-directed: In this case, we use the pH meter to decide when to stop adding phosphoric acid (for example, when the meter reads 3.00).

B) Gravimetric: In this case, we calculate the amounts each reagent ahead of time, and repeat that recipe each time, only measuring the pH of the solution when the buffer is complete.

The nominal procedures for the two methods, and the amounts of reagents added for the six buffers used to obtain the data shown in Figure 4, are shown in Table II.

Figure 4 shows the mean relative retention of hexylaniline measured for six different buffers prepared by the same analyst, three by the pH meter-directed method (all using the same meter and electrode), and three by the gravimetric method. The results are quite clear. They show that the buffers prepared using the gravimetric method lead to much better repeat-

ability of retention time in different buffers, relative to the repeatability observed for different buffers made using the pH meter-directed approach. These results are evidence that the answer to our question posed early in this article is "no". In other words, the pH values reported by the meter are not sufficiently repeatable to guide preparation of the buffer when buffers of highly repeatable composition are needed.

Having settled on the protocol shown in Table II for the gravimetric method, three other analysts from our laboratory each prepared three replicate buffers using the pH meter-directed approach, and three using the gravimetric approach. The results are shown in Table III, where we see that all four analysts were able to produce buffers that led to highly repeatable retention time using the gravimetric approach, whereas the buffers prepared using the pH meter-directed approach always led to much more variable retention times.

Closing Thoughts

Clearly not all work involving buffered solutions requires the level of repeatability in pH that we explored in this work. However, we believe these results show that, when working with analytes that have a significant retention dependence on pH of the eluent, the gravimetric approach to buffer preparation is worth considering seriously. Simply put, in most cases weighing reagents using a balance is a simpler operation than measuring pH using a glass electrode, and can be done with extraordinary precision compared to most other analytical methods. When the recipe for a particular buffer is known, and repeating the preparation of the buffer in a precise way is desirable, then the gravimetric approach is most precise. Readers interested in learning more about factors that influence the accuracy and precision of pH measurement at this level are referred to Bates's book on the topic (7). Finally, readers interested in tools for calculation of buffer recipes that can be used with gravimetric approach are referred to free web-based tools developed by Professor Rob Beynon (https://www.liverpool.ac.uk/pfg/Research/Tools/BuffferCalc/Buffer.html), and Professor Peter Carr and Aosheng Wang (http://zirchrom.com/Buffer.asp) It is important to recognize that the latter tool does not correct pH calculations to account for activity effects, which affect calculated pHs of solutions of high ionic strength and multiply charged buffer components (for example, phosphate at pH 7).

Acknowledgements

We would like to acknowledge the effort of Hayley Lhotka, Alex Florea, and Dr. Gabriel Leme and their willingness to participate in the experiments described here. We also thank Professor Peter Carr and Dr. William Tindall for their willingness to share their knowledge of this subject with us. DM was supported by a grant from the Camille and Henry Dreyfus Foundation.

References

(1) G.W. Tindall, *LCGC North Am.* **20,** 1114–1118 (2002).

(2) J.W. Dolan, *LCGC North Am.* **33,** 18–22. (2015).

(3) G.W. Tindall, *LCGC North Am.* **21,** 28–32 (2003).

(4) G.W. Tindall, *LCGC North Am.* **20,** 1028–1032 (2002).

(5) D.R. Stoll and C. Seidl, *LCGC North Am.* **36,** 170–177 (2018).

(6) L.W. Potts, *Quantitative Analysis: Theory and Practice* (Harper & Row, New York, New York, 1987).

(7) R.G. Bates, *Determination of pH: Theory and Practice* (John Wiley and Sons, New York, New York, 2nd ed.,1973).

ABOUT THE CO-AUTHOR

Devin Makey
is an undergraduate student in his fourth year of study in chemistry at Gustavus Adolphus College in St. Peter, Minnesota.

ABOUT THE COLUMN EDITOR

Dwight R. Stoll
is the editor of "LC Troubleshooting." Stoll is a professor and co-chair of chemistry at Gustavus Adolphus College in St. Peter, Minnesota. His primary research focus is on the development of 2D-LC for both targeted and untargeted analyses. He has authored or coauthored more than 50 peer-reviewed publications and three book chapters in separation science and more than 100 conference presentations. He is also a member of *LCGC*'s editorial advisory board. Direct correspondence to: LCGCedit@ubm.com

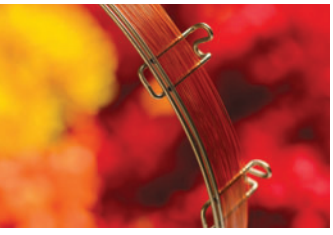

GC CONNECTIONS

Temperature Programmed GC: Why Are All Those Peaks So Sharp?

Temperature programming is used for most separations in capillary gas chromatography (GC) today. Despite this, many of the principles by which we understand temperature-programmed capillary column separations are based on ideas developed using packed columns and isothermal conditions. This installment of "GC Connections" dives into temperature programming. First, the differences in peak widths and retention times between temperature programmed and isothermal chromatograms are examined. Why are all the peaks so sharp in temperature programmed GC, yet they get broader (and shorter) in isothermal GC? Next, we explore some early ideas about temperature programming and peak broadening that explain why the peaks are so sharp in temperature-programmed GC, and why the peak spacing is different from isothermal GC. Finally, we examine an important consequence of our ability to program temperature: the need for temperature programming in splitless and other injections that use "solvent effects" and other peak focusing mechanisms. These points are illustrated using several historical figures and chromatograms from the early days of GC.

Nicholas H. Snow

Nearly every student of gas chromatography (GC) has seen chromatograms like the ones shown in Figure 1. These chromatograms were originally published in 1959, in one of the first papers describing an apparatus for temperature programming (1). Although developed on a handmade packed column with firebrick as the stationary phase, this work shows the same comparison and contrast between isothermal and temperature-programmed GC seen today. Starting from the bottom, Figure 1c shows an isothermal separation of normal alkanes. Notice that as the retention times get longer, the peaks get broader, and the last peak appears to exhibit fronting. Also notice that the retention time difference between each peak appears to nearly double with each successive alkane. The difference between C9 and C10 (the last two peaks) is about twice the difference between C8 and C9. Notice also that nearly 30 min is required to separate the six alkanes.

This chromatogram illustrates the main limitations of isothermal GC. First, the range of analytes that can be separated in a reasonable time is relatively small. Second, as the retention times get longer, the peaks get significantly broader (band broadening), and, as a result, they get shorter and harder to detect. If the peak area is constant, as a peak becomes broader, it must become shorter, limiting sensitivity. Third, the fronting of the later peaks is caused by the column temperature being too low for effective adsorption on the surface of the stationary phase. The liquid analyte condenses on the surface, causing some to be evaporated into the mobile phase more quickly and to therefore elute too soon. This is a form of column overload.

Moving up, Figure 1b shows a temperature-programmed separation of the same mixture of n-alkanes with a temperature programming rate of 5 °C per min and Figure 1a shows the same separation with a rate of 30 °C per min. Note the significant differences from the isothermal separation. First, the run time is reduced from 30 min to 10 and 5 min, respectively. Second, the peaks are spaced evenly. The retention time difference between each successive alkane is about the same. Finally, all of the peaks are sharper (remember this was a handmade packed column); they appear to have about the same peak width and as a result all have about the same peak height, while the isothermal peaks get broader and shorter.

Figure 1 raises two critical questions:

1. Why are the retention times evenly spaced in the temperature programmed separation, while the spacing doubles from peak to peak in the isothermal run?
2. Why are all the peaks sharp in the temperature-programmed separation, while the later peaks get significantly broader in the isothermal separation?

We will address these questions by drawing some simple pictures of the chromatographic process, followed

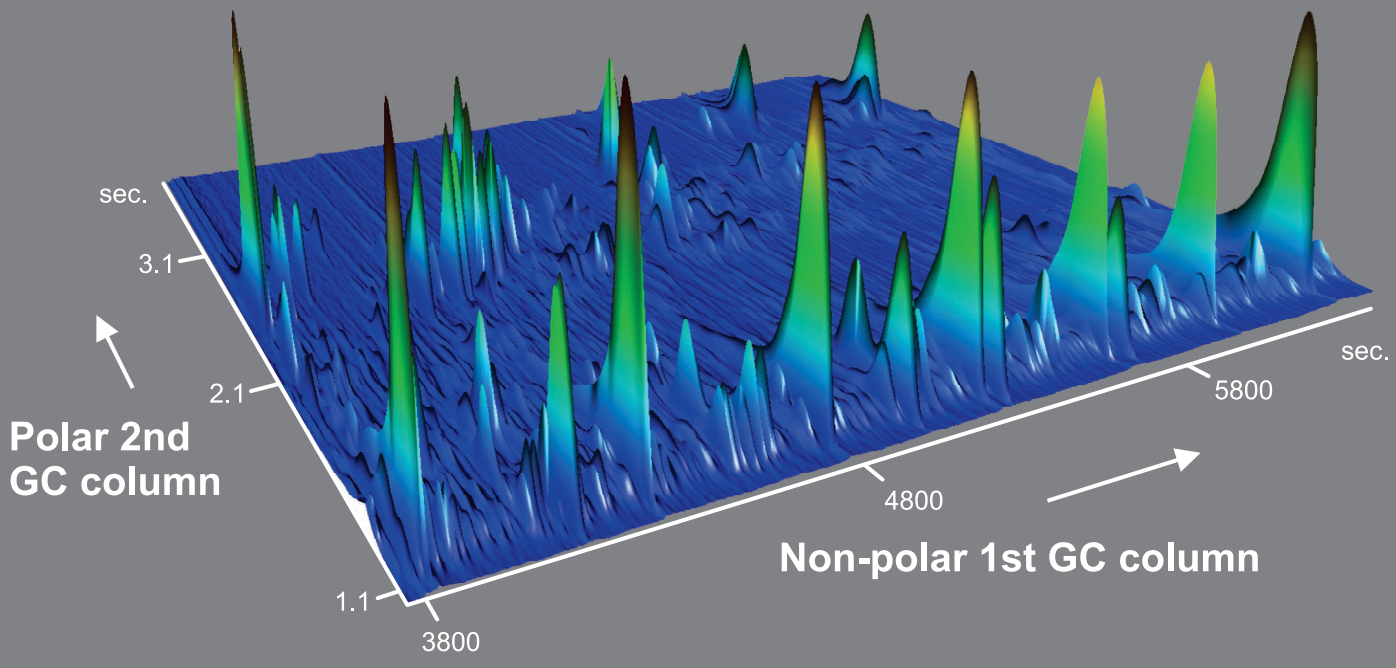

The power of GC×GC-TOFMS for your samples!

Simplify the Way You Perform GC×GC

Our benchtop GC-TOFMS solution, the Pegasus® BT, has the power to both screen and quantify from the same injection. Yet what if you could take your analysis one-step further and add a second dimension of separation? The Pegasus BT now offers our new FLUX™ GC×GC flow modulator, which inexpensively and easily enables you to perform GC×GC analysis. This option takes away the need for cryogens and makes GC×GC more accessible and routine to the everyday analyst.

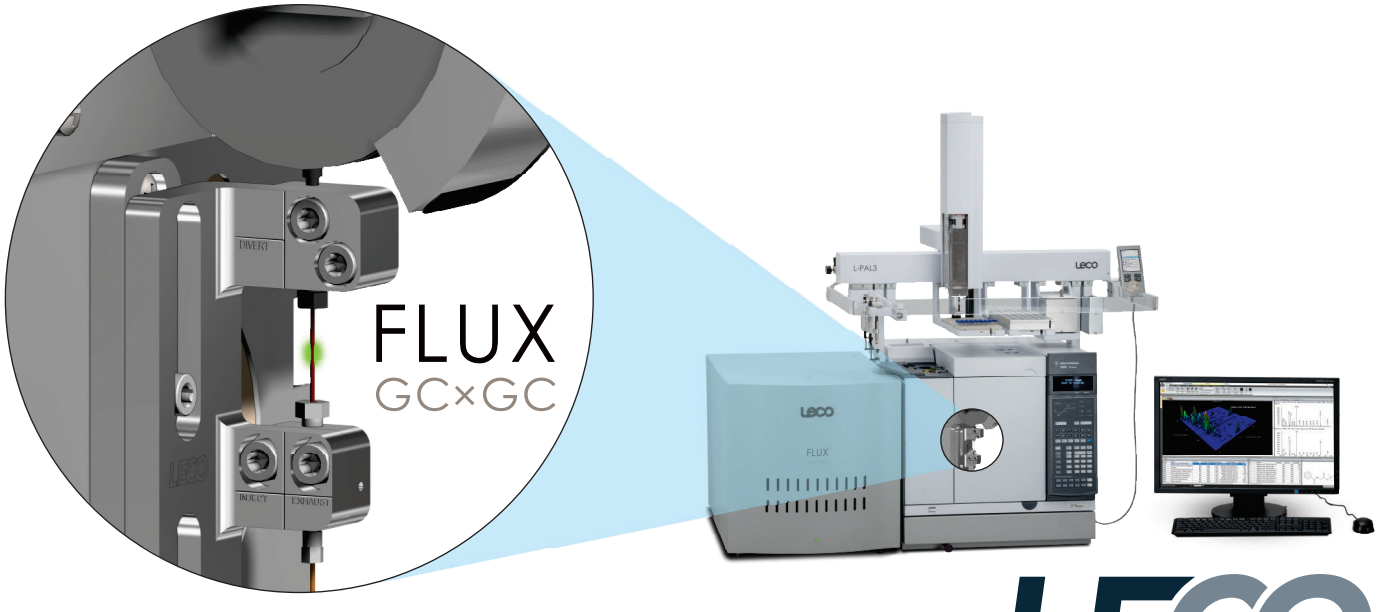

Phone: 1-800-292-6141 | info@leco.com
www.leco.com | © 2019 LECO Corporation

LECO
EMPOWERING RESULTS

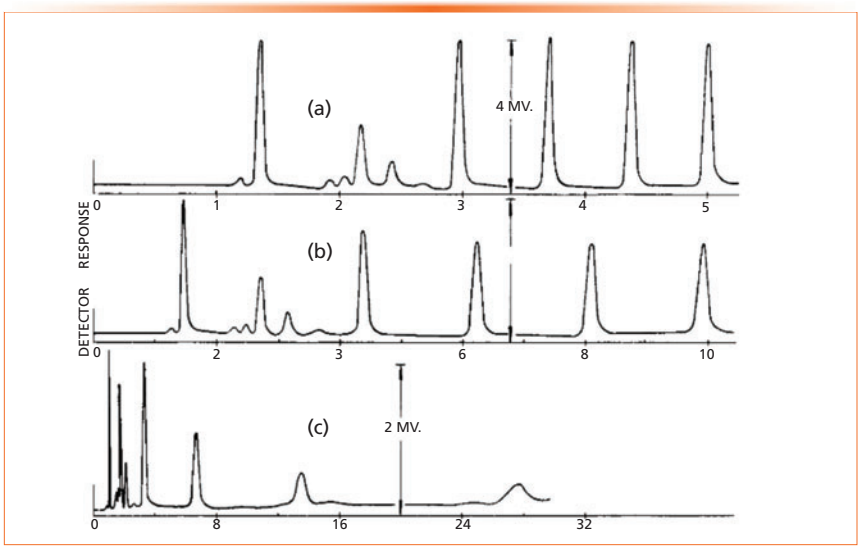

FIGURE 1: Temperature-programmed and isothermal chromatograms of a C_5–C_{10} alkane mixture. The temperature program in (a) is 30 °C per minute starting at 40 °C and in (b) is 5 °C per minute starting at 40 °C, and (c) is isothermal at 75 °C. Reproduced with permission from Reference 1, copyright 1959, American Chemical Society.

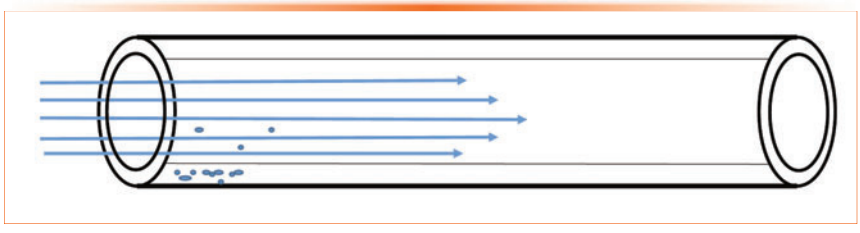

FIGURE 2: Simplified picture of analyte partitioning in a capillary GC column. Analyte molecules are represented by dots. There are nine dots in the stationary phase and three in the mobile phase, giving $k = 3$. Reprinted from Reference 2 with permission of the author.

by descriptions based on theories for both isothermal and temperature-programmed GC that were developed in the first 10 years of GC.

For an analyte to move along a GC column, it must have a vapor pressure of at least a few torr at the operating temperature. Remember that this vapor pressure is affected by both the normal vapor pressure and any change resulting from interactions with the stationary phase. Figure 2 shows a simplified picture of the inside of a capillary column, with the analyte molecules represented as dots (2). This compound has nine dots in the stationary phase and three in the mobile phase, giving a retention factor (k) of 3. A higher value of k indicates that more of the dots, a larger mass of the analyte, will be in the stationary phase, causing the analyte to be retained longer. The carrier gas forces the three dots in the mobile phase to move along the column. When they encounter fresh stationary phase, their attraction to the stationary phase and low (but finite) vapor pressure cause them to condense onto and dissolve in this new region of stationary phase. In isothermal GC, the thermodynamics of the partitioning process between the mobile phase and the stationary phase is governed by the enthalpy of vaporization (the change in heat content) for the analyte from the stationary phase into the mobile phase. For the alkanes seen in Figure 1, the enthalpy of vaporization increases linearly as each -CH_2- unit is added to the carbon chain. Through the Gibbs equation, which relates enthalpy and temperature, this results in an exponential increase in K and k, leading to an exponential increase in retention time. The full theory and thermodynamics are discussed elsewhere in more detail with the relevant equations (3–5).

In temperature programming, the column temperature usually increases linearly with time as the separation proceeds. This has the effect of increasing the vapor pressure and decreasing k of the analytes with time. From general and physical chemistry courses, we know that vapor pressure increases exponentially with temperature, with the linearized form of the relationship expressed by the Clausius-Clapeyron equation:

$$\ln P_{vap} = \frac{-\Delta H_{vap}}{R}\left(\frac{1}{T}\right) + \ln \beta \qquad [1]$$

where P_{vap} is the vapor pressure, ΔH_{vap} is the enthalpy of vaporization, R is the gas constant, T is the temperature in degrees Kelvin and β is $\Delta S/R$. Gas chromatographers often use a similar expression, the van't Hoff equation, which relates the equilibrium constant for a reaction and the temperature, assuming a constant change in enthalpy ΔH, and entropy ΔS:

$$\ln K = \frac{-\Delta H}{R}\left(\frac{1}{T}\right) + \frac{\Delta S}{R} \qquad [2]$$

where K is the partition coefficient which in GC is related to the retention factor (k) by the phase ratio (β), the ratio of the volume of the stationary phase to the volume of the mobile phase. In 1963, less than 10 years after the initial inception of GC, Giddings provided a model for temperature programming, depicted in Figure 3, based on the Clausius-Clapeyron equation, modified for the specific case of GC and on relationships derived previously by Dal Nogare and Harris and Habgood (6–9). One equation for describing temperature programming and relating it to the same thermodynamic quantities as seen in isothermal GC, derived by Harris and Habgood is seen in equation 3:

$$\int_{T_o}^{T_R} \frac{dT}{t_M(T)\left(1+\left(\frac{\alpha}{\beta}\right)e^{\Delta H/RT}\right)} = Rate \qquad [3]$$

where T_o is the initial temperature of the temperature program, T_R is the elution temperature of the analyte, $t_M(T)$ is the gas hold-up time at temperature T, $\alpha = \Delta S/R$, and β is the column phase ratio. Rate is the slope (°C/min) of the linear temperature program. Equation 3 must be solved numerically for the second integration constant, which provides the elution temperature of the analyte (easily translated into retention time using the starting temperature and programming rate), and provides the basis for several of the computer simulation programs for GC that have been developed over the years (10,11). For computer simulations of GC, ΔH and ΔS are easily measured and have been termed *thermodynamic retention indices* (12). With knowledge of these for a given analyte and stationary phase, and equation 3, it is possible to predict the retention time of any analyte on that same stationary phase under any conditions.

In Figure 3, the exponential curve describes the rate of zone or peak migration as the column temperature in increased. This exponential curve resembles a vapor pressure curve, and can be approximated as such, with the addition that acceleration of the analyte along the column is faster than predicted by vapor pressure alone, due to expansion of the carrier gas as it travels from the higher pressure at the column inlet to the lower pressure at the outlet. This demonstrates that, as the column temperature is increased, the peak accelerates as it simultaneously travels along the column, because its vapor pressure increases and the carrier gas is expanding inside the column as it flows from the inlet to the outlet.

In order to simplify the model, the

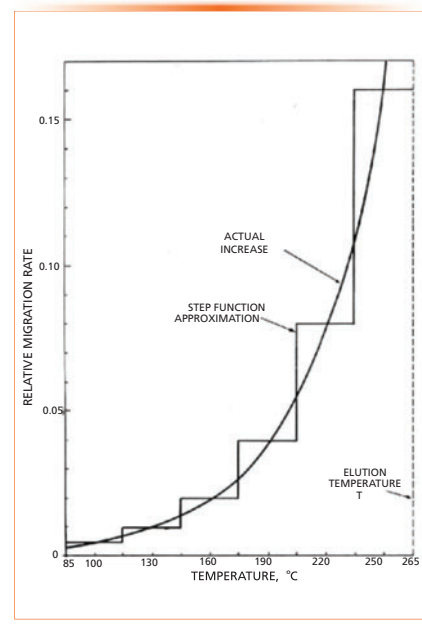

FIGURE 3: Step function approximation for the rate of zone migration in temperature-programmed gas chromatography. Reprinted with permission from Reference 6, American Chemical Society (1962).

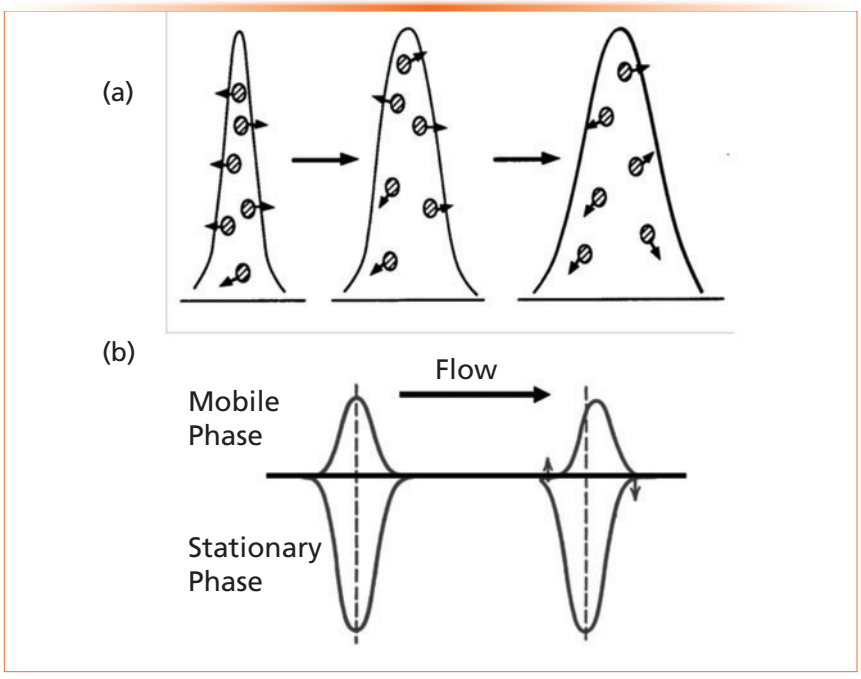

FIGURE 4: Diffusion and mass transfer in a capillary column: (a) molecular diffusion occurring in the mobile phase and relating to the *B* term in the Golay equation; (b) mass transfer occurring in both the mobile and stationary phases and referring to the *C* terms in the Golay equation.

exponential curve is broken up into six 30 °C steps, a so-called "step approximation" for temperature programming. As seen in Figure 3, with temperature programming conditions, in contrast to isothermal conditions, analytes move slowly when first injected, and accelerate exponentially as the temperature is increased and the chromatographic run proceeds. This exponential acceleration has the practical effect of linearizing the relationship between carbon chain length and retention time for the n-alkanes, as seen in Figure 1.

As an example of using the step approximation, Giddings described a temperature program from 85 to 265 °C, with the steps being six 30 °C intervals. He demonstrated that 50% of a peak's migration down the column occurs in the final 30-degree segment. In short, the peak travels about half of the column length in the last 1/6 of the retention time, and about 3/4 of the column length in the last 1/3 of the total retention time. Likewise, at the beginning of the run, the peak travels about 1/64 of the column length in the first 1/6 of the retention time, and about 3/32 of the column length in the first 1/3 of the retention time.

From this discussion, we see that retention times in temperature-programmed GC are based on the same thermodynamic quantities as in isothermal GC. However, in temperature programming, in contrast to isothermal conditions, the relationship between the enthalpy of vaporization and the retention time becomes linear, due to the linear increase in temperature giving rise to an exponential increase in vapor pressure, as seen in the Clausius-Clapeyron equation, or in *K* as seen in the van't Hoff equation. This explains the first aspect of the temperature programmed chromatogram seen in Figure 1: Alkane peaks are evenly spaced.

Turning to the second observation about Figure 1, that all of the peaks in the temperature-programmed run are of similar width, the step approximation can help explain that, as well. Giddings developed the step approximation so that the six segments could be further approximated as isothermal segments at the mean temperature of the segment. This allows us to think about each segment as a single isothermal portion of the run, and to apply the Golay equation, shown below in abbreviated form, to the conditions in each segment:

$$H = \frac{B}{\bar{u}} + (C_s + C_M)\,\bar{u} \qquad [4]$$

where *H* is the height equivalent to a theoretical plate, *B* is related to solute diffusion rates in the mobile phase, C_S and C_M are related to mass transfer rates in the stationary and mobile phases, respectively, and $\bar{u}$ is the average velocity of the carrier gas. A full explanation of the Golay equation and the principles related to the kinetics of band broadening is provided in References 4 and 5. The Golay equation reminds us that the rate of band broadening (expressed by *H*, the height equivalent to a theoretical plate) is a consequence of diffusion in the mobile phase, mass transfer in the mobile phase, and mass transfer in the stationary phase, as well. Simplified views of diffusion and mass transfer are shown below in Figure 4.

From the Golay equation, we see that band broadening caused by diffusion in the mobile phase, illustrated in Figure 4a, is inversely related to the average linear carrier gas velocity. Using the step model, we see that, in the first segments immediately following the injection, the bulk of analyte molecules reside in the stationary phase, so they are not affected much by mobile phase diffusion. As the separation proceeds in the later segments, the bulk of analyte molecules are in the mobile phase, and moving very rapidly as they approach the column outlet. This minimizes band broadening due to molecular diffusion, because of the inverse relationship with the carrier gas velocity.

Next, we turn to band broadening due to mass transfer, which is somewhat more complicated, but can be explained using similar logic. In capillary columns, there are terms

related to mass transfer in both the mobile and stationary phases. In this case, the rate of band broadening is directly proportional to the average velocity of the carrier gas, and is related to *k* and the respective mobile phase and stationary phase diffusion constants, illustrated in Figure 4b. On the left side of the figure, a symmetrical peak with $k = 3$ is shown, with its relative portions in both phases. On the right side of Figure 4b, the peak is seen to distort, or spread, caused by the mass in the mobile phase being shifted down the column (to the right in the figure), followed by the resulting evaporation of new analyte on the left of the figure.

The step approximation is useful here, as well. In the early steps, with the bulk of analyte molecules in the stationary phase, mass transfer is limited by the low temperature at the start of the temperature program. The analyte band is essentially "frozen" in place. In later segments, when the bulk of the analyte molecules are in the mobile phase, the time spent to traverse 50% of the column is short—1/6 of the total retention time—limiting the effect of mass transfer in the mobile phase. For mass transfer in the stationary phase, *k* gets smaller as the temperature increases, pushing the analyte more and more out of the stationary phase into the mobile phase, also limiting stationary phase mass transfer. In short, the narrow initial band, once it starts to move, accelerates and moves very quickly along most of the column length, minimizing the time for significant mass transfer as it is moving. The Golay equation and the step approximation together explain why the peaks are all sharp and about the same width in temperature-programmed GC.

The step approximation also provides a useful explanation for many practical aspects of temperature-programmed GC beyond the appearance of the chromatogram in Figure 1. Best practice in performing splitless injections provides a good example. The basics of splitless injection were recently reviewed in this column, and are the subject of an excellent review and book by Konrad Grob, so they will not be reviewed again in detail here (13–15). For this discussion, the important principles in splitless injections are that the injection process itself may require up to 60 s to complete, and splitless injection is always used in combination with temperature programming. Despite the long time required for the injection process, the peaks seen in separations that employ splitless injection are often very sharp. The step model of temperature programming can help to explain this phenomenon.

In a splitless injection, there are two peak focusing mechanisms at work once the sample reaches the column:

solvent effects, and thermal focusing or "cold trapping". The step approximation explains how both can work in combination with temperature programming to generate sharp peaks. First, assume a splitless injection in combination with a temperature program that starts at a temperature well below the boiling point of the sample solvent, and even further below the boiling points of the analytes. For example, if using hexane as solvent, which has a normal boiling point of 68 °C, I start my temperature programs at 40 °C. As the sample and solvent transfer into the column, the low initial column temperature causes the solvent to condense as a long plug of liquid at the head of the column. Analytes with higher boiling points or strong affinity for the stationary phase will be strongly retained by the stationary phase. This is cold trapping. Analytes with lower boiling points or stronger affinity to the solvent will be initially retained in the solvent plug, followed by retention as a narrow initial band on the stationary phase as the solvent evaporates. This is the solvent effect. A detailed description of solvent effects is provided in the text and article by Grob (14,15)

The step approximation applies to splitless injections whether the peaks are refocused by solvent effects or by cold trapping. All the peaks are broadened as the splitless injection process proceeds during the initial purge-off time, with the peak width determined by the length of the purge-off time. The cold initial column temperature effectively condenses the analytes into a narrow band at the column head. As the column is heated, the analytes begin to move down the column one by one, determined by their heat of vaporization from the stationary phase to the mobile phase. The process is similar for solvent effects, except that the initial bands are focused by evaporation of the solvent plug during the early stages of the separation. As an example, picture two analytes, one with a retention time of 12 min, and one with a retention time of 18 min. When the first analyte elutes after 12 min, the second analyte will have traveled about 1/4 of the column length. It will travel the final 3/4 of the column in the remaining 6 min. As discussed above, this process of refocusing, either by cold trapping or solvent effects, followed by temperature programming, keeps all of the peaks in a splitless injection sharp.

Temperature-programmed GC has been in common use for about six decades, and continues to be among the most powerful, yet easy to use, high resolution separation methods available. However, much of the theory of GC was developed assuming isothermal conditions, and continues to be discussed on that basis. The theory of temperature-programmed GC is much more complex than for isothermal GC, but is still based on the same fundamental thermodynamic and kinetic principles. In temperature-programmed GC, retention time relates linearly to the enthalpy of vaporization, while in isothermal GC the relationship is exponential. Combined with the high temperature stability of columns, this allows a wide range of analytes to be separated in a single run. The temperature-program step approximation provides a simple means for understanding how the peaks in temperature programmed GC remain sharp throughout the run, based on acceleration of the migration rate along the column as the temperature program proceeds. These principles make temperature-programmed capillary GC still the most powerful chromatographic separation technique available today.

References

(1) S. Dal Nogare and J.C. Harden, *Anal. Chem.* **31**(11) 1829–1832 (1959).

(2) N.H. Snow, *LCGC North Am.* **36**, 806–811 (2018).

(3) N.H. Snow, *J. Chem. Educ.* **73**(7), 592–597 (1996).

(4) L.M. Blumberg, *Gas Chromatography*, C.F. Poole, Ed. (Elsevier, Amsterdam, 2012), pp. 19–78.

(5) H.M. McNair, and J.M. Miller, *Basic Gas Chromatography* (John Wiley and Sons, New York, New York, 2nd ed., 2008), pp. 29–52.

(6) J.C. Giddings, *J. Chem. Educ.* **39**, 569–573 (1962).

(7) H.W. Habgood and W.E. Harris, *Anal. Chem.* **32**, 450–453 (1960).

(8) H.W. Habgood and W.E. Harris, *Anal. Chem.* **32**, 1206 (1960).

(9) S. Dal Nogare, *Anal. Chem.* **35**, 19R–25R (1960).

(10) N.H. Snow and H.M. McNair, *J. Chromatogr. Sci.* **30**, 271–275 (1992).

(11) Pro EZGC Chromatogram Modeler https://www.restek.com/proezgc (Accessed May 16, 2019).

(12) E. Dose, *Anal. Chem.* **59**, 2414–2419 (1987).

(13) N.H. Snow, *LCGC North Am.* **36**(7) 448–454 (2018).

(14) K. Grob, *Split and Splitless Injection for Quantitative Gas Chromatography: Concepts, Processes, Practical Guidelines, Sources of Error* (John Wiley and Sons, New York, New York, 4th. ed., 2008).

(15) K. Grob, *Anal. Chem.* **66**(20) 1009A–1019A (1994).

ABOUT THE COLUMN EDITOR

Nicholas H. Snow is the Founding Endowed Professor in the Department of Chemistry and Biochemistry at Seton Hall University, and an Adjunct Professor of Medical Science. During his 30 years as a chromatographer, he has published more than 60 refereed articles and book chapters and has given more than 200 presentations and short courses. He is interested in the fundamentals and applications of separation science, especially gas chromatography, sampling, and sample preparation for chemical analysis. His research group is very active, with ongoing projects using GC, GC–MS, two-dimensional GC, and extraction methods including headspace, liquid–liquid extraction, and solid-phase microextraction.

John V. Hinshaw "GC Connections" editor John V. Hinshaw is a Senior Scientist at Serveron Corporation in Beaverton, Oregon, and a member of LCGC's editorial advisory board. Direct correspondence about this column to the author via e-mail: LCGCedit@ubm.com

FOCUS ON ENVIRONMENTAL ANALYSIS

Environmental Method Development: Key Challenges and Unmet Needs

Whether working in commercial environmental laboratories or academia, many analytical chemists agree that the number and variety of pollutants requiring analysis today is straining the capabilities of current methods and technologies, the introduction of new standard methods is far too slow, and the community sorely needs a system by which new and up-to-date methods are more easily developed, shared, and adopted. These issues were all raised in some recent *LCGC* roundtable discussions.

Michael MacRae

In February 2019, the U.S. Environmental Protection Agency (EPA) unveiled (1) a comprehensive plan to deal with one of today's most persistent and pervasive classes of pollutants: per- and polyfluoroalkyl substances (PFAS). Used since the 1940s in a vast array of industrial and consumer products, including food packaging, firefighting foams, and fabric protectants, PFAS has been shown in laboratory studies to be associated with reproductive and developmental problems, liver and kidney function, immunological effects, and cancer. Among other actions, the EPA plans to develop new tools to characterize PFAS in the environment, and to set maximum levels for two common PFAS chemicals—perfluorooctane sulfonate (PFOS) and perfluorooctanoic acid (PFOA)—in drinking water.

The new EPA policies build on the agency's 2018 expansion of its Method 537 (2,3), which specifies the use of solid-phase extraction (SPE) and liquid chromatography–tandem mass spectrometry (LC–MS/MS) for the determination of PFAS in drinking water. The changes reflect a move to regulate a wider range of PFAS compounds, including so-called GenX chemicals and other newer products developed to replace specific PFAS compounds no longer on the market.

Although some environmental activists have welcomed the plan as a step in the right direction, the PFAS story is emblematic of a larger challenge facing today's environmental laboratories. Tens of thousands of chemicals of emerging ecological concern are released into the environment daily, posing a daunting array of scientific and regulatory issues for analytical chemists working in testing laboratories, academia, and the scientific instrument manufacturing industry. New findings about the health impacts of compounds such as glyphosate-based herbicides, microplastics, and dioxane are currently making headlines. The myriad of largely undisclosed chemicals used by the oil and gas industry in hydraulic fracturing ("fracking") are a source of ongoing public controversy. Meanwhile, a large class of persistent organic compounds, including dichloro-diphenyl-trichloroethane (DDT) and polychlorinated biphenyls (PCBs), continues to cycle through the environment, appearing decades after the compounds were last manufactured. Whether working in commercial environmental laboratories or academia, many analytical chemists agree that the number and variety of pollutants requiring analysis today is straining the capabilities of current methods and technologies, the introduction of new standard methods is happening far too slowly, and the community sorely needs a system by which new and up-to-date methods are more easily developed, shared, and adopted. These issues were all raised in some recent *LCGC* roundtable discussions. This reporting on trends in environmental analysis was underwritten by GE Healthcare.

Regulatory Ambiguity

Testing laboratories are often unsure of which regulatory statutes apply to certain sample types, says William A. Lipps, the chief science officer at Eurofins Eaton Analytical (Monrovia, California). For example, although the existing EPA guidelines for PFAS analysis in drinking water take the guesswork out of that particular application, the guidelines do not address one of the largest sources of PFAS contamination: wastewater. "As far as I know, there's really no activity to make a method for wastewater," said Lipps.

Lipps says that with more than 6000 known PFAS compounds in the environment, more up-to-date methods could help laboratories face an array of tough questions: "Who knows which ones to look for? How do you run them? Do you use this column or that column? This mobile phase or that mobile phase? Is it an ion? Is it an organic? At commercial laboratories, we don't really have time to deal with that stuff anymore."

PFAS compounds as a class comprise molecules across a wide size range, and the challenge of selecting the appropriate chromatographic technique is yet another consequence of the lack of PFAS standards, says Kevin Schug, the Shimadzu Distinguished Professor of Analytical Chemistry at the University of Texas at Arlington. "If you look at the thousands of variants of these PFAS compounds, you're talking about small molecules that are easily LC-able, and then [on the other end], you have really big polymeric species," he said. "There are very different analytical challenges with characterizing those and—again—there are no standards."

Similar ambiguity surrounds the selection of analytical methods for recycled water: processed wastewater that is increasingly being used in agriculture, landscaping, and other applications that increase the risks of human exposures to hazardous pollutants. In principle, Lipps notes, recycled water could fall under either wastewater or drinking water regulations, but there are consequences of the choice, and important implications for which methods would be used and how the laboratory would apply quality control. "Wastewater methods allow you to make some modifications, but drinking water methods don't," he explained. "If there's significant turbidity, the drinking water method won't work. You're probably going to need a combination of both, but there's really no EPA statute that handles recycled water as it is."

Laboratories working to measure the environmental impact of fracking chemicals face special challenges, due to the large array of chemicals currently in use by the oil and gas industry, most of which are not publicly reported because they're part of proprietary processes. "Even the oil and gas operators don't know exactly what they're using, in some cases," Schug adds.

One of the many issues is that there are a lot of different chemicals being used, in extremely high volumes, to stimulate the ground when companies are trying to extract oil and gas. "There's the potential for waste to be mishandled and to touch the environment, to get into drinking water and groundwater," said Schug. "There's not the kind of EPA standard methods to look at water quality through the lens of all those different chemicals."

Lipps agrees. "Nobody knows what they're sticking down that hole, and they're not going tell anybody, because it's proprietary," he said. "And so [fracking involves] all these different compounds. We have no methods for them. We don't know what they are."

Industry's response to the regulation of certain toxic compounds is often to develop chemically similar variants that offer similar performance, but sidestep existing regulatory statutes. The manufacturer creates a new compound that does the same job as the original substance, but has an unknown toxicity profile. "It's almost like a designer street drug type of situation," Schug remarked.

These issues underscore the concern raised by many environmental chemists that the EPA's development of new methods has simply not kept pace with the dramatic changes in the volume and variety of pollutants needing analysis. They say that the agency's methods are largely focused on compounds that are no longer manufactured, and, that when the EPA does develop a new method, it often is based on the capabilities of outdated analytical equipment.

"The EPA methods were written for priority pollutants, like organochlorine pesticides, or organochlorine solvents," Lipps said. "We're sitting around monitoring things that were banned 40 years ago, and yet there are absolutely no methods for the new things that are coming out. EPA just doesn't move fast enough." And by the time the agency does release a new method, he added, it may have been developed on a piece of equipment that may be more than a decade old.

"We're sitting around monitoring things that were banned 40 years ago, and yet there are absolutely no methods for the new things that are coming out."
William A. Lipps,
Chief Science Officer,
Eurofins Eaton Analytical

Jennifer Field, a professor in the Department of Environmental and Molecular Toxicology at Oregon State University (Corvallis, Oregon), said that, although she isn't required to follow EPA methodology in her research, she also believes that existing EPA methods often call for the use of older techniques that add complexity to the analytical process without substantially improving performance. "PFAS is where my laboratory spends 99% of its time now, so we're watching the development of EPA methods," she says. "EPA methods tend to be lagged in time, technology-wise."

Field points to the mandated use of SPE in many EPA methods as a prime

example of the agency's adherence to older technologies that may not be necessary or even appropriate. "I personally want to see the use of SPE decline," she stated. "It's really not necessary for so many applications. I think SPE has a history and [exists for] a reason, but there are a lot of problems that come with it, in terms of cost, time, and waste."

Field considers SPE a "crude tool," that requires inordinate amounts of time, labor, and sample matrix to obtain just the few microliters needed for analysis. "People have been told from infancy that SPE protects columns and mass spectrometers. I haven't had an application yet where that's true," she said, citing her laboratory's alternative practice of using the mass spectrometer's divert valve to eliminate salts and other components that are eluted prior to the analytes of interest. "I get the same functionality with much better control and resolution [than with SPE]. If you know your LC instrument very well, you can essentially achieve everything for water samples you can achieve with SPE. It's greener, faster, there's less labor, there are fewer problems with lot changes, and you just have much finer control. But this is a hard sell."

Lipps shares Field's concerns about SPE, but says he has no choice other than to use it. "As a commercial lab, we're stuck with it, especially for drinking water. There's really no reason for it, but we have to do it. So, we take an analysis that is maybe 15–30 minutes per sample on the instrument, and we add four hours to a day of sample preparation to it."

Filling the Method Development Void

Academic environmental laboratories and volunteer organizations, such as American Society for Testing and Materials (ASTM) International, are positioned to fill the void in analytical method development. However, many chemists say that it's difficult to secure the time, resources, and human capital for a task that is typically under-valued inside an organization, and under-utilized by the chemistry community at large.

"Developing methods for wider use is kind of the goal," said Sascha Usenko, an associate professor in the Department of Environmental Science at Baylor University (Waco, Texas). "But with the variations in approaches and technologies—which are somewhat competitive—it's kind of hard to get even a good method broadly accepted."

"Even the oil and gas operators don't know exactly what they're using, in some cases."
Kevin Schug,
Professor of Analytical Chemistry,
University of Texas at Arlington

Field agrees that academic laboratories face barriers in transferring methods to the broader community and commercial environment. "For example, our main vector is to put papers in peer-reviewed journals," she said. "But not everybody outside academia has subscriptions to those, nor wants them." The open-source vehicles for disseminating methods might facilitate more efficient technology transfer, she added.

As a contract laboratory scientist who also serves as a volunteer chairman of ASTM International's Committee D19 on Water, Lipps views the issue of standard method development from a unique vantage point. "ASTM is all-volunteer, so the speed at which we can bring a method forward is based on the speed of the volunteers and the voting process," he explained. "We've had some methods go through in as fast as a year, and others take five years." Finding qualified volunteers willing to sign on for the tedious, time-consuming work of ASTM method development is no small task, he added. "For the most part, it's roughly 20 or 30 people in the United States doing all the methods being developed at ASTM," he said. "There is just not that much interest. It's hard, it's a challenge, it takes a lot of time. And it's a very expensive endeavor."

Lipps said that the environmental analysis community is reluctant to adopt non-EPA methods, even though the agency recognizes many standards developed by others. He cited past efforts to develop three EPA-approved ASTM methods for cyanide that significantly reduced sample preparation time. "Roughly eight years after the fact, I only know of two laboratories that are running one of them," he said. "You would think that commercial laboratories would jump at this, but the adoption is almost nothing."

ASTM has developed "probably about 10 LC–MS/MS methods that don't use SPE…[for] polar pesticides, herbicides, other organic compounds like glycols—those are the types of methods we're developing at ASTM that do a modified form of direct injection LC–MS/MS," Lipps added. "They are published. They are standardized. And the world just absolutely rejects them."

A fundamental challenge for academics who seek to spend time or money on method development is the widespread lack of appreciation for the complexity of the method development process itself. "In the environmental world, a lot of my colleagues and collaborators are engineers," Field remarked. "They just want you to measure stuff. They think these methods grow on trees. They don't realize that method development is a whole discipline that requires a very systematic validation for each matrix of interest. The time and effort are simply undervalued by everybody except an analytical chemist." As a result, she continued, academic chemists are rarely able to secure funding specifically for the time and materials required to develop new methods, and often end

A Q&A

Flash Chromatography: Discover What's New in an Old Field

Dr. J Preston, PhD
Manager, Applications Laboratory
Global Product Manager for Chiral, Prep, Bulk and Flash Products
Phenomenex

What makes Flash a power purification technique for several industries?

Flash has been around for decades and its primary use has been in pharmaceutical drug discovery R&D. When an organic chemist or medicinal chemist synthesizes a new drug candidate molecule, the compound of interest must be "cleaned up" or purified before it can be further studied and evaluated. The crude reaction mixture is typically passed through a flash chromatography column and the pure drug compound is isolated by selective elution. If you have ever taken a prescription medication, the chances are very high that flash chromatography was used at some point in the research and development of that drug.

So, even though flash is an "old" chromatography, it is still the primary purification technique used in the pharmaceutical R&D enterprise because it is fast (Flash!), easy to use, and versatile.

Because of these characteristics, flash chromatography is also finding use in the purification of natural products and is being used to isolate and purify cannabinoids for use in edible products.

LCGC recently spoke with Dr. J Preston, PhD, manager of the Applications Laboratory and Global Product Manager for Chiral, Prep, Bulk, and Flash products, at Phenomenex about where flash chromatography fits in the scope of purification solutions, the advanced technologies of flash chromatography, and tips and techniques for flash product selection.

LCGC: How would you compare flash chromatography today to previous years?

Dr. J Preston: Flash chromatography is one of the oldest versions of chromatography, dating back more than 100 years. It has been updated and modified over the years, but the current version is a breakthrough from previous versions. Before, flash chromatography was a low-pressure gravity-fed system; now, instrumentation pumps the fluid through the flash cartridges. You no longer have to hand-pack glass columns. You can now use pre-packed plastic cartridges, which are faster, more convenient, and more reproducible. This change allows for better chromatographic media to be packed into each cartridge/column, which produces better results.

LCGC: How do these advantages affect how flash chromatography is used in purification?

Preston: In purification, flash chromatography is now a mainline tool that produces a high-quality material. It can also be used

to clean up very dirty samples that would then be used by more high-powered purification techniques.

LCGC: What are the advantages of using flash chromatography compared with prep or similar techniques?

Preston: One advantage of flash chromatography is that it typically utilizes a pre-packed, disposable column. You can put some of the dirtiest synthetic mixtures or natural product extracts onto the column and subsequently receive reasonably pure or highly pure material without worrying about the cost related to an expensive prep column.

In addition, the instrumentation to use flash chromatography can be simpler and the cost of those instrumentations is more affordable.

> "The instrumentation has pushed flash chromatography into a much wider realm and made it a legitimate step in the purification process."

LCGC: What are some popular applications for Phenomenex Claricep™ Flash columns?

Preston: The Claricep flash product line includes a range of standard cartridges that can be used in all the normal organic methodology, whether in early development or a specialty chemical area. Additional development of newer reversed phase and hydrophilic interaction liquid chromatography (HILIC) stationary phases has helped align the product line for purification of peptides, natural products, and other industries.

Continuous innovation within the Claricep brand has lead to the availability of both irregular and spherical particle morphologies, a large range of stationary phases, many particle size offerings and media that has been base deactivated to increase inertness.

LCGC: What are the emerging industries for flash chromatography?

Preston: The cannabis industry is interested in using flash chromatography for isolating desired components and for removing some of the impurities, solvents, pesticides, and fungicides that go into the production.

Another emerging industry for flash chromatography has been the peptide industry, which has traditionally depended on low-pressure, large-scale purification. They have recently found that flash fits nicely as a quick purification tool, especially because of the availability of pre-packed reversed-phase cartridges.

Historically, flash chromatography only focused on normal phase chromatography, but with pre-packed cartridges and better instrumentation, both HILIC and reversed-phase are becoming more popular.

LCGC: Who is currently using flash chromatography?

Preston: We are having a hard time finding places not using flash chromatography. Pharmaceutical companies, universities, peptide companies, the cannabis industry, and natural product isolation groups all use flash chromatography. The key has been the advancement of both instrumentation and pre-packed plastic bodies for flash chromatography cartridges that has allowed the technique to become widespread in many industries.

The instrumentation has pushed flash chromatography into a much wider realm and made it a legitimate step in the purification process.

up doing the work while in the process of performing other funded studies.

Technological Challenges

Many environmental chemists also say they feel current analytical technologies do not adequately meet their current needs, although they cite a wide variety of reasons for that view. Many environmental chemists share the perception that innovation in environmental analytical instrumentation and methods has lagged behind the more lucrative pharmaceutical and life science markets. Other scientists, typically those working in unregulated academic laboratories, seek instrumentation for highly specific, complex measurements that aren't possible with standard commercial systems. Furthermore, for many laboratories across the spectrum of environmental analysis, advanced instrumentation and the skilled personnel required to operate it to its full potential are economically out of reach.

Lipps, who formerly worked in marketing and product management for several instrument manufacturers, described something of an innovation stalemate in the environmental sector. Instrument manufacturers are hesitant to spend money to develop a new technology for environmental applications because the EPA continues to base its methods on older technologies, and laboratories are reluctant to buy new instrumentation unless it is specifically blessed by EPA-approved methods.

Usenko said that if laboratories can't afford to acquire the technologies they need, they have to "ask different questions, based on the technology they have in hand." He said that he personally devotes significant time and money to modifying instruments to achieve desired measurements. "For my proton-transfer reaction (PTR) MS system, I actually built a cold trap system so I could reduce the amount of moisture" when measuring compounds like formaldehyde in atmospheric samples. "All of a sudden, I've got to put a $50,000 modification onto that instrument—and that's just me building stuff."

Laboratories that do manage to acquire advanced instrumentation, such as high-resolution mass spectrometers for chromatographic analysis, can feel hindered by the incompatibility of the various manufacturers' proprietary data platforms. Field said in the case of her laboratory's recent purchase of a quadrupole time-of-flight (Q-TOF)-MS system intended to be used in collaboration with another laboratory, the decision was based more on the need to share data than on the capabilities of the data collection hardware. "There are people trying to fix that with independent programs and ways to translate files so they are comparable, but it's not routine and not commercially available yet, to my knowledge," she remarked.

"In the environmental world, a lot of my colleagues and collaborators are engineers. They think these methods grow on trees. They don't realize that method development is a whole discipline that requires a very systematic validation for each matrix of interest."
Jennifer Field,
Professor of Environmental and Molecular Toxicology,
Oregon State University

Role of Untargeted Analysis

Advances in full-scan mass spectrometry in recent years have enabled analytical chemists to determine large numbers of substances in a variety of sample types without knowing in advance what they were looking for. Untargeted analysis also enables users to search stored data from previous samples for the presence of compounds of emerging interest. The environmental analysis community seems to be gradually moving in the direction of untargeted analysis, although the change isn't happening overnight.

"There's absolutely a wave in that direction," Field stated. "The amazing power—and the challenge, resource-wise—is in the reduction and analysis of the data. The files are huge. They collect everything all the time." Advanced tools like Q-TOF, she said, can determine targeted analytes, suspected compounds of interest, and complete unknowns. "The instrument has all these capabilities," she said, "but the magic and the mystery and the challenge is dealing with the data. There's tremendous strength and power, but it's going to require a very talented workforce. It's going to take very expensive instrumentation. It takes faster computers just to deal with it. And, of course, data storage is a monster. The regulatory world isn't even close to dealing with things for which there are no standards—which is where this instrument shines."

Lipps agrees. "In my opinion, there's a very big demand to do untargeted testing, but it takes somebody that really, really knows what they're doing to ensure the resulting data is actually useful," he said.

Sample Preparation Issues

Problems with sample collection, preparation, and introduction are perpetual challenges in environmental analysis, and account for the vast majority of errors. Sample preparation is a complicated, and often tedious, step in the experimental process that many experienced chemists take pains to avoid, and, like method development, the time and expertise required for efficient sample prep is rarely appreciated by colleagues from other disciplines.

Despite these challenges, not everyone dislikes this part of the analytical process. "I enjoy sample prep" admitted Usenko. "There's a lot of opportunity within sample preparation to improve your overall analytical throughput, where you have less instrument downtime because the bulk of the heavy lifting is done with sample prep."

Field has taken the opposite approach in her lab. "I have dumped as much sample prep as I humanly can," she said. "Our lab hasn't run SPE for anything through an LC–MS in probably 12 years."

Nevertheless, laboratories using EPA methods are routinely required to perform SPE before analysis, adding to the sample handling complexity of analyzing samples like those containing PFAS-containing substances. PFAS samples typically contain high concentrations of suspended particulate matter and organics that can clog SPE columns and cause matrix effects. Removal of suspended solids before extraction using conventional filtration can absorb analytes of interest, contaminate the sample, and results in the determination of only the dissolved fraction of the sample.

EPA methods mandate other sample-handling procedures that cause headaches for contract laboratories. For example, according to EPA methods, PFAS samples cannot be held for more than two weeks before analysis. "The PFAS has been out in the environment for 20 years and hasn't changed," Field said. "But contract laboratories are stuck with a lot of things that are mandated for which there just simply isn't any scientific basis. As an academic, I would love to create methods for that community, yet these laboratories are constrained."

Potential Solutions

Acknowledging his bias as an editor of ASTM standards, Lipps believes closer collaboration between the EPA and ASTM would help method development proceed more quickly. He gets the impression that the EPA is reluctant to share information with volunteer consensus bodies, because of legal or other concerns. He says EPA worked much more closely with organizations like ASTM in the 1980s and 1990s, but those close collaborations aren't as common anymore.

"It would really help if [academics] were able to get their methods out there a little bit quicker and EPA could just adopt them or post them in the *Federal Register* and say, 'These things are allowed,'" As it is, he stated, contract laboratories are unable to use methods unless they first appear in the *Federal Register*. "People at universities develop methods, and we just can't use them. Even though we know we're going to get the right number with it [a new method], it doesn't matter. We know that we might be reporting the wrong number [by using an outdated but approved method], but that doesn't matter. The wrong number is EPA-approved, so that's what we report."

"With the variations in approaches and technologies—which are somewhat competitive—it's kind of hard to get even a good method broadly accepted."
Sascha Usenko,
associate professor of Environmental Science,
Baylor University

From the academic perspective, Usenko believes policy-makers, regulators, and research funders must return to the idea that investing in new technologies and method development work is worth taxpayer dollars. "There are always going to be new threats or new issues, but if we want to do the best for environmental and human health, it's a worthwhile investment."

Another step forward—although "a bit of a pipe dream"—said Field, would be for the United States to follow the European Union's lead in requiring manufacturers to disclose more data (and analytical methods) about their new compounds before they are permitted to market them. "One of my beefs," she said, "is that I get federal dollars to reverse-engineer proprietary formulations that were released on a large scale to the environment. Taxpayers are getting hit over and over again in this country to pay for solving problems they didn't create. This is how you basically let industry slide on their responsibilities toward environmental stewardship and public health."

Future Outlook

Environmental chemists may face some significant challenges, but the next generation of environmental chemists is a source of optimism that things will get better. "There's a lot of talent out there," Field said. "There are a lot of young people who want to make a difference. It's a wonderful field to be in, and I've really enjoyed watching it unlock the ingenuity and creativity in students. Method development is challenging, it's fun, and it's our way of saving the world."

Disclaimer

The views expressed here are the views of the individuals quoted, and do not necessarily reflect the views of Eurofins or any other organization.

References

(1) *EPA's Per- and Polyfluoroalkyl Substances (PFAS) Action Plan,* EPA 823R18004, February 2019, www.epa.gov/pfas.

(2) J. Shoemaker, P. Grimmet, and B. Boutin, *Method 537, Determination of Selected Perfluorinated Alkyl Acids in Drinking Water by Solid Phase Extraction and Liquid Chromatography/Tandem Mass Spectrometry* (LC/MS/MS), U.S. Environmental Protection Agency, Washington, DC, 2008.

(3) J. Shoemaker and Dan Tettenhorst, *Method 537.1, Determination of Selected Per- and Polyfluorinated Alkyl Substances in Drinking Water by Solid Phase Extraction and Liquid Chromatography/Tandem Mass Spectrometry (LC/MS/MS).* U.S. Environmental Protection Agency, Washington, DC, 2018.

Underwriting

This reporting on trends in environmental analysis was underwritten by GE Healthcare.

ABOUT THE AUTHOR

Michael MacRae writes about science, technology, and society. A former editor of *LCGC North America* and its sister publication, *Spectroscopy*, he lives in Portland, Oregon. Direct correspondence to: msmacrae@yahoo.com.

The Determination of Trace Per- and Polyfluoroalkyl Substances and Their Precursors Migrated into Food Simulants from Food Contact Materials by LC–MS/MS and GC–MS/MS

The determination of multiple per- and polyfluoroalkyl substances (PFAS) migrating from food contact material gained in importance as an increasing range of PFAS has been found migrating from food contact material into food. In this study, an integrated analytical approach that combines high performance liquid chromatography–tandem mass spectrometry (HPLC–MS/MS) and gas chromatography–tandem mass spectrometry (GC–MS/MS) was established for detecting 36 PFAS migrating from food contact materials into four food simulants (3% acetic acid, 10% alcohol, 50% alcohol, and olive oil). The response surface methodology was applied to optimize the selection of solvents in sample treatment. This target analytical method was appropriate for the determination of multiple PFAS, with recoveries ranging from 81.8 to 118.7%. The relative standard deviations (RSDs) ranged from 2.4 to 7.8%, and detection limits were in the range of 0.3 to 10 µg/kg in relevant food simulants.

Dan Li, Zi-hao Zhang, Huai-ning Zhong, Lei Zhu, Jing-jing Pan, Jian-guo Zheng, Qin-bao Lin, and Hui Liu

Per- and polyfluoroalkyl substances (PFAS) are a family of synthetic substances that do not occur naturally in the environment. They are a concern due to their stable physical and chemical properties with strong C-F bonds, including their chemical inertness, thermal stability, high surface activity, and hydrophobic-oleophobic properties (1–3). PFAS are widely used in consumer goods, household products and food contact materials (4–5). In food contact material (FCM), PFAS are mainly used in nonstick cookware, as well as the coatings of paper and other resistant materials, due to their oil- and water-repellent properties (6–7). Studies have indicated that the migration of PFAS from FCM into food is likely to be the main route of consumer exposure to these substances (8–11).

PFAS have been found to be highly resistant, and could persist in the environment for long periods of time, as well as in human serum, milk, and tissues (12–17). Certain type of PFAS, such as perfluorocarboxylic acids (PFCA) and perfluorosulfonic acids (PFSA), are likely to be toxic and bioaccumulate, posing adverse effects on human health (18–21). Perfluorooctane sulfonic acid (PFOS) and perfluorooctanoic acid (PFOA) are two of the most studied PFCA and PFSA. There is suggestive evidence from human epidemiology studies that PFOS and PFOA may cause abnormal liver enzymes, antibody response, and cancer (21–23). To reduce the occurrence of PFOS and PFOA, a number of PFAS, such as perfluoro-alcohol and its derivatives, have been used as substitutes to replace PFCA and PFSA in FCM. However, studies indicated that these substitutes could also pose health risks to humans, as PFSA and PFCA precursors are more toxic than the PFSA or PFCA themselves (24). In addition, these precursors could be absorbed into the human body, and degrade into PFOA and PFOS by an oxidation mechanism (25). For example, 8:2FTOH (flurotelomer alcohol) and 10:2FTOH could be converted into PFOA, and PFDA, and N-methyl perfluorooctane sulfonamido ethanol (N-MeFOSE) and N-ethyl perfluorooctane sulfonamido ethanol (N-EtFOSE) could be capable of conversion into PFOS. Therefore, besides known harmful PFAS, the migration of PFAS precursors from food contact material must also be taken into account to ensure its safety.

To protect consumers from exposure to PFAS migrated from FCM, stringent regulatory approaches have been adopted to control their production, application, and migration. The Danish Food and Veterinary Administration set a recommended limit for the total organic fluorine content in paper and cardboard at 0.35 µg per square decimeter of paper. The U.S. Food and Drug Administration (FDA) finalized an amendment to regulations that certain type of PFAS were not permitted as additives used in the manufacture of FCM (26). In China, the National Food Safety Standard GB 9685, which is the regulation for the use of additives in FCM, added an amendment in 2016 that no longer authorized PFAS as additives in the manufacture of FCM (27). In 2017, The European Chemicals Agency (ECHA) added seven types of

PFCAs and PFSAs to the Substances of Very High Concern (SVHC) list (28), which attracted much attention concerning the occurrence of PFAS, and their effects on the environment and human health.

Comparable results for measurement of PFAS migration from FCM is crucial for official control purposes. To achieve this objective, the guidance for choice of food simulants and migration test conditions for plastics have been provided in relevant regulations (29), which define the food simulants that should be used to mimic a specific foodstuff, and what standardized conditions of time, temperature, and contact should be performed. Various analytical approaches have been investigated for measuring the migration of PFAS from FCM (30–35). GC–MS is usually used for detecting volatile fluorine-containing compounds, such as perfluoroalcohols and perfluoroalcohol acrylates. LC–MS/MS, a highly sensitive and selective tool, was applied to detect more than 10 PFAS that mainly refer to straight-chain perfluorinated carboxylic acids or perfluorinated sulfonic acids. However, an analytical approach that is suitable for determination of multiple PFAS to detect migration from food contact materials has not been well established, especially for the increasing range of precursors, including PFCAs and PFSAs. In addition, the previous studies mainly focused on measuring the residue of PFAS in different matrices of FCM, such as extracts of paper. Few studies have been carried out on detecting migration of PFAS by using conventional simulants that represent the specific foodstuff.

To meet official control purposes, this present study aims to establish an effective method for simultaneously measuring multiple PFAS migrated from FCM, and possibly containing both PFAS and their precursors, including fluorinated carboxylic acid, hydrogen-substituted fluorinated carboxylic acid, and hydrogen-substituted fluorinated alkyl acid amides. To achieve this objective, the optimization of sample treatment was carried out by using a response surface methodology. An integrated analytical approach of combining high performance liquid chromatography–tandem mass spectrometry (HPLC–MS/MS) and gas chromatography–tandem mass spectrometry (GC–MS/MS) was established in four conventional food simulants (3% acetic acid, 10% alcohol, 50% alcohol, and olive oil) that are considered to represent specific foodstuffs.

Experimental

Reagents and Materials

Ultrapure water was purified using a Milli-Q system (Millipore, Milford, Massachusetts). Alcohol and methanol (HPLC-grade) were purchased from TEDIA Company. Ammonium acetate and acetic acid were purchased from Guangzhou Chemical Reagent Factory (Guangzhou, China), and olive oil was purchased from Sinopharm (Shanghai, China).

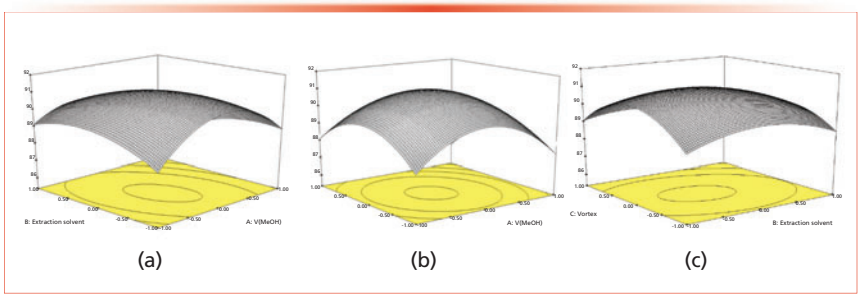

FIGURE 1: The recovery for PFNA shown in 3D plots of response surface and contour map, where the *z*-axis is the recovery rate for all figures: (a) acetonitrile concentration (A, %) versus volume of extraction solvent (B, mL); (b) acetonitrile concentration (A, %) versus vortex time (C, min); and (c) extraction solvent (B, mL) versus the vortex time (C, min).

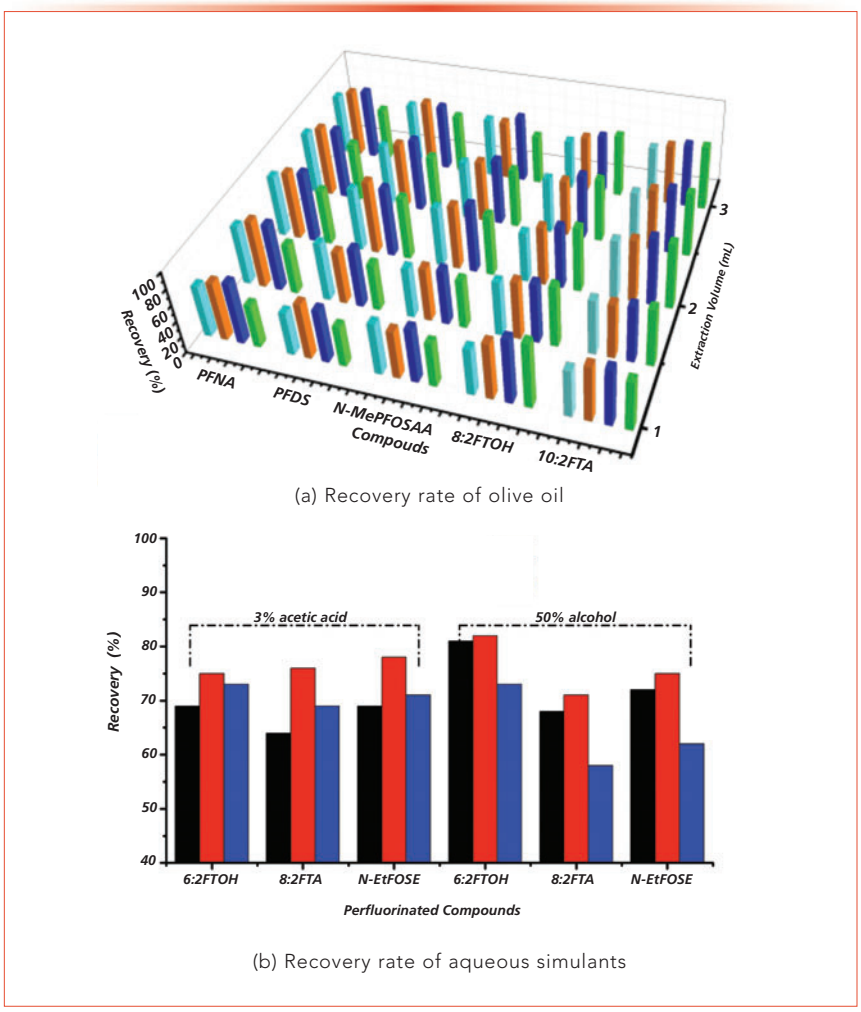

(a) Recovery rate of olive oil

(b) Recovery rate of aqueous simulants

FIGURE 2: Extraction efficiency by recovery rate of solvents: (a) recovery rate (%) of olive oil, and (b) recovery rate (%) of aqueous simulants.

A total of 36 PFAS standards (Table I) were purchased from Wellington Laboratories (Guelph, Ontario, Canada), Dr. Ehrenstorfer Company (Augsburg, Germany), Chiron Company (Trondheim, Norway), and TRC Company (North York, Ontario, Canada). An intermediate standard solution containing 27 PFAS (0.1 µg/mL, Group 1) was prepared by dissolving the commercial standards in methanol. An intermediate standard solution containing nine PFAS standards (1.0 µg/mL, Group 2) was prepared by dissolving the commercial standards in dichloromethane.

The standard working solutions used for LC–MS/MS analysis were prepared by transferring the intermediate standard (1.0 µg/mL), containing 27 PFAS (Group 1), into a 10 mL volumetric flask, spiked with 50 µL (1.0 µg/mL) 1,2,3,4-$^{13}C_4$ perfluorooctanoic acid (MPFOA) of internal standard, and then made up to 10 mL with the food simulants (10% [v/v] ethanol, 3% [w/v] acetic acid, and 50% [v/v] ethanol), respectively. The standard working solutions used for GC–MS/MS analysis were prepared by transferring the intermediate standard (1.0 µg/mL) containing nine PFAS (Group 2) into a 10 mL volumetric flask, spiked with 50 µL (0.2 µg/mL) methyl margarate-d33 of internal standard, and then made up to 10 mL with the food simulants (10% [v/v] ethanol, 3% [w/v] acetic acid, and 50% [v/v] ethanol), respectively. Then, 2 mL dichloromethane was added, vortexed for 5 min, allowed to separate, and the lower solvent layer was collected for further analysis.

The standard working solutions for the food simulant (olive oil) were prepared by transferring the intermediate standard of Group 1 (0.1 µg/mL) and Group 2 (1.0 µg/mL) into 10 g olive oil, spiked with internal standard of 10 µL MPFOA (1.0 µg/mL) and 50 µL (0.2 µg/mL) methyl margarate-d33. Then, 2 mL acetonitrile was added, vortexed for 5 min to allow stratification, and the upper solvent layer was taken for further analysis.

Equipment

An LC–triple quadrupole mass spectrometer and a GC–triple quadrupole mass spectrometer (6410 Triple Quad LC–MS, 7000c Triple Quad GC–MS, Agilent Technologies, Palo Alto, California) equipped with automatic injectors, were employed for the identification and quantification of PFAS.

The LC column employed was a 15 cm Poroshell120 EC-C18 column (2.7-

µm particle diameter and 2.1-mm i.d., Agilent Technologies), while the GC column employed was 30 m DB-5 column (0.25-µm particle diameter and 0.25-mm i.d., Agilent Technologies). The LC mobile phase consisted of water (solvent A) and HPLC grade methanol (solvent B). The gradient elution procedure was as follows: 0–3 min, 10% B; 3–4 min, 20% B; 4–5 min, 45% B; 5–11 min, 70% B; 11–18 min, 85% B; 18–19 min, 100% B; 19–20 min, 75% B; 20–21 min, 50% B; 21–24 min, 20% B; 24 min, 10% B. The injection volume was 5 µL, and the flow rate was 0.2 mL/min. ESI was used in negative mode with the following conditions: spray ion voltage, 4000 V; nebulizer, 20 psi; gas flow, 8 L/min; and capillary temperature, 350 °C. The GC temperature program was as follows: 75 °C for 3 min, 30 °C/min to 250 °C for 0 min, 50 °C/min to 300 °C for 6 min. The injection volume was 2 µL and pulsed splitless. The gas flow was 1.5 mL/min, with an electron ionization (EI) source and multiple reaction monitoring (MRM) mode. All of the ionization parameters and collision cell parameters were optimized for each analyte (Table I).

Migration Experimental

Migration experiments were carried out in accordance with European Union (EU) regulation 10/2011 for plastic materials and articles intended to be in contact with food (29).

Each sample was exposed to the food simulants with a ratio of contact area-to-volume at 1000 mL:6 dm^2, and then placed in an incubator at 70 °C. The food simulants were collected from each sample at 2 h, followed by cooling at room temperature, and then further analysis.

Instrumental Analysis

The majority of PFAS being investigated are fatty acid compounds that can ionize protons, and negatively charged parent ions in aqueous solution. For this reason, LC–MS/MS was used to detect 27 of this type of PFAS (Group 1). For the rest of the nine PFAS being investigated (Group 2), these are generally considered volatile compounds in which perfluoroalcohols and perfluoroalcohol acrylates would not easily be ionized in aqueous solutions; these compounds are more susceptible to ionization in an EI source than in an ESI source, therefore GC–MS/MS was preferred for their analysis.

The PFAS analytes were extracted from the relevant food simulant collected following an exposure step. For the determination of 27 PFAS (Group 1), the food simulants (10% ethanol, 3% acetic acid, and 50% ethanol) were transferred into a 10 mL volumetric flask, and filtered by a 0.22 µm syringe filter, followed by direct LC–MS/MS analysis.

The aqueous simulants containing nine PFAS (Group 2) were extracted

TABLE I: Optimized parameters of GC–EI-MS/MS and LC–ESI-MS/MS for 36 PFAS standards.

No	Compound (Abbreviation)	CAS Number	Structure	Retention Time (min)	Precursor Ion (m/z)	Product Ion (m/z)	Fragmentor (V)	Collision Energy (eV)
Group 1								
1	Perfluorobutyric acid (PFBA)	375-22-4	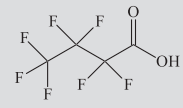	12.36	213.0	168.9	60	1
2	Perfluoropentanoic acid (PFPeA)	2706-90-3		13.18	262.9	218.9, 69.1	61	1, 47
3	Perfluorohexanoic acid (PFHxA)	307-24-4		13.94	313.0	269.0, 118.9	67, 68	5, 20
4	Perfluoroheptanoic acid (PFHpA)	375-85-9		14.76	362.8	319.0, 168.9	75, 75	5, 15
5	7H-Dodecafluoroheptanoic acid(HPFHpA)	1546-95-8		14.97	344.9	280.9, 131.1	70, 70	5,25
6	Perfluorooctanoic acid (PFOA)	335-67-1		15.76	413.0	369.0, 168.9	90, 90	5, 15
7	Perfluorononanoic acid (PFNA)	375-95-1		16.71	462.8	419.0, 218.9	106, 106	5, 10
8	Perfluorodecanoic acid (PFDA)	335-76-2		17.69	512.8	468.9, 218.9	90, 90	10, 15
9	2H,2H-Perfluorodecanoic acid (H2PFDA)	27854-31-5		17.59	476.9	393.0, 243.0	90, 90,	20, 25
10	Perfluoro-3-7-dimethyl octane carboxylate (PF-3,7-DMOA)	172155-07-6	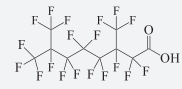	17.69	512.8	218.9, 168.9	88, 88	20, 33
11	Perfluoroundecanoic acid (PFUnA)	2058-94-8		18.74	562.9	518.9, 268.9	90, 90	5, 15
12	2H,2H,3H,3H-Perfluoroundecanoic acid (H4PFUnA)	34598-33-9		20.76	490.7	366.9, 386.9	96, 96	23, 11
13	Perfluorododecanoic acid (PFDoA)	307-55-1		19.74	613.0	569.1, 168.9	96, 96	4, 24
14	Perfluorotridecanoic acid (PFTRIDA)	72629-94-8		20.69	663.1	619.0, 168.9	101, 101	8, 28
15	Perfluorotetradecanoic acid (PFTEDA)	376-06-7		21.60	713.0	669.1, 168.9	114, 114	8, 24
16	Perfluorohexadecanoic acid (PFHeDA)	67905-19-5		23.27	813.0	768.9, 168.9	100, 100	5, 26
17	Perfluorobutanesulfonic acid (PFBS)	375-73-5	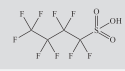	13.28	299.1	80.0, 99.0	120, 120	35, 35
18	Perfluorohexanesulfonic acid (PFHxS)	355-46-4		14.77	398.8	80.0, 99.0	161, 161	48, 36
19	Perfluoroheptanesulfonic acid (PFHpS)	375-92-8	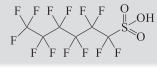	15.74	448.9	80.0, 99.0	114, 114	61, 56

(*Table continued on page* 470)

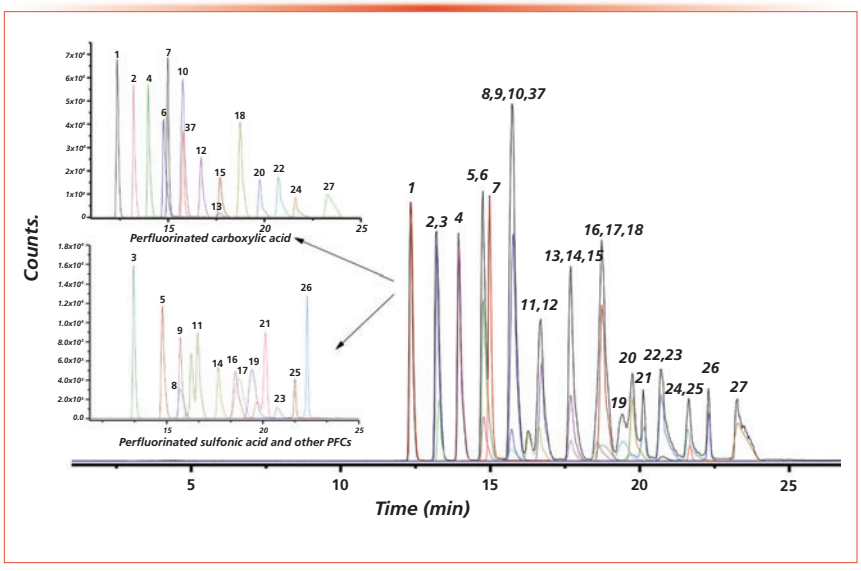

FIGURE 3: The MRM chromatogram of 27 PFAS compounds by HPLC–MS/MS (0.02 mg/kg)(1: PFBA, 2: PFPeA, 3: PFBS, 4: PFHxA, 5: PFHxS, 6: PFHePA, 7: HPFhpA, 8: H4PFOS 6:2, 9: PFHpS, 10: PFOA, 11: PFOS, 12: PFNA, 13: H2PFDA, 14: PF-3,7-DMOA, 15: PFDA, 16: PFDS, 17: N-MeFOSAA, 18: PFUnA, 19: N-EtFOSAA, 20: PFDoA, 21: PFOSA, 22: PFTRIDA, 23: H4PFUnA, 24: PFTEDA, 25: N-MeFOSA-M, 26: N-EtFOSA-M, 27:P FHeDA, 37: MPFOA).

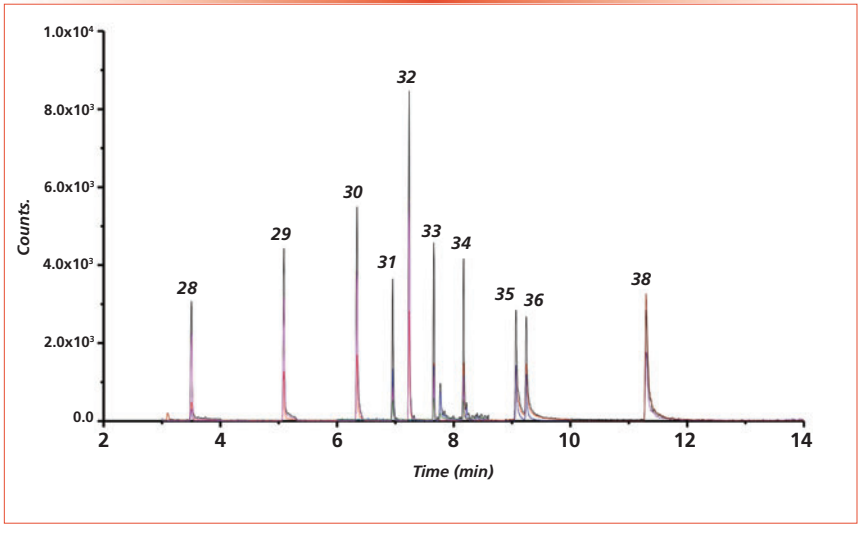

FIGURE 4: The MRM chromatogram of nine perfluorinated alcohols or esters by GC–MS/MS (0.01mg/kg) (28: 4:2FTOH, 29: 6:2FTOH, 30: 8:2FTOH, 31: 6:2FTA, 32: 10:2FTOH, 33: 8:2FTA, 34: 10:2FTA, 35: N-MeFOSE, 36: N-EtFOSE, 38: methyl margarate-d33).

with dichloromethane, and a volume of 10 mL of aqueous food simulants was transferred into the headspace bottle, with 50 µL (0.2 µg/mL) methyl margarate-d33 added as the internal standard. Dichloromethane was then added, and vortexed for stratification. The bottom layer was filtered, and used for GC–MS/MS analysis.

For treatment of the olive oil, 10 g of olive oil was transferred into the headspace bottle, and 10 µL (1.0 µg/mL) MPFOA and 50 µL (0.2 µg/mL) methyl margarate-d33 were added as the internal standards. After acetonitrile was added and vortexed for stratification, the supernatant liquor was filtered and analyzed by LC–MS/MS and GC–MS/MS.

(*Table continued from page 468*)

No	Compound (Abbreviation)	CAS Number	Structure	Retention Time (min)	Precursor Ion (m/z)	Product Ion (m/z)	Fragmentor (V)	Collision Energy (eV)
20	Perfluorooctanesulfonic acid (PFOS)	1763-23-1		16.65	498.8	80.0, 99.0	120, 120	60, 60
21	1H,1H,2H,2H-Perfluorooctanesulphonic acid (H4PFOS6:2)	27619-97-2		15.71	426.8	407.0, 81.1	124, 124	43, 5
22	Perfluorodecanesulfonic acid (PFDS)	335-77-3		18.56	598.8	80.0, 99.0	195, 195	80, 60
23	Perfluorooctanesulfonamide (PFOSA)	754-91-6		20.14	497.9	77.9, 147.9	161, 161	49, 29
24	N-Methyl-Perfluorooctanesulfonamide (N-MeFOSA-M)	31506-32-8		21.67	511.8	168.9, 218.9	116, 116	31, 29
25	N-Ethyl-Perfluorooctanesulfonamide (N-EtFOSA-M)	4151-50-2		22.32	526.1	168.9, 219.1	124, 124	31, 28
26	N-Methyl-Perfluorooctanesulfonamido acetic acid (N-MeFOSAA)	n.a.	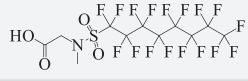	18.75	570.2	511.9, 418.9	135, 135	24, 28
27	N-Ethyl-Perfluorooctanesulfonamidoacetic acid (N-MeFOSAA)	n.a.	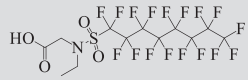	19.42	584.2	525.9, 418.9	135, 135	23, 25
Group 2								
28	1H,1H,2H,2H-Perfluoro-1-hexanol (4:2FTOH)	2043-47-2	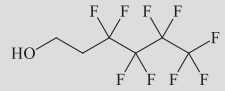	1.78	196.0, 94.8	50.9, 69.0	/	25, 25
29	1H,1H,2H,2H-Perfluoro-1-octanol (6:2FTOH)	647-42-7		2.46	94.9, 131.0	69.0, 69.0	/	23, 27
30	1H,1H,2H,2H-Perfluoro-1-decanol (8:2FTOH)	678-39-7		3.69	94.9, 131.0	69.0, 69.0	/	25, 25
31	1H,1H,2H,2H-Perfluoro-1-dodecanol (10:2FTOH)	865-86-1		4.78	94.9, 131.0	69.0, 69.0	/	26, 25
32	1H,1H,2H,2H-Perfluorooctylacrylate (6:2FTA)	27619-97-2	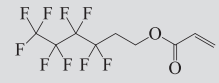	4.40	55.1, 131.0	27.2, 69.0	/	15, 30
33	1H,1H,2H,2H-Perfluorodecylacrylate (8:2FTA)	17527-29-6	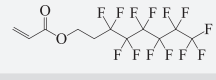	5.34	55.1, 131.0	27.2, 69.0	/	5, 20
34	1H,1H,2H,2H-Perfluorodecylacrylate (10:2 FTA)	27905-45-9	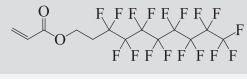	6.05	55.1, 131.0	27.2, 69.0	/	60, 45
35	N-Methyl-Perfluorooctanesulfonamidoethanol (N-MeFOSE)	24448-09-7	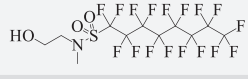	7.29	130.9, 526.0	69.0, 169.0	/	25
36	N-Ethyl-Perfluorooctanesulfonamidoethanol (N-EtFOSE)	1691-99-2	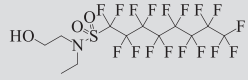	7.53	130.9,540.0	69.0, 169.0	/	25
Internal Standard								
37	1,2,3,4-13C4- Perfluorooctanoic acid(MPFOA)	n.a.	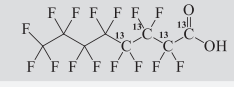	15.76	417.0	371.9, 168.9	95	5, 15
38	Methyl Margarate-d33	1219804-81-5		11.28	155.0	107.0, 78.9, 62.0	/	10, 15, 20

Results and Discussion

The Choice of Mobile Phase

A mixture of 27 PFAS comprising a standard at a concentration of 100 ng/mL was used to check the mass spectrometric response and separation power of four different mobile phases, including methanol–water solution, methanol–10 mmol/L ammonium acetate solution (pH = 7), methanol–(containing 0.1% ammonia) water solution, and acetonitrile–10 mmol/L ammonium acetate solution.

The results indicated that the weakest MS signal for target analytes was observed for acetonitrile–10 mmol/L ammonium acetate solution, and the strongest MS signal was observed for methanol–aqueous solution (containing 0.1% ammonia). This is likely due to the MS signal of PFAS analytes being related to the formation of the negative parent ion of PFAS, and the degree of ionization of the proton as well. Methanol allows analytes to generate target ions more easily, and be atomized on the electrospray ionization process, while acetonitrile may decrease the ionization of analytes. The poor peak shapes and baseline disturbances were observed for certain analytes, such as PFBA and PFPeA when methanol–water (containing 0.1% ammonia) was applied. Therefore, methanol–water (containing 0.1% ammonia) was not chosen as the mobile phase for further experiments.

Either methanol–water solution or methanol–10 mmol/L ammonium acetate solution was considered satisfactory as a suitable mobile phase, given that a similar ion peak response was obtained, and good chromatographic peak shapes were observed. It can be explained that the ionization of a proton occurs more often in a neutral or weak alkaline mobile phase, leading to an increase of formation of parent ions. Considering the methanol–water solution has the advantage of making maintenance of instrument pipelines simpler and more effective, the methanol–water solution was preferred for further experiments.

The Choice of Chromatography Column

Three different LC columns, including Agilent Zorbax SB-C18 (150 mm × 4.6 mm, 5-µm), Poroshell 120 EC-C18 (150 mm × 3.0 mm, 2.7-µm), and Eclipse XDB C-18 (150 mm × 4.6 mm, 3.5-µm), were compared in the separation of a mixture of standards (27 PFAS), at a concentration solution of 100 ng/mL.

The results indicated that all three columns could effectively separate the target analytes, particularly n-alkane PFAS. However, due to the occurrence of a high number of target PFAS analytes, the chromatographic peaks of various analytes may overlap each other, causing difficulty in further analysis. The Poroshell 120 EC-C18 was shown to be able to completely separate 27 PFAS analytes in 25 min with the same gradient elution program. Therefore, the Poroshell 120 EC-C18 was chosen as the stationary phase for further experiments.

For the selection of a GC column, baseline separations could be achieved for nine target PFAS using a low or medium polarity column. Therefore, the DB-5, DB-17, or DB-35 column could be chosen to perform the analysis.

The MRM chromatogram of 36 PFAS compounds is shown in Figures 3 and 4.

The Choice of Extraction Solvent for Olive Oil

Olive oil, as a fatty simulant, cannot be directly analyzed due to interference from compounds it contains. Therefore, it must be converted into a suitable solution before analysis. To achieve the objective, a recovery experiment was conducted in an olive oil blank spiked with 0.1 mL PFAS standards (10 µg/mL), aimed at selecting a suitable solvent to extract the PFAS from the olive oil. Four different solvents—methanol, acetonitrile:water (1:1), acetonitrile:water (3:1), and acetonitrile—with serial extraction volumes (1 mL, 1.5 mL, 2 mL, 2.5 mL, 3 mL), were investigated. The recovery rate for each solvent is indicated in Figure 2a.

The results indicated that acetonitrile:water (3:1) and acetonitrile had the highest extraction efficiency, and a slightly higher recovery rate was obtained for acetonitrile compared with that of acetonitrile:water (3:1). One of the reasons might be that the PFAS being investigated are long-chain aliphatic compounds, and the pure organic phase is more favorable for the extraction of the target analytes. For methanol, the separation of the methanol and olive oil layers was not clearly observed after mixing because of the emulsification effect, although

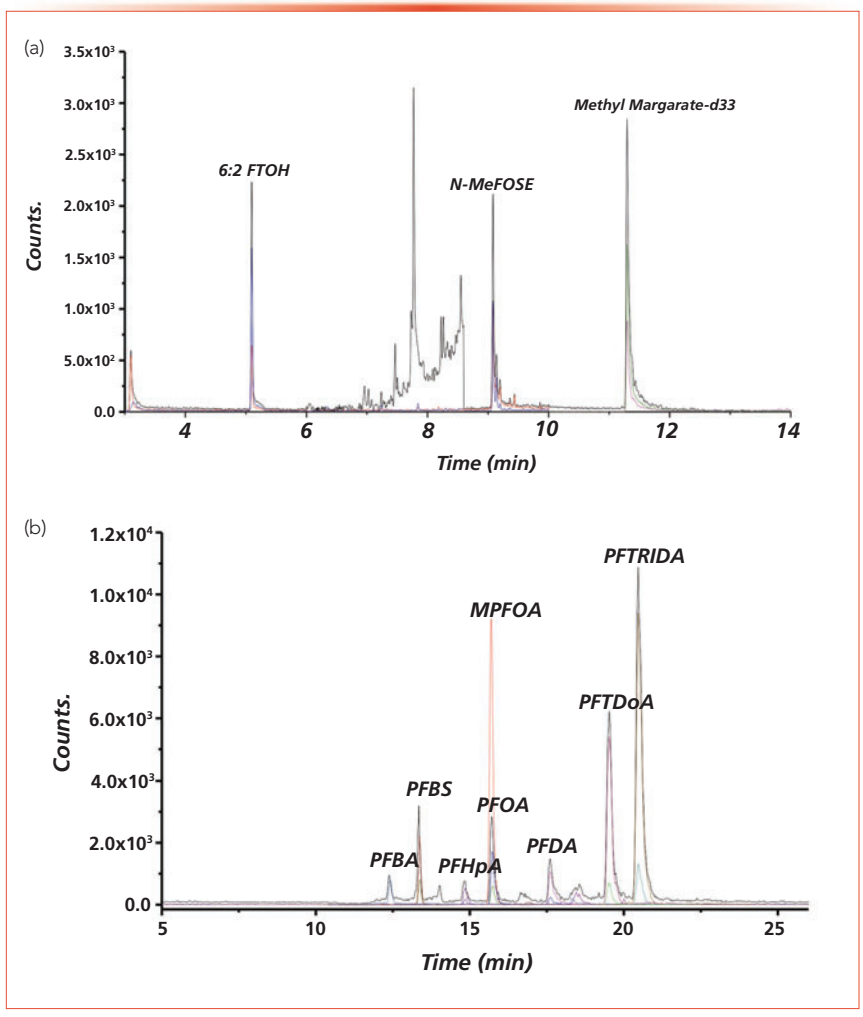

FIGURE 5: The chromatograph profiles of a coated cardboard using (a) GC–MS/MS and (b) LC–MS/MS.

the fluorinated fatty alcohol and some perfluorinated carboxylic acids had the highest recovery rates. In the case of acetonitrile:water (1:1) solvent, delamination was not clear, and the recovery rate was low, therefore acetonitrile:water (1:1) was not suitable for GC–MS analysis. Given the test results indicted, acetonitrile was chosen as the solvent to extract the PFAS from the olive oil.

The extraction conditions of PFAS in olive oil were optimized by applying a single-factor experiment derived from the response surface methodology. PFNA was taken as the sample to be investigated, and the acetonitrile concentration (A, %), volume of extraction solvent (B, mL), and the vortex time (C, min) were assigned as independent variables. The recovery rate of PFAS were taken as the response value based on the principle of the Box-Behnken central composite design. A secondary polynomial regression model was obtained from 15 experiments with three factors and three levels: recovery = 72.46 + 7.77 × A + 1.47 × B + 5.23 × C - 1.35 × A × B + 0.50 × A × C + 1.75 × B × C + 3.70 × A^2 + 0.60 × B^2 + 0.69 × C^2. The results of the recovery of PFNA obtained by the response surface methodology are shown in Table II and Figure 1.

It can be found from the F-value (Table II) that the sequence of influence of a single factor on the recovery rate was A > C > B, suggesting that the influence of A^2 was significant in the quadratic term, while B^2 and C^2 were not. Thus, 100% acetonitrile was considered an appropriate extraction solution. The highest extraction efficiency was observed when the extraction time was 5 min, and the extraction volume was 2 mL.

The Choice of Extraction Solvent for Aqueous Simulants

In this study, GC–MS was employed for detecting fluorinated fatty alcohols, fluorinated fatty alcohol acrylates, and fluoro-sulfonamide fatty alcohols in the extraction of aqueous simulants. A comparison experiment was conducted on two aqueous simulants (3% acetic acid and 50% ethanol) to check the extraction efficiency of the solvents n-hexane, dichloromethane, and ethyl ether:n-heptane (1:1).

The results showed that all selected solvents were well able to extract the analytes of the aqueous simulants. However, n-hexane was not a suitable solvent to extract fluorinated fatty alcohols, due to its weak polarity. A mix of solvents consisting of ethyl ether and n-heptane did not demonstrate sufficient extraction efficiency. In addition, ethyl ether may cause a hazard to the analyst during vortexing at high pressures. The data indicated that the highest recovery rate was obtained when dichloromethane was applied for measuring fluorinated fatty alcohols and fluorinated fatty alcohol acrylates, which may be due to its medium polarity and strong density that is lower than water-based solutions. Thus, dichloromethane was chosen as the extraction solvent. Figure 2b shows the extraction efficiency for three different solvents by measured recovery rate. The highest extraction efficiency was achieved with a 5 min extraction time with a 2 mL extraction volume.

Optimization of Mass Spectrometry

The mass spectrometry methods for 27 PFAS in Group 1 and 9 PFAS in Group 2 were optimized to directly detect each PFC (1 mg/L) in methanol. Standard solutions were scanned by performing a first-stage mass spectrometry full

scan in negative ion ESI mode with corresponding transmission voltages. The results showed that the strongest peaks of the perfluorocarboxylic acid, hydrogen substituted fluorocarboxylic acid, or perfluorosulfonamide compounds were the quasi-molecular ion peaks $[M-1]^-$ or the molecular ion peaks following the loss of the carboxyl group $[M-45]^-$. The strongest signal of the perfluorosulfonic acid or hydrogen substituted perfluorosulfonic acid compounds observed were quasi-molecular ion peaks $[M-1]^-$ and sulfonic acid group molecular ion peaks $[SO_3]^-$. Nine types of PFAS from Group 2 were scanned by conducting a first-stage mass spectrometry full scan under the positive EI mode. The results indicated that the fluorinated fatty alcohols and fluorinated fatty alcohol acrylates formed smaller fragmentary ion peaks $[C_3H_5F_2O]^+$ (M = 95), $(C_3H_3O]^+$ (M = 55) or $[C_3H_3F_4O]^+$ (M = 131), which are shown in Figures 3 and 4.

Ion beam scanning was performed with a collision energy of 0–60 eV targeting each quasi-molecular ion to obtain the daughter ion information and the collision energy values that were suitable for the daughter ion response sizes. Daughter ions of perfluorocarboxylic acid compounds are a series of molecular ions following the loss of the carboxyl group, and there are several CF_2 fragments between each molecule, including the ionic fragment of $[C_3F_7]^-$, $[C_4F_9]^-$, $[C_5F_{11}]^-$, having a general structural formula of $[C_nF_{2n+1}]^-$. The ions of the perfluorosulfonic acid compounds were those molecular ions that lost several $[C_nF_{2n+1}]^-$ saturated carbon chain groups and had sulfonic acid functional groups, such as $[C_nF_{2n}SO_3]^-$, $[SO_3]^-$, and $[FSO_3]^-$ ions. Both the fluorinated fatty alcohols and fluorinated fatty alcohol acrylates contained the ion-pair $[C_3H_3F_4O]^+$ (M = 131) to $[CF_3]^+$ (M = 69). Therefore, the fragment ions with the largest response and least interference were chosen as the quantitative and qualitative ions. To obtain better sensitivities, the parameters including the selection of daughter ions, fragmentation voltage, and collision energy were optimized (see Table I).

Quantification and Validation

Linear Range and Quantitative Limit

Using the method described above, the 36 PFAS compounds were analyzed in the multiple reaction monitoring mode (MRM). The concentration and peak area of each compound was taken as the abscissa and ordinate, and a standard curve was drawn. The linear range of the recovered curve was between 1 and 1000 ng/mL, and the limits of quantification (10 S/N) were 0.35–9.72 µg/kg in 3% acetic acid, 0.29–8.43 µg/kg in 10% alcohol, 0.28–8.73 µg/kg in 50% alcohol, and 0.43–9.86 µg/kg in olive oil.

TABLE II: F-values of PFNA by Box-Behnken central composite design

Source	Model	A	B	C	AB	AC	BC	A^2	B^2	C^2
F-value	4.21	22.78	0.82	10.29	0.34	0.05	0.58	2.71	0.07	0.10

Recovery and Precision

An experiment was carried out where samples were spiked with 10 and 100 ng standards in 3% acetic acid, 10% alcohol, 50% alcohol, and olive oil, respectively. The recovery rates for the four different food simulants ranged from 81.8 to 118.7%, and the relative standard deviations (RSDs) ranged from 2.4 to 7.8%.

Analysis of Real Samples

A total of 70 food contact materials were collected from local supermarkets, which include coated paper board, multilayer paper packaging, multilayer plastic food packaging, heat-resistant rubber articles, and coated heat-resistant metallic containers. The novel analytical approach was applied to perform the analysis. Some specific PFAS compounds were found in paper samples with concentrations of 0.01 mg/kg to 0.05 mg/kg of food simulants, which accounted for 5% of the total number of samples analyzed. Multilayer cardboard and coated paper board were the main types of packaging in which PFAS compounds were found with average concentrations of 0.02 mg/kg. The highest migration of PFAS was 0.08 mg/kg. The type of PFAS compounds found were mainly straight-chain perfluorinated acids and perfluorinated alcohol compounds. The chromatogram profiles of the PFAS in typical samples are shown in Figure 5.

Conclusion

A target approach was established for the determination of 36 PFAS migrating from food contact material into food simulants of 3% acetic acid, 10% alcohol, 50% alcohol, and olive oil. A total of 36 PFAS were divided into two groups, and measured by LC–MS/MS and GC–MS/MS. LC–MS/MS was used to detect 27 fatty acid PFAS, while 9 PFAS with volatile properties, including fluorinated fatty alcohols and fluorinated fatty alcohol acrylates were measured by GC–MS/MS. The response surface methodology was a useful tool to simplify the selection of solvents with optimized conditions. This integrated analytical approach was appropriate for the determination of multiple PFAS with recovery rates that ranged from 81.8 to 118.7%, the relative standard deviation (RSD) ranged from 2.4 to 7.8%, and the detection limits ranged from 0.35 to 9.72 µg/kg in 3% acetic acid, 0.29 to 8.43 µg/kg in 10% alcohol, 0.28 to 8.73 µg/kg in 50% alcohol, and 0.43 to 9.86 µg/kg in olive oil. This target approach had the advantage of simultaneously measuring the migration of multiple PFAS from food contact materials with satisfactory sensitivity, accuracy, and reliability. The test results showed that PFAS were found in coated paper and board at mg/kg levels, suggesting that further investigation is needed for the migration of PFAS from coated paper and board.

Funding

The authors acknowledge funds given by national quality infrastructure program (No. 2016YFF0203705), and the General Administration of Quality Supervision Inspection and Quarantine Science-Technology Programs (Grant 2014IK078, Grant 2015IK049). The authors have declared no conflict of interest.

References

(1) F. Kissa, *Fluorinated Surfactants and Repellents* (Marcel Dekker Inc., New York, 2nd ed., 2001).

(2) M.P. Krafft and J.G. Riess, *Chemosphere* **129,** 4–19 (2015).

(3) M.M. Schultz, D.F. Barovsky, and J.A. *Environ. Eng. Sci.* **20,** 487–501 (2003).

(4) R. Renner, *Environ. Sci. Technol.* **35,** 154A–160A (2001).

(5) J. Jeon K. Kannan, H.K. Lim, H.B. Moon, and S.D. Kin, *Environ Toxicol.* **29,** 2529–2535 (2010).

(6) T.H. Begley, K. White, P. Honigfort, M.L. Twaroski, R. Neches, and R.A. Walker, *Food Addit. Contam.* **22**(10), 1023–1031 (2005).

(7) DuPont. Information on PFOA.2008. http://repanet.de/PFOA2/en_US/index.html. April 07. 2008.

(8) L.S. Haug, C. Thomsen, and G. Bechert, *Environ. Sc. Technol.* **43,** 2131–2136 (2009).

(9) X. Trier, K. Granby, and J.H. Christensen, *Environ. Sci. Pollut. Res.* **118,** 108–1120 (2011).

(10) M/P. Martinez-Moral and M.T. Tena, *Talanta* **101,** 104–109 (2012).

(11) E. Zafeiraki, D. Costopoulou, I. Vassiliadou, E. Bakeas, and L. Leondiadis, *Chemosphere* **4,** 169–176 (2014).

(12) G.W. Olsen, K.J.Hansen, L.A. Stevenson, J.M. Burris, and J.H. Mandel, *Environ. Sci. Technol.* **37**(5), 888–891 (2003).

(13) K. Inoue, F. Okada, R. S. Kato, S. Sasaki, S. Nakajima, A. Uno, Y. Saijo, F. Sata, Y. Yoshimura, R. Kishi, and H. Nakazawa, *Environ. Health Perspect.* **112**(11), 1204–1207 (2004).

(14) G.W. Olsen, H-Y Huang, K.J. Helzlsouer, K.J. Hansen, J.L. Butenhoff, and J.H. Mandel, *Environ. Health Perspect.* **113**(5), 539–545 (2005).

(15) M.K. So, N. Yamashita, S. Taniyasu, Q. Jiang, J.P. Giesy, K. Chen, and P.K.S. Lam, *Environ. Sci. Technol.* **40**(9): 2924–2929 (2006).

(16) L. Liu, J. She, X. Zhang, J. Zhang, M. Tian, Q. Huang, S.A. Musstjab, A.S. Eqani, and H. Shen, *J. Sep. Sci.* **38,** 247–253 (2015).

(17) T. Zhang, H.W. Sun, Q. Wu, X.Z. Zhang, S.H. Yun, and K. Kannan, *Environ. Sci. Technol.* **44(**9), 3572–3579 (2010).

(18) C. Lau, J.R. Thibodeaux, R.G. Hanson, M.G. Narotsky, J.M. Rogers, A.B. Lindstrom, and M.J. Strynar, *Toxicol. Sci.* **90**(2), 510–518 (2006).

(19) N. Johansson, P. Eriksson, and H. Viberg, *Toxicol. Sci.* **108,** 412–418 (2009).

(20) Y. Lin and J. Li, *Environ. Chem.* **34,** 649–655 (2015).

(21) EFSA (European Food Safety Authority), *EFSA Journal* **653,** 1–131 (2008).

(22) EPA, *Health Effects Support Document for Perfluorooctanoic Acid (PFOA),* U.S. Environmental Protection Agency EPA822R16003. https://www.epa.gov/sites/production/files/201605/documents/pfoa_hesd_final-plain.pdf. (May, 2016; accessed July 6, 2017).

(23) EPA, *Health Effects Support Document for Perfluorooctane Sulfate (PFOS),* U.S. Environmental Protection Agency EPA822R16002. https://www.epa.gov/sites/production/files/201605/documents/pfos_hesd_final_508.pdf. (May, 2016; accessed July 6, 2017).

(24) I. Zabaleta, E. Bizkarguenaga, and D. Bilbao, *Talanta* **152,** 353–363 (2016).

(25) M.J.A. Dinglasan, Y. Ye , E.A. Edwards, and S.A. Mabury, *Environ. Sci Technol.* **38**(10), 2857–2864 (2004).

(26) FDA, *Indirect Food Additives, Paper and Paperboard Components,* https://www.federalregister.gov/articles/2016/01/04/2015-33026/indirect-food-additives-paper-and-paperboard-components (2016).

(27) GB 9685-2016, *Standard for the Use of Additives in Food Contact Materials and Articles,* http://www.nhfpc.gov.cn/sps/s7891/201611/06ed87a09dad4cf6aee48cd89efbef35.shtml (2016).

(28) ECHA, *Background Document to the Opinion on the Annex XV Dossier Proposing Restrictions on Perfluorooctanoic Acid (PFOA), PFOA Salts and PFOA-related Substances,* ECHA/RAC/RES-O-0000006229-7002/F, ECHA/SEAC/RES-O-0000006229-70-03/F (2015).

(29) *Commission Regulation (EU) No. 10/2011 of 14 January 2011 on Plastic Materials and Articles Intended to Come into Contact with Food,* https://www.fsai.ie/uploadedFiles/Reg10_2011.pdf (2011).

(30) W.M. Henderson, E.J. Weber, S.E. Duirk, J.W. Washington, and M.A. Smith, *J. Chromatogr B* **846,** 155–161 (2007).

(31) M. Stadalius, P. Connolly, K.L. Empereur, J.M. Flaherty, T. Isemura, M.A. Kaiser, W. Knaup, And M. Noguchi,*J. Chromatogr. A* **1123,** 10–14 (2006).

(32) F. Gosetti, U. Chiuminatto, D. Zampieri, E. Mazzucco, E. Robotti, G. Calabrese, M.C. Gennaro, and E. Marengo, *J. Chromatogr. A* **1217,** 7864–7872 (2010).

(33) A.S. Lloyd, V.A. Bailey, S.J. Hird, A. Routledge, and D.B. Clarke, *Rapid Commun. Mass Spectrom.* **23,** 2923–2938 (2009).

(34) S. Poothong, S.K. Boontanona, and N. Boontanon, *Hazard Mater.* **205–206,** 139–143 (2012).

(35) B.M. Surma , W. Wiczkowski, H. Zieliński, and E. Cieślik, *Packag. Technol. Sci.* **28,** 789–799 (2015).

Dan Li, Zi-hao Zhang Huai-ning Zhong, Jing-jing Pan, Jian-guo Zheng and Hui Liu are with the Guangdong Inspection and Quarantine Technology Centre and the Guangdong Provincial Key Laboratory of Import and Export Technical Measures of Animal, Plant and Food, in Guangzhou, China. Lei Zhu is with the China National Center for Food Safety Risk Assessment, in Beijing, China. Qin-bao Lin is with the Department of Food Science and Engineering at Jinan University, in Guangzhou, China. Direct correspondence to: zhulei@cfsa.net.cn or marco_zhong@iqtc.cn

A Q&A

Preparing for Those Nasty Samples: Solid Phase Extraction with Challenging Matrices

Andrew Taylor
Applications Chemist
Biotage

The catch-all solution for solid-phase extraction with challenging matrices

Solid-phase extraction (SPE) is a powerful sample preparation technique capable of extracting and pre-concentrating hundreds of semivolatile organic compounds, even in the most challenging matrices. And as any analytical scientist knows, some matrices are challenging, indeed.

That's why proper disk choice is so critical to recouping valuable results from an extraction. The right SPE disk needs the chemical and physical capacity to handle the sample matrix—whether it's high in suspended solids, particulates, or…restaurant grease. After all, no one wants to risk losing a sample—let alone accurate quantitative results—just because a disk clogged during the extraction.

LCGC recently sat down with Andrew Taylor, applications chemist at Biotage, to hear his tips on how to customize your extraction to process even the nastiest sample matrices and ensure success every time.

LCGC: Can you give some examples of challenging sample matrices?

Taylor: Some of the more challenging sample matrices that I encounter are around the Environmental Protection Agency (EPA) Methods for wastewater such as: 608, 625, and 1664. These samples can include high total suspended-solid influence from a wastewater treatment plant, particulate-laden industrial wastewater samples, and even restaurant grease trap samples. In one instance, we actually analyzed a food sample; it was a commercially available can of olives and we were looking for the oil and grease content in the olive brine. It was particularly challenging because, not only did the sample have particulates, but it also had a high salt content and a lot of organic matter.

LCGC: Why do these samples have to be filtered before they can be extracted?

Taylor: There are a few different reasons why you need to filter a sample before SPE can take place. The first is to ensure that the entire sample can be processed through the disk. Many EPA methods require that a full one-liter sample be extracted. If you're dealing with samples that have high total suspended-solids content, it's important that pre-filters be used to ensure that this whole sample can be processed through.

The second major reason is regarding the capacity of the disk. The SPE disks that are used for EPA Methods 608 and 625 are 47 mm in diameter, which allows for faster flow rates. But without proper pre-filtration, the active sites of the solid-phase media can actually become physically blocked by particulates, which can adversely affect the ability of the disk to capture the analytes.

SPONSORED BY

Biotage

LC GC north america

LCGC: When preparing a disk for extraction, what are some things you should consider?

Taylor: When you're preparing a disk for SPE, you really need to examine the sample matrix first. The first thing you look for is clarity. A transparent sample makes life a lot easier. You can visibly see particulates in the sample, if there are any. And if there aren't, you may not even need pre-filtration.

In contrast, if you have a completely opaque sample, you will need a fair amount of pre-filters built in to ensure the sample can process through.

LCGC: Can you process samples that contain obvious particles such as pebbles, leaves, or sticks?

Taylor: Absolutely. Those types of particulates are actually easier to capture than some of the finer particulates. In that case, you can just place a fine mesh screen on top of your pre-filter stack and that will capture the larger sticks, leaves, and pebbles. These things are more commonly observed in groundwater samples, but the principle still is the same.

LCGC: Can you use glass wool as a pre-filter?

Taylor: Glass wool is an incredibly useful pre-filter when you're dealing with particulate-laden samples. When you're assembling a disk holder for really dirty samples, you want to start with a 1-µm pre-filter and stack a 5-µm pre-filter on top. Then, glass wool can be placed on top of the pre-filters themselves. When you use the glass wool, it's good practice to pull it apart to ensure that the fibers are going in all different directions. This allows the filtration to be more effective.

A fine-mesh screen can be placed on top of the glass wool to compress it down to ensure you get consistent flow through the whole area and catch large particulates with that, as well. And if it's absolutely necessary, a filter aid such as diatomaceous earth can even be placed on top of this. This layering technique allows for the analysis of those really tough samples.

LCGC: What happens if your disk clogs partway through an extraction?

Taylor: This is a really interesting scenario. If proper pre-filtration is not used and the disk clogs or becomes too dirty for the sample to flow through, you can do a few different things.

The first scenario is only applicable if you have multiples of a sample. In that case, you can completely abandon that sample, select another replicate of that sample, dilute it to reduce the concentration of the matrix components, and try the extraction again. If you do this, it's vital to multiply the final calculated concentration by your dilution factor.

In most cases, though, this isn't applicable because the customer gives you only one sample. This creates a challenging problem. The first thing I would do is stop the flow through the disk of that clogged filter. Then, I would set up another disk holder on another station and pack it with the proper amount of pre-filter material, and I would extract the remaining sample on another station. When you do this, you need to combine both the extracts that you get at the end to make sure that all the extracted material is accounted for.

LCGC: How do you know how many pre-filters to use?

Taylor: That's a great question. The number of pre-filters to use can only be determined by trial and error. I always like to err on the side of caution the first few times I'm running a dirty sample. It's better to have too many pre-filters than not enough, and you can always back off on the amount later.

Once the extraction is complete, I lay out all the components that were used in the filtration process. I put a paper towel in the hood and I take the pre-filters out layer by layer. This allows you to visibly see which pre-filters are dirty and which ones are clean, which tells you exactly which ones are useful in the filtration process. This gives you a better idea of how you should configure the pre-filter stack next time a sample like this needs to be analyzed.

LCGC: Should you use a 47-mm disk or a 90-mm disk for extracting very challenging samples?

Taylor: When following EPA Method 1664, you always want to use a 90-mm SPE disk if you're analyzing dirty samples. The larger surface area of this disk provides higher flow rates, and it's also more difficult to clog.

The same principle applies for Methods 625 and 608, however, a 47 mm disk is used instead of a 90 mm disk. For these applications, a fast flow disk holder can be used to tackle really challenging sample matrices. This disk holder allows a 47 mm SPE disk to be used, however, it allows for high-surface-area, 90-mm pre-filters to be stacked on top of the 47-mm disk, while leaving plenty of room for things like glass-wool filter aids. This disk holder is the key to being able to process through those dirty samples.

LCGC: How do you complete your extraction if you form an emulsion?

Taylor: In SPE, it is rare to have an emulsion, but in the few instances when you do, the best thing to do is to use a phase-separation membrane to physically separate out the emulsion.

LCGC: What should you do if your sample is oily or soapy?

Taylor: If your sample has a visible layer of oil, or if it has something resembling a surfactant in it, the best thing to do is stack several pre-filters on top of your SPE disk and add a layer of diatomaceous earth. That diatomaceous earth will most likely catch whatever oil and soap you're looking at, and you'll be able to process through the rest of the sample.

Chromatography Fundamentals, Part VII: Influence of Peak Broadening on Detection Sensitivity, Solute Dilution, and Efficiency of Coupled Columns

In this contribution, we examine the degree to which injected samples become diluted during chromatographic elution, reducing detection sensitivity. Equations are also introduced for estimating the plate count of column sets that comprise different column lengths and efficiencies.

Howard G. Barth

The purpose of this tutorial is to present equations for estimating the extent of broadening that a solute undergoes as it migrates through a chromatographic column in high performance liquid chromatography (HPLC). These relationships can then be used for predicting the degree of solute dilution that in turn will influence detection sensitivity, as well as the effectiveness of semipreparative HPLC. Furthermore, equations are derived for estimating the number of theoretical plates generated when joining columns of different efficiencies and lengths.

Background

Peak broadening is a complex process involving the resistance of mass transfer and molecular diffusion of solutes, coupled with hydrodynamic-flow properties of the mobile phase as it permeates through the packed bed. As a result of these mechanisms, solutes emerge from the column as broadened peaks that take the form of a Gaussian distribution (1,2).

Chromatographic peaks are characterized by a mean and standard deviation, σ, better known as the peak-maximum retention time, t_r, and peak width, w, such that $w = 4\sigma$. Although 4σ includes only 95.6% of the peak area, it is, nevertheless, a good approximation, considering that chromatographic peaks are usually slightly tailed or asymmetric.

The number of theoretical plates, N, is the figure of merit that defines column efficiency as

$$N = t_r^2/\sigma^2 = 16\, t_r^2/w^2 \qquad [1a]$$

where t_r is the retention time of a test solute; typically, but not necessarily, an unretained solute. Since retained components include additional peak broadening caused by the stationary phase, plate count measured in this manner is significantly lower than with an unrestrained solute. Because the units of retention time and peak width are the same, N is a dimensionless property of a column measured at specific conditions. Please note that the accepted definition of theoretical plates is now equation 1b, where $w_{0.5}$ is peak width at half height.

$$N = 5.54\,(t_r^2/w_{0.5}) \qquad [1b]$$

To a first approximation, the number of theoretical plates generated by a column is defined by the column packing, most notably particle size, shape, and particle-size distribution. This value, however, can be increased to some extent by decreasing the flow rate, reducing injection volume, or increasing column temperature.

The impact that peak broadening has on separations cannot be overstated. To fully appreciate its importance, it is instructive to compare hypothetical chromatograms with and without broadening. In the absence of peak dispersion, components would be eluted as razor-sharp, rectangular-shaped peaks, each with a peak volume corresponding to the injection volume. Thus, a 5-µL injection at a flow rate of 0.5 mL/min would produce geometrically shaped peaks with 0.15-s peak widths. Under these conditions, a peak that is retained for 10 min, for example, would generate roughly 1.6 x 10^7 plates, as compared to about 10^4 plates with normal broadening with a high-efficiency column. With these extraordinarily high numbers of theoretical plates, it would be feasible to separate compounds based on subtle chemical or structural differences.

Influence of Peak Broadening on Solute Concentration

The Gaussian distribution function,

$$f(x) = (1/\sigma\sqrt{2\pi})\exp[-(x-\mu)^2/2\sigma^2] \qquad [2]$$

forms the basis of chromatographic theory (1,2), where the pre-exponential term, $(1/(\sigma\sqrt{2\pi})$, is a normalization factor that ensures that all peaks have an area of unity. The first moment of the distribution, μ, is the peak-maximum retention time of a Gaussian-shaped peak, and x is the retention time with a corresponding peak height, $f(x) = y$. As peaks broaden, $f(x)$ or peak height decreases at each elution-volume increment along the peak.

With the use of equation 2, we can derive the following relationship:

$$\frac{c_{max}}{c_0} = \frac{V_{inj}\sqrt{N}}{V_r\sqrt{2\pi}} \qquad [3]$$

Here, c_{max}/c_0 is the ratio of the solute concentration at peak maximum, c_{max}, relative to the initial injected concentration, c_0, V_{inj} is the injection volume, and V_r is the retention volume. The ratio, c_{max}/c_0, is also equal to the dilution factor of an eluting solute.

TABLE I: Influence of theoretical plates, *N*, and injection volume, V_{inj}, on solute dilution ratio[a] or percent solute dilution[b], using equation 1, where V_r = 4 mL.

Column	Solute Dilution Ratio (Percent Solute Dilution)				
	N	V_{inj} = 5 µL	V_{inj} = 10 µL	V_{inj} = 20 µL	V_{inj} = 40 µL
1	1,000	0.016[a] (98%)[b]	0.032[a] (97%)[b]	0.064[a] (94%)[b]	0.13[a] (87%)[b]
2	5,000	0.035 (96%)	0.070 (93%)	0.14 (86%)	0.28 (72%)
3	10,000	0.050 (95%)	0.10 (90%)	0.20 (80%)	0.40 (60%)
4	20,000	0.071(93%)	0.14 (86%)	0.28 (72%)	0.56 (44%)
5	30,000	0.087 (91%)	0.17 (83%)	0.34 (66%)	0.68 (32%)

[a] c_{max}/c_0
[b] Percent sample dilution is defined as 100 x (1 − c_{max}/c_0).

TABLE II: The influence of column length, *L*, and elution volume, V_r, on detection sensitivity[a] of a hypothetical solute, assuming V_{inj} = 5 µL, 1 mL/min flow rate, and 4.6-mm i.d. columns (see equation 3).

Column	L (mm)	Vr (mL)	*Theoretical Plates (N)*	*Theoretical Plates/250 mm*	*Injection Volume (µL)*	*Rel. Detection Sensitivity at Peak Max (%[a])*
1	250	4	20,000	20,000	5	7
2	100	1.6	20,000	50,000	5	18
3	50	0.8	20,000	100,000	5	35

[a] (c_{max}/c_0) x 100 is the ratio of the detector response at peak maximum relative to the detector response of the solution before injection, that is, with no peak broadening. This ratio is also equivalent to solute concentration at peak maximum to solute concentration before injection.

Equation 3 is useful for monitoring the extent of solute dilution, especially for semipreparative fractionation; if collected fractions are too dilute, a concentration step may be required before proceeding to the next step. This equation tells us that solute dilution is proportional to retention. In other words, the greater the peak broadening, the more dilute the solute becomes, as would be expected.

Example calculations are given in Table I, which shows the effects of column efficiency and injection volume on sample dilution. Plates per column range from 1000 to 30,000, with injection volume ranging from 5 to 40 µL; these data do not take into account efficiency loss with increasing injection volume, which would further increase sample dilution.

It is interesting to note the high degree of solute dilution that occurs even when injecting a small volume with respect to the elution volume of the solute. With a low-efficiency of 1000 plates, an injection of 5 µL would result in 98% dilution; at these same experimental conditions, a high-efficiency 30,000-plate column would dilute the solute by 91%. However, with increased injection volume, and by keeping elution volume constant, solute dilution decreases. For example, a 40-µL injection using a 1000-plate column, would result in 87% dilution, as compared to 32% for the 30,000-plate column. (For semipreparative separations, the injection volume should be as large as possible.)

Equation 3 is applicable only for isocratic elution; with gradients, peaks can be compressed, depending upon the gradient program, and analytes are eluted in a more concentrated form.

Effect of Peak Broadening on Detection Sensitivity

Equation 3 can also be used for predicting *relative detection sensitivity*, an important HPLC parameter, which is defined as the slope of detector response of a solute versus injection concentration, a value used for calculating detection limits. As discussed in the previous section, peak broadening has a pronounced effect on detection limits, influencing both accuracy and reproducibility. Thus, another consequence of peak broadening is decreased peak height at peak maximum, characterized by the ratio c_{max}/c_0.

In Table II, we define detection sensitivity as the relative percentage of detector response: (c_{max}/c_0) x 100. This value is calculated for three hypothetical columns that have the same plate number (20,000), but different lengths: 250, 100, and 50-mm, packed with decreasing particle size. The injection volume is kept constant at 5 µL. As shown in Table II and in equation 3, the elution volume of a given solute decreases with decreasing column length, and the relative detection sensitivity increases with decreasing column length. For example, the detection sensitivity of a 250-mm column is only 7%, but increases to 35% for a 50-mm column of corresponding efficiency. The reason for this trend is that c_{max}/c_0 scales with V_{inj}/V_r at constant plate count. From a practical consideration, a relative detection sensitivity of about 10% should be adequate for most applications, except for trace analysis, where a higher ratio would be required to overcome baseline noise.

Keeping the same LC conditions and column dimensions, we can also estimate the required number of theoretical plates, N_2, to obtain a given, relative detector response $(c_{max})_2$, using the following ratio:

$$\frac{(c_{max})_2}{(c_{max})_1} = \frac{\sqrt{N_2}}{\sqrt{N_1}} \quad [4]$$

For example, increasing plates from 2000 to 10,000 would more than double detector response for a given method.

Equation 3 can be rearranged to estimate the injection volume V_{inj} needed to obtain a given c_{max}/c_0 ratio, for a solute with retention volume V_r and number of plates,

TABLE III: The influence of theoretical plates on peak broadening and relative detector response. Injection volume is 10 µL; retention volume is 4 mL (see equations 6 and 10).

Column	Theoretical Plates (N^a)	Peak Width (μL^b)	Relative Detection Sensitivity (%^{c})
1	400	800	2%
2	1.6×10^3	400	4%
3	6.4×10^3	200	8%
4	1×10^4	160	10%
5	4×10^4	80	20%
6	16×10^4	40	40%
7	1×10^6	16	100%

a. See equation 3.
b. $w = 4\sigma_v$; see equation 7.
c. $c_{max}/c_0 \times 100\%$; see equations 3 and 7

$$V_{inj} = (c_{max}/c_0)(V_r\sqrt{2\pi}/\sqrt{N}) \quad [5]$$

For example, an injection volume of 50 µL would be needed to obtain a relative detection sensitivity of 0.5 using a 10,000-plate column for a solute with a 4-mL retention volume. For a 12-mL retention-volume peak, a 150 µL injection would be required to obtain a comparable detector response.

An interesting relationship is obtained by expressing equation 3 in terms of the peak standard deviation, σ_v, by substituting

$$N = (V_r/\sigma_v)^2 \quad [6]$$

into equation 3, and canceling out retention volume to give

$$\frac{c_{max}}{c_0} = \frac{V_{inj}}{\sigma_v\sqrt{2\pi}} \quad [7]$$

Although equations 3 and 7 are equivalent, we can obtain insight into the separation process by examining results from both. Such an application is given in Table III, which shows the influence of theoretical plates on peak width ($w = 4\sigma_v$), and relative detector response of a 10-µL injection with a 4-mL peak retention volume. With a conventional, low-efficiency column of 400 plates (column 1), there would be considerable peak broadening: The initial 10-µL injected volume would spread by a factor of 80x to about 800 µL, with a relative detection sensitivity of only 2%. Detection limit can be improved by a factor of five-fold with a 10,000-plate column (column 4). To achieve a peak width of only 16 µL, we would have to generate close to one million plates (column 7). With modern HPLC columns, we typically can keep the relative detection sensitivity to about 8–20%.

Coupling Columns

A practical approach for increasing plate counts is to simply couple together columns of the same packing that have equivalent lengths and theoretical plates. The total plate count of a multiple-column set consisting of columns that have the same length is simply the sum of the theoretical plates of the individual columns,

$$N_t = \sum_{i=1}^{n} N_i \quad [8]$$

The number of theoretical plates can correspond to either an unretained or retained compound, depending on the situation, but it must be either one or the other. The reason why we add theoretical plates, rather than variances (2), is that variance and plate counts are interrelated through $\sigma^2 = t_r^2/N$.

Difficulty arises when coupling columns of different lengths or plate counts, in which case equation 8 is no longer valid. When a solute leaves a highly efficient column (column 1) and enters a second column (column 2) of lower efficiency, the peak will broaden to a greater extent. Conversely, if column 2 has higher efficiency than column 1 (such as when adding a precolumn to a column), the peak cannot reverse course, but would continue to broaden. In other words, once a peak broadens, it cannot be reversed or remedied by entering a column of higher efficiency. (We can, however, concentrate the solute onto the head of a second column by decreasing eluent strength, but this involves employing a different strategy not considered in this paper.)

For a single column, the number of theoretical plates, using either an unretained or retained component with units of time, is calculated with

$$N = t^2/\sigma_t^2 \quad [9]$$

where t is elution time, and σ_t^2 is the peak variance of the corresponding peak in units of time. For column sets comprising columns with different lengths or efficiencies, the total plate count of either an unretained or retained peak is

$$N_{total} = (t_1 + t_2)^2/(\sigma_{t,1}^2 + \sigma_{t,2}^2) = (t_1 + t_2)^2/(t_1^2/N_1 + t_2^2/N_2) \quad [10]$$

where subscripts 1 and 2 refer to the two columns. The general equation for calculating the total plate count of an unretained or retained peak of a bank of n columns is therefore

$$N_t = [\sum_{i=1}^{n} t_i]^2/\sum_{i=1}^{n}(t_i^2/N_i) \quad [11]$$

Likewise, for a single column, the number of theoretical plates of an unretained component using column length as the unit of measure is

$$N = L^2/\sigma_L^2 \quad [12]$$

where L is column length and σ_L^2 is the peak variance of an unretained peak in units of length. For a coupled column comprising two columns, the total plate count of an unretained peak is

$$N_{total} = (L_1 + L_2)^2/(\sigma_{L,1}^2 + \sigma_{L,2}^2) = (L_1 + L_2)^2/(L_1^2/N_1 + L_2^2/N_2) \quad [13]$$

where subscripts 1 and 2 refer to the two separate columns. The general equation for calculating the total

(Continued on page 489)

Under Pressure to Perform: Impact of UHPLC Technology on Pharmaceutical Research and Development

An informal survey of industrial chromatographers reveals some insights into the different ways that ultrahigh-pressure liquid chromatography (UHPLC) technology has had an impact on modern pharmaceutical research and development.

Christopher J. Welch

I recently spoke at the James L. Waters Symposium on Ultrahigh-Pressure Liquid Chromatography (UHPLC) at Pittcon 2019 in Philadelphia, Pennsylvania, where I had the honor of sharing the stage with Jim Jorgenson, Pete Carr, Ed Bouvier, and Bill Barber, key figures in the origin of UHPLC (1,2) (Figure 1). The James L. Waters symposium has become an important part of the annual Pittcon meeting and provides a window on the creation and evolution of a significant new analytical technology. Privately endowed by Jim Waters and now in its 30th year, this year's James L. Waters Symposium was organized and chaired by Steve Weber, who explained to me that my role was to describe the many ways in which UHPLC technology has transformed pharmaceutical research. While I had some personal opinions, the scope of the assignment led me to choose a survey approach, in which I discussed the matter with colleagues, then compiled the results into a short presentation. I received several requests to share this information, so I have reprised some of the content here for this article.

I recently retired from industry, and now, in the post-retirement phase of my career, I am leading the Indiana Consortium for Analytical Science and Engineering (ICASE), a joint venture between Purdue, Notre Dame, and Indiana University, focusing on research collaborations in measurement science and instrumentation. My work with ICASE often brings me into contact with industrial scientists, so I began the project by surveying friends, associates, and contacts in the pharmaceutical industry for testimonials and examples of how UHPLC technology has transformed research in their areas.

I soon learned that the "UHPLC advantage" means different things to different people. I spoke with chromatographers interested in analytical release testing, high throughput screening, drug metabolism, bioanalysis, drug discovery, formulation studies, and preparative separations. Researchers in drug discovery and early development often focused on speed advantages, while researchers from late-stage development, commercialization, and manufacturing often touted performance advantages relating to quality. There are many types of chromatographers in industry, some with formal training in the subject who know the equations and the theoretical underpinnings, and others who have learned on the job, developing a fine-tuned chromatographic sensibility derived from decades of practical experience. I set out to survey both extremes as well as those in the middle. Attribution is provided whenever possible, although a number of informants preferred to remain anonymous.

UHPLC Means Faster Separations

Naijun Wu, a well-known chromatographer from Celgene, provided an overview of UHPLC's impact on pharma, noting that in the drug discovery sector, fast "universal" sub-minute UHPLC methods for routine samples have now replaced the 5 to 10 min HPLC methods that were previously used. This increase in speed allows for faster decision making and overall shorter experimental cycle times.

Comparable speed advantages have profoundly changed the field of high throughput synthesis (where different catalysts and reaction conditions are rapidly screened) and in drug metabolism and pharmacokinetics studies (where thousands of plasma or urine samples are often analyzed). UHPLC speed advantages have also revolutionized in-process control (IPC) analysis, where 50 min end-of-reaction HPLC assays have been replaced by <5 min UHPLC methods. This faster turnaround allows for denser monitoring of reaction progress, and the ability to quickly intervene and adjust reaction conditions when necessary.

UHPLC has also allowed automated multicolumn screening for method development (such as six columns × three pH levels × two mobile phases) to evolve from an overnight or even multiday task in the era of HPLC to a job that can be accomplished in a single morning using UHPLC (3). The pace of research is greatly increased when method development can be performed within a single day, as opposed to waiting for several days.

The impact on the pharmaceutical commercialization and manufacturing sector has also been profound, with batch release (the task of ensuring quality of newly prepared batches of active pharmaceutical ingredients [APIs]) shrinking from two workday shifts in the HPLC era to a couple of hours with UHPLC. Naijun noted that this batch release constitutes more than a dozen chromatographic runs, for example, two blanks, eight system suitability samples, two reference standards, and three batch samples, analyzed in duplicate.

Several chromatographers from major pharmaceutical companies observed that it is important to place the UHPLC speed advantage in the proper context, noting that, in the days before the introduction of UHPLC, many separations in pharma were

FIGURE 1: Speakers and organizers from the James A. Waters Symposium on ultrahigh-performance liquid chromatography (UHPLC) at Pittcon 2019, l to r, Stephen Weber, Peter Carr, James Jorgenson, Christopher Welch, Ed Bouvier, William Barber. Used with permission: Photo Copyright Notice: 2019 Roy Engelbrecht – royephoto.com

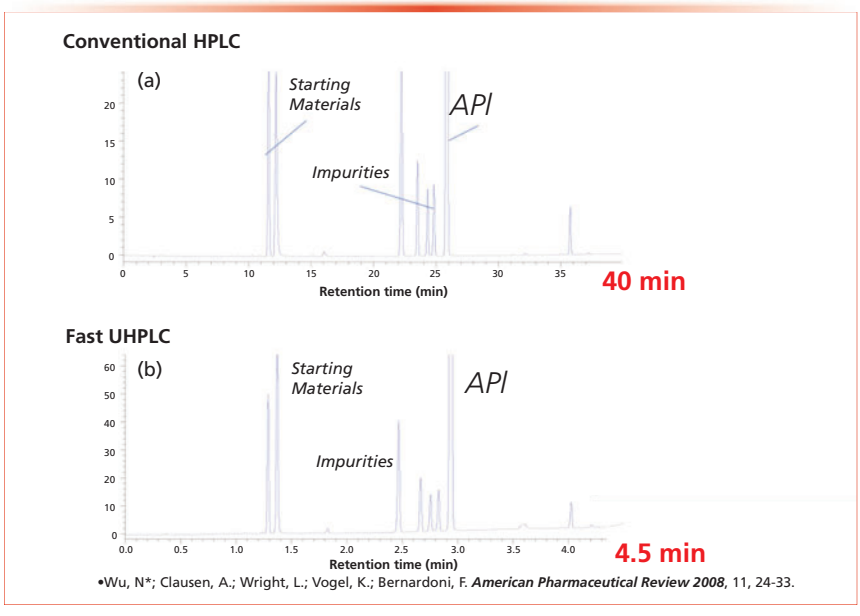

•Wu, N*; Clausen, A.; Wright, L.; Vogel, K.; Bernardoni, F. ***American Pharmaceutical Review 2008***, 11, 24-33.

FIGURE 2: Fast UHPLC for reaction monitoring. Representative example of the speed advantage of (a) conventional HPLC analysis relative to (b) modern UHPLC analysis with a speed advantage of nine times. Conventional HPLC conditions: column 250 mm x 4.6 mm, 5-µm symmetry C18, 210 nm detection at 5 Hz, 10 µL injection, 40 °C, Agilent 1100, 1.0 mL/min 1450 psi, 60:40 to 5:95 1% phosphoric acid–acetonitrile in 40 min, 10 min post run. UHPLC conditions: column 100 mm x 2.1 mm, 1.7-µm Acquity BEH C18, 210 nm detection at 40 Hz, 2 µL injection, 40 °C, Waters Acquity system, 0.60 mL/min, 13,000 psi, 60:40 to 5:95 0.1% phosphoric acid–acetonitrile in 4.5 min, 2 min post run.

incompletely optimized, with 45 min purity assays and 10 min reaction screening methods being regarded by researchers as normal. In those days, it was not uncommon to see 10 min chromatographic runs used for monitoring single component dissolution assays. Simply put, optimizing the speed of HPLC separations was often not emphasized, perhaps owing to a less compelling need for speed and a historical emphasis on data quality, with researchers often doubling safety margins "just to be certain." When UHPLC arrived on the scene, there were some exaggerated claims of improvement in analysis speed, resulting from the comparison of nicely optimized UHPLC separations to essentially unoptimized HPLC separations.

Nevertheless, there is an actual UHPLC speed advantage compared to HPLC that can be profound. An example is shown in Figure 2, where both the HPLC and the UHPLC chromatograms are nicely optimized, resolution is comparable for the two methods, and substantial speed advantage for the UHPLC separation is observed.

In this example, a ninefold increase in pressure (1450 psi for HPLC, 13,000 PSI for UHPLC) coincidentally affords a ninefold improvement in separation speed; however, several factors in addition to pressure and the nearly fivefold increase in linear velocity in the UHPLC method contribute to the observed speed advantage. In particular, the HPLC column is packed with 5 µm particles, whereas the UHPLC column is packed with 1.7 µm particles. Figure 3 illustrates the well-established improvements in chromatographic efficiency that are observed with columns packed with smaller particles (4). This increased efficiency generally leads to enhanced resolution, which can be traded for increased speed (5,6). In addition, the significantly lower extracolumn volume of current UHPLC instruments enables the use of smaller columns and faster gradients without a significant falloff in performance (7).

Irrespective of the various factors contributing to the UHPLC advantage, users have been quick to derive practical advantage from faster UHPLC techniques. An example of the tremendous gains in separation speed in recent years can be seen in the realm of chiral chromatography, which is primarily concerned with resolving the two peaks corresponding to the two enantiomers of a chiral substance (8). Figure 4 shows the historical evolution of the "world speed record" for resolution of the enantiomers of flurbiprofen, a representative chiral molecule. Other compounds show similar precipitous drops over time, reflecting dramatic improvements brought about by the introduction of new UHPLC and supercritical fluid chromatography (SFC) instrumentation, as well as introduction of new stationary phases containing smaller particles.

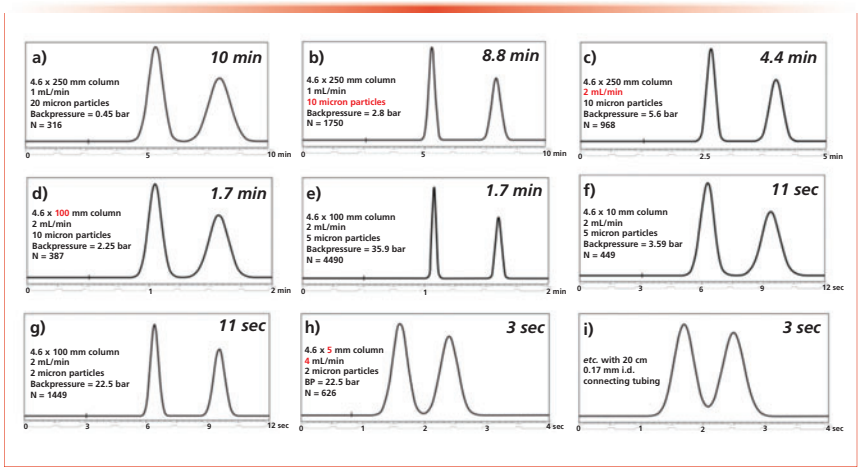

FIGURE 3: Impact of decreasing particle size on improving efficiency, resolution, and speed of chromatographic separations (4). Note chromatograms (a) through (i) with improvements in speed from 10 min to 30 s.

Greener Separations Using UHPLC

Kelly Zhang and Pete Yehl from Genentech commented on the importance of speed, but also brought up another factor that was widely reported among respondents—the green chemistry solvent savings afforded by UHPLC. The green chemistry movement in pharma seeks to reduce the use of toxic materials and the generation of waste in the discovery, development, and manufacturing of pharmaceuticals (9). While the greatest impacts are often obtained in the manufacturing realm, green chemistry is very much an endeavor where "every little bit counts," thus chromatographers have been focusing for some time on the various ways that solvent use can be minimized during pharmaceutical analysis (10). Mike Hicks from Merck reported that UHPLC counts among the greatest contributions to green analytical chemistry, and that it has revolutionized modern pharmaceutical analysis. Christine Aurigemma from Pfizer noted that the advent of UHPLC, as well as next-generation SFC systems, means that solvent consumption and waste generation have been drastically reduced while separation speed has increased tremendously.

Faster Injections Needed to Compete With MS

Xiaoyi Gong from Merck cautioned that, while the UHPLC speed advantage has revolutionized many pharmaceutical workflows, UHPLC is still too slow for addressing many of the challenges of high throughput analysis. The pace of analysis of 96 well microplates was greatly increased by the development of fast analysis techniques such as MISER (multiple injections in single experimental run) (11), and multiplexed HPLC (12) and capillary electrophoresis (CE) (13) techniques. But the challenge of same day analysis of 1536 well microplates by UHPLC requires additional innovations. Conventional UHPLC analysis of 1536 samples currently takes more than 9 h, owing to limitations in the speed of injection via the robotic autosampler (14). A recent study reported a 2.4 h "plate time" for 1536 samples using MISER UHPLC–MS, although this approach relied on an eightfold mass spectrometry (MS) multiplexing strategy, in which groups of eight wells containing mass-differentiated products were combined prior to analysis (15). In contrast, direct MS measurement of 1536 well microplates can be completed in only 8 to 10 min using droplet microfluidics-MS (16), matrix-assisted laser desorption–ionization (MALDI) (17), or desorption electrospray ionization (DESI) (18) analysis. With the next generation of UHPLC separations sometimes taking less than a second (19), new ideas and approaches for sample injection will have to be developed to maintain the competitiveness of UHPLC for high throughput analysis.

Enabling the Investigation of New Modalities

In a phone conversation, Genentech's Pete Yehl pointed out that UHPLC has greatly enabled the exploration of the new therapeutic modalities that have been a significant focus for pharma over the past decade. Newly found resolving power provided by UHPLC was immediately put to use to study problems of ever-increasing complexity including small interfering RNA and other oligonucleotides (20), proteolysis-targeting chimeras (PROTACs), antibody–drug conjugates (ADC), and peptidic macrocycles. In addition, conventional small molecule drug candidates continue to increase in complexity, especially with regard to the presence of multiple stereocenters. Analysis and characterization of this next generation of pharmaceuticals is incredibly complex, taxing conventional HPLC and even the improved resolving power of UHPLC. Increasingly, multidimensional chromatographic separation approaches with orthogonal detection techniques are used to address these thorny problems (21,22).

Increasing Focus on Instrument Utilization

Several interviewees mentioned that the initial wave of UHPLC instrument introductions created an increased focus in pharma on instrument utilization rates, with instrument companies arguing that purchases of the more expensive UHPLC instruments would be justified by increased productivity, with a single UHPLC instrument doing the work of two conventional HPLC instruments. Irrespective of the merits of this argument or the actual UHPLC for HPLC replacement metric (several sources suggest that the actual ratio was more like 1:1), this focus on instrument productivity captured the attention of corporate procurement accountants and efficiency experts, who began to be increasingly involved in coordinating instrument lifecycle management.

Instrument utilization rates in certain areas of pharmaceutical discovery and development are often quite low, owing to the dedication of individual instruments to specific tasks, either on a project-by-project basis or on the basis of function—such as method development screening, walk-up "standard gradient" systems, and high throughput analysis systems. Consequently, the UHPLC revolution did little to either reduce instrument numbers or increase utilization. Going

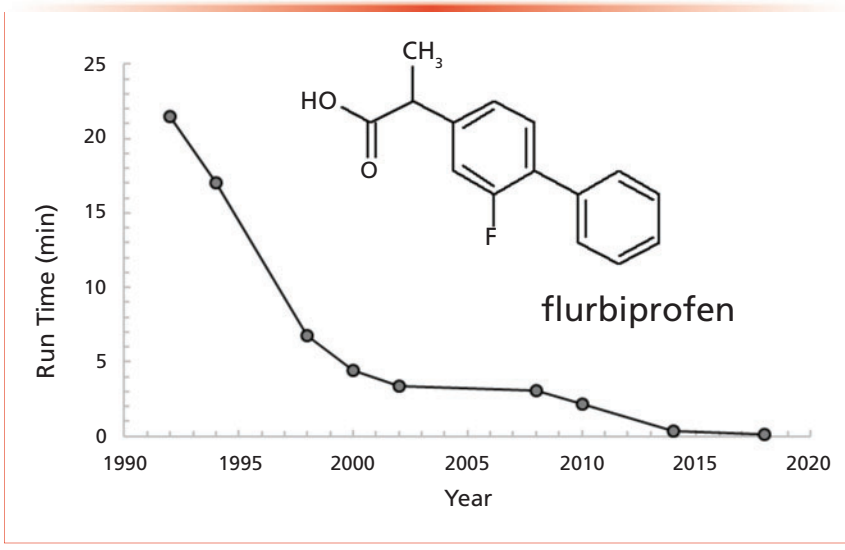

FIGURE 4: Evolution of "world speed record" for chromatographic resolution of the enantiomers of flurbiprofen over time. Advances in UHPLC and SFC instrumentation, new stationary phases, and smaller chromatographic particles have similar increases in speed for most chiral compounds. Data from ChirBase database.

forward, improved software to better facilitate automated transitions between several discreet functions within a single instrument is an area of considerable interest among pharmaceutical researchers (3). Bill Farrell from Pfizer cites the series of solvent washes required to transition an instrument from reversed-phase mode to normal-phase mode and then back again as a potentially easily automated routine task that currently requires too much user oversight and guidance.

Larry Miller from Amgen reports that instrument utilization software that is now commonplace on newer HPLC and UHPLC instruments helps him track the number of injections for each instrument, which guides instrument maintenance and replacement scheduling, and also informs decisions on how best to place open-access instruments around the laboratories to best serve users. Larry claims that this data is also helpful when justifying the purchase of new instruments.

In the End, It's All About Performance

Tim Olah from Bristol Myers Squibb summed things up nicely by noting that for many researchers in pharma, it's all about performance. The significant impact of UHPLC on research operations has often been more about resolution and specificity than about speed (although, of course, these factors are linked). Tim and his colleagues have been able to develop and implement very sensitive and specific multiple component bioanalytical methods using UHPLC and MS detection that are capable of simultaneously quantifying therapeutic agents and definitive biomarkers in small biological samples, including tissue biopsies and dried blood spots (DBS) in a way that was simply not possible before the advent of modern UHPLC technology. They and other researchers are glad that UHPLC has become an integral technology that underpins research activities across the entire spectrum of pharmaceutical discovery, development, and manufacturing.

References

(1) J.E. MacNair, K.C. Lewis, and J.W. Jorgenson, *Anal. Chem.* **69,** 983–989 (1997).

(2) J. Nawrocki, C. Dunlap, A. McCormick, and P.W. Carr, *J. Chromatogr. A* **1028,** 1–30 (2004).

(3) F.T. Mattrey, A.A. Makarov, E.L. Regalado, F. Bernardoni. M. Figus, M.B. Hicks, J. Zheng, L. Wang, W. Schafer, V. Antonucci, S.E. Hamilton, K. Zawatzky, and C.J. Welch, *TrAC* **95,** 36–46 (2017).

(4) C.J. Welch, *ACS Cent. Sci.* **3,** 823–829 (2017).

(5) C.J. Welch and E.L Regalado, *J. Sep. Sci.* **37,** 2552–2558 (2014).

(6) B. A. Rogers, Z. Wu, B. Wei, X. Zhang, X. Cao, O. Alabi, and M.J. Wirth, *Anal. Chem.* **87,** 2520–2526 (2015).

(7) N. Wu, A C. Bradley, C. J. Welch, and L. Zhang, J. *Sep. Sci.* **35,** 2018–2025 (2012).

(8) C.L. Barhate, L.A. Joyce, A.A. Makarov, K. Zawatzky, F. Bernardoni, W.A. Schafer, D.W. Armstrong, C.J. Welch, and E.L. Regalado, *Chem. Commun.* **53,** 509–512 (2017).

(9) P.T. Anastas and M.M. Kirchoff, *Acc. Chem. Res.* **35,** 686–694 (2002).

(10) C.J. Welch, N. Wu, M. Biba, R. Hartman, T. Brkovic, X. Gong, R. Helmy, W. Schafer, J. Cuff, and Z. Pirzada, *TrAC* **29,** 667–680 (2010).

(11) C.J. Welch, X. Gong, W. Schafer, E.C. Pratt, T. Brkovic, Z. Pirzada, J.F. Cuff, and B. Kosjek, *Tet. Asymm.* **21,** 1674–1681 (2010). P. Sajonz, W. Schafer, X. Gong, S. Shultz, T. Rosner, and C.J. Welch, *J. Chromatogr.* **1147,** 149–154 (2007).

(12) Y. Zhang, X. Gong, H. Zhang, R.C. Larock, and E.S. Yeung, *J. Comb. Chem.* **2,** 450–452 (2000).

(13) K. Zawatzky, C.L. Barhate, E.L. Regalado, B.F. Mann, N. Marshall, J.C. Moore, and C.J. Welch, *J. Chromatogr. A* **1499,** 211–216 (2017).

(14) A. Buitrago Santanilla, E.L. Regalado, T. Pereira, M. Shevlin, K. Bateman, L-C Campeau, J. Schneeweis, S. Berritt, Z-C Shi, P. Nantermet, Y. Liu, R. Helmy, C.J. Welch, P. Vachal, I.W. Davies, T. Cernak, and S.D. Dreher, *Science* **347,** 49–53 (2015).

(15) X. Diefenbach, I. Farasat, E. Guetschow, C.J. Welch, R. Kennedy, S. Sun, and J. Moore, *ACS Omega* **3,** 1498–1508 (2018).

(16) S. Lin, S. Dikler, W.D. Blincoe, R.D. Ferguson, R.P. Sheridan, Z. Peng, D.V. Conway, K. Zawatzky, H. Wang, T. Cernak, I.W. Davies, D.A. DiRocco, H. Sheng, C.J. Welch, and S.D. Dreher, *Science* **361,** 6236 (2018).

(17) M. Wleklinski, B.P. Loren, C.R. Ferreira, Z. Jaman, L. Avramova, T.J.P. Sobreira, D.H. Thompson, and R.G. Cooks, *Chem Sci.* **9,** 1647–1653 (2018).

(18) M.F. Wahab, R.M. Wimalasinghe, Y. Wang, C.L. Barhate, D.C. Patel, and D.W. Armstrong, *Anal. Chem.* **88,** 8821–8826 (2016).

(19) M. Biba, E. Jiang, B. Mao, D.Zewge, J.P. Foley, and C.J. Welch, *J. Chromatogr. A* **1304,** 69–77 (2013).

(20) C.J. Venkatramani,S.R. Huang, M. Al-Sayah, I. Patela, and L. Wigman, *J. Chromatogr. A* **1521,** 63–72 (2017).

(21) CL. Barhate, E.L. Regalado, J. Lee, N.D. Contrella, J. Jo, A.A. Makarov, D.W. Armstrong, and C.J. Welch, *Anal. Chem.* **89,** 3545–3553 (2017).

Christopher J. Welch
is with the Indiana Consortium for Analytical Science & Engineering, in Indianapolis, Indiana. Direct correspondence to: Chris.Welch@ICASE.center

PRODUCTS & RESOURCES

IEX column

Imtakt's Intrada organic acid ion exchange (IEX) column is designed for the analysis of organic acids. According to the company, the silica-based column does not require the use of ion-paring reagents or analyte derivatization to provide retention and separation of organic acids and can distinguish between multiple charge variants. **Imtakt USA,** Portland, OR. www.imtaktusa.com

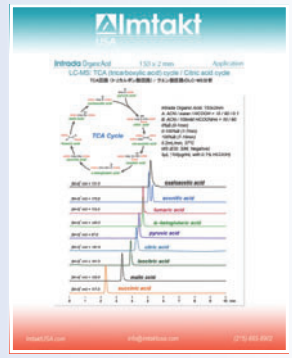

Liquid-filled permeation tube

Kin-Tek's Trace Source liquid-filled permeation tube is designed for use in Kin-Tek gas calibration systems to generate moderate-to-high concentration mixtures of low-vapor liquids or solids such as water, benzene, various sulfur compounds, and formaldehyde. According to the company, the tubes are small compared to high-pressure gas cylinders, and contain only a small amount of chemical, eliminating the possibility of acute exposure. **Kin-Tek Analytical,** Inc., La Marque, TX. www.kin-tek.com

Work assignment and resource planning module

A work assignment and resource planning module available from LabVantage is designed to let laboratory managers assign work based on technician availability, work capacity, and training status, and instrument certification status and availability. According to the company, testing master data can be configured to identify preferred laboratory instruments and users so that incoming work can be assigned and optimized. **LabVantage Solutions, Inc.,** Somerset, NJ. www.labvantage.com

Fraction collector for HPLC

Shimadzu Scientific's FRC-40 fraction collector is designed for high-performance liquid chromatography. According to the company, the collector incorporates fraction simulation to ensure pure fractions, and users can change system parameters, such as the pump flow rate and detector settings, during analysis to maximize efficiency. **Shimadzu Scientific Instruments,** Columbia, MD. www.ssi.shimadzu.com

Adsorbents

Sorbtech's high-purity adsorbents for chromatography and purification processes are designed to perform simple to complex analytical and preparative chromatographic techniques for laboratory, pilot, and industrial process applications. According to the company, a broad selection of adsorbents, including silica gel, bonded phases, alumina, polymeric resins, and size-exclusion media, allows researchers to have one source for a project and a continuous scale-up path without variability. **Sorbent Technologies, Inc.,** www.sorbtech.com

Benchtop mass spectrometer

Thermo Fisher's Orbitrap Exploris 480 mass spectrometer is designed for rigorous, high-throughput protein identification, quantification, and structural characterization of biotherapeutics and translational biomarkers within a compact, benchtop instrument. According to the company, the system allows researchers to conduct rapid, multiplexed analysis of proteins within complex biological matrices. **Thermo Fisher Scientific,** San Jose, CA. www.thermofisher.com

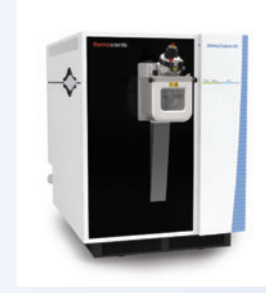

Headspace syringe

Hamilton Company's HDHT headspace syringe is designed for high-temperature applications up to 200 °C. According to the company, the syringe's high-dynamic HD plunger uses a spring in the plunger tip that compensates for the materials' different expansion coefficients. **Hamilton Company,** Reno, NV. www.hamiltoncompany.com

Flow modulator

The FLUX flow modulator from LECO is designed for routine GC×GC analysis. According to the company,the flow modulator does not require cryogens to carry out GC×GC analysis, and a simplified method development feature requires the user to manage only two parameters. **LECO Corporation,** St. Joseph, MI. www.leco.com/flux-gcxgc-flow-modulator

Multitechnique sample preparation system

Markes' Centri multitechnique system is designed for sample automation and concentration for gas chromatography–mass spectrometry. According to the company, four sampling modes are available: HiSorb high-capacity sorptive extraction; headspace, solid-phase microextraction; and thermal desorption.

Markes International, Llantrisant, UK. chem.markes.com/Centri

Laboratory water system

MilliporeSigma's redesigned Milli-Q IQ 7003/7005 Ultrapure and Pure laboratory water system is designed to provide Type 1 and Type 2 water directly from tap water. According to the company, the system's design features include system auto-rinsing prior to production; an integrated vent filter; a built-in ech2o bactericidal UVC LED lamp, and automatic recirculation of stored water through the purification loop.

MilliporeSigma, Burlington, MA. www.emdmillipore.com

Artificial body fluids

Pickering's artificial body fluids are designed to meet official product testing specifications from AATCC, ISO, DIN, BS, EN, and other worldwide standards organizations. According to the company, the artificial body fluids are suitable for product development, quality testing, and research applications.

Pickering Laboratories, Mountain View, CA. www.pickeringlabs.com

Column

Tosoh's TSKgel FcR-IIIA-NPR column is designed for the analysis of IgG glycoforms. According to the company, the stationary phase uses a recombinant human Fcγ receptor III as a ligand bound to a nonporous polymethacrylate polymer, providing an elution profile of the glycoprotein that mimics antibody-dependent cellular cytotoxicity activity, which is correlated to the composition of the N-glycans.

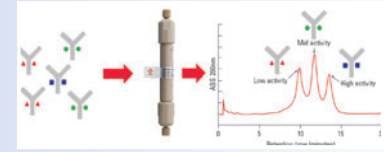

Tosoh Bioscience LLC, King of Prussia, PA. www.tosohbioscience.com

Syringes

VICI Precision Sampling Pressure-Lok analytical syringes are made with polytetrafluoroethylene (PTFE) plunger tips. According to the company, the tips are designed to remain smooth, without the seizing or residue of conventional metal plunges, and have leak-proof seals.

Valco Instruments Co., Inc., Houston, TX. www.vici.com

MALS instruments

The NEON generation of multi-angle light scattering (MALS) refractive index and intrinsic viscosity instruments are designed with updated optical, electrical, and mechanical components. According to the company, its Smart Services platform provides customer-first enhancements for ease-of-use.

Wyatt Technology, Santa Barbara, CA. www.wyatt.com/nextgen

LC accessories

Accessories from Restek are designed for use in liquid chromatography analysis. According to the company, products include bottle top inlet valves, outlet valves, couplers, fittings, unions, tees and crosses, PEEK stainless steel tubing, mobile-phase maintenance and safety products, bottle tops, valves, filters, spargers, replacement parts, and supplies.

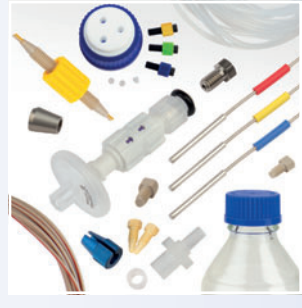

Restek Corp., Bellefonte, PA. www.restek.com

Ion chromatograph

Metrohm's Eco IC ion chromatograph is designed for the routine analysis of anions, cations, and polar substances in water. According to the company, the chromatograph includes a suppressor, a conductivity detector, and software, and allows for automatic analysis of up to 36 samples.

Metrohm USA, Riverview, FL. www.metrohmusa.com

CALENDAR

25–29 August 2019
American Chemical Society Fall 2019 National Meeting & Exposition
San Diego, CA
www.acs.org/content/acs/en/meetings/national-meeting.html

1–4 September 2019
ITP 2019: 26th International Symposium on Electroseparation and Liquid-Phase Separation Techniques
Toulouse, France
www.itp2019.com/index.php

1–5 September 2019
EuroAnalysis 2019
Istanbul, Turkey
http://euroanalysis2019.com/

4–6 September 2019
Cannabis Science Conference
Portland, OR
www.cannabisscienceconference.com

3–5 September 2019
40th British Mass Spectrometry Society Annual Meeting
Manchester, UK
www.bmss.org.uk/bmss-annual-meeting-2019

6–12 September 2019
AOAC Annual Meeting and Exposition
Denver, CO
https://www.aoac.org/

11–13 September 2019
12th Balaton Symposium on High-Performance Separation Methods
Siófok, Hungary
http://www.balaton.mett.hu/

15–18 September 2019
30th International Symposium on Pharmaceutical and Biomedical Analysis
Tel-Aviv, Israel
www.pba2019.org

15–18 September 2019
25th International Symposium on Separation Science (ISSS 2019)
Lodz, Poland
www.isss2019.p.lodz.pl

17–20 September 2019
16th Symposium on the Practical Applications of Mass Spectrometry in the Biotechnology Industry (Mass Spec 2019)
Chicago, IL
www.casss.org/page/MS1901

23–26 September 2019
23rd International REID Bioanalytical Forum
Cambridge, UK
https://chromsoc.com/event/23rd-international-reid-bioanalytical-forum/

24–26 September 2019
Analytica Latin America
São Paulo, Brazil
www.analiticanet.com.br/en

29 September–1 October 2019
SFC 2019: International Conference on Packed Column SFC
Philadelphia, PA
www.greenchemistrygroup.org/current-conference/sfc-2019

29 September–2 October 2019
Society of Forensic Toxicologies (SOFT 2019)
San Antonio, TX
http://www.soft-tox.org/

8–11 October 2019
American Council of Independent Laboratories (ACIL) 2019 Annual Meeting
Nashville, TN
https://acil.events.idloom.com/acil-annual-meeting-2019

13–18 October 2019
CE in the Biotechnology & Pharmaceutical Industries
Bethesda, MD
www.casss.org/page/CE1900

15–16 October 2019
Gulf Coast Conference
Galveston, TX
https://gulfcoastconference.com/

27-31 October 2019
Microtas 2019: The 23rd International Conference on Miniaturized Systems for Chemistry and Life Sciences
Basel, Switzerland
https://microtas2019.org/

5–8 November 2019
9th International Symposium on Recent Advances in Food Analysis
Prague, Czech Republic
www.rafa2019.eu/

18–20 November 2019
Eastern Analytical Symposium and Exhibition
Princeton, NJ
www.eas.org

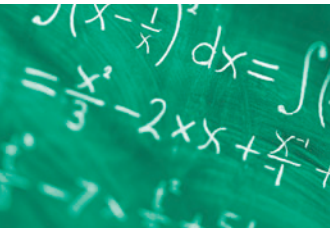

SHORT COURSES

Hyphenated

17–18 November 2019
LC–MS: Theory, Instruments, and Applications
Princeton, NJ
easinc.org/wordpress/?page_id=947

18–20 November 2019
Practical LC–MS Method Development for Small Molecules
Princeton, NJ
easinc.org/wordpress/?page_id=5953

HPLC

On Demand 2019
High Performance Liquid Chromatography Basics
proed.acs.org/content/proed/en/on-demand/high-performance-liquid-chromatography-basics.html

26–27 August 2019
Fundamentals of High Performance Liquid Chromatography
San Diego, CA
proed.acs.org/content/proed/en/in-person/fundamentals-high-performance-liquid-chromatography.html

1–4 October 2019
High Performance Liquid Chromatography: Fundamentals, Troubleshooting, and Method Development
Chicago, IL
proed.acs.org/content/proed/en/lab-component/high-performance-liquid-chromatography-fundamentals-troubleshooting-method.html

2-16 October 2019
Modern HPLC/UHPLC for Practicing Scientists 1: Fundamentals
Online Live
proed.acs.org/content/proed/en/online-live/modern-hplc-uhplc-practicing-scientists1-fundamentals.html

8 October 2019
Modern HPLC/UHPLC for Practicing Scientists 2: UHPLC, Method Development, HPLC Operation, and Troubleshooting
Online Live
proed.acs.org/content/proed/en/in-person/modern-hplc-uhplc-practicing-scientists2-method-development-biopharmaceutical-applications.html

21–23 October 2019
Solutions and Workflows in (Environmental) Molecular Screening and Analysis
Erding, Germany
www.swemsa.eu

17–18 November 2019
Fundamentals & Best Practices in Method Development and Operation/Troubleshooting
Princeton, NJ
easinc.org/wordpress/?page_id=4022

18–20 November 2019
HPLC & UHPLC for Practicing Scientists 1 and 2: Fundamentals & Best Practices in Method Development and Operation/Troubleshooting
Princeton, NJ
easinc.org/wordpress/?page_id=4022

19–20 November 2019
Systematic LC and GC Troubleshooting
Princeton, New Jersey
easinc.org/wordpress/?page_id=961

19–20 November 2019
How to Develop Validated HPLC Methods: Rational Design with Practical Statistics & Troubleshooting
Princeton, New Jersey
easinc.org/wordpress/?page_id=961

Mass Spectrometry

17–18 November 2019
Modern Mass Spectrometry: Fundamentals to Frontiers
Princeton, NJ
easinc.org/wordpress/?page_id=5953

Other

17 November 2019
High-Performance TLC, Planar Chromatography Beyond the Ordinary!
Princeton, New Jersey
easinc.org/wordpress/?page_id=5975

17–18 November 2019
Chemometrics Without Equations Parts 1 & 2
Princeton, New Jersey
easinc.orgwordpress/?page_id=1002

19–20 November
Quality-by-Design: A New Paradigm for the Analytical Laboratory Part 1 & 2
Princeton, New Jersey
easinc.org/wordpress/?page_id=967

Sample Prep

18 November 2019
Analytical Sampling and Sample Preparation for Chromatography
Princeton, NJ
easinc.org/wordpress/?page_id=5205

(Continued from page 480)

plate count of an unretained peak of a bank of *n* columns is

$$N_t = [\sum_{i=1}^{n} L_i]^2 / \sum_{i=1}^{n} (L_i^2/N_i) \quad [14]$$

The total number of theoretical plates of column sets, like those seen in equations 11 and 14, is a weighted average, not an arithmetic sum. Note that the efficiency of a bank of columns is independent of column sequence; similar results would be obtained if the column order were to be reversed. Furthermore, consider the mathematical order of the numerators in equations 11 and 14; column lengths or retention times are first added together, and then squared, while in the denominators, time or lengths are first squared, then divided by their corresponding plates, and finally added together.

A practical application of these concepts would be attaching a well-used 50-mm precolumn with 500 plates to a new 250-mm analytical column with 30,000 plates. According to equation 11, the total estimated plate count of the 300-mm column set would be about 13,000, representing a 60% efficiency loss.

Conclusions

When an injected sample undergoes peak broadening, the concentrations of eluted components are greatly reduced. Based on a Gaussian distribution model, relationships are presented that show that the degree of solute dilution is proportional to retention volume, and inversely proportional to injection volume and the square-root of column plate count. Solute dilution not only reduces the efficacy of analytical and semipreparative HPLC fractionation, but also lowers detection sensitivity.

A convenient approach for increasing column efficiency is simply to couple columns together. As a result of peak broadening, however, a weighted-average plate count, rather than an arithmetic mean, must be used to calculate the total plate count of column sets that consist of different length or efficiency columns. Calculations show that connecting a short, but low-plate, count column in series with a high-plate analytical column has a deleterious effect on the total efficiency of the column bank.

Our next contribution will discuss the impact that peak broadening has on chromatographic resolution.

Dedication

This paper is dedicated to Prof. Barry L. Karger, Director Emeritus of the Barnett Institute, and the James L. Waters Chair and Distinguished Professor Emeritus at Northeastern University, in honor of his 80th birthday.

References

(1) H.G. Barth, *LCGC North Am.* **36**(11), 830–835 (2018).

(2) H.G. Barth, *LCGC North Am.* **37**(4), 269–273 (2019).

Howard G. Barth
is with Analytical Chemistry Consultants, Ltd., in Wilmington, Delaware. Direct correspondence to: howardbarth@gmail.com

Ad Index

THE ESSENTIALS

Excerpts from *LCGC's* professional development platform, CHROMacademy.com

Electron Capture Detectors

The invention of the electron capture detector (ECD) is attributed to Lovelock in 1957 (1). The detector measures the electrical conductivity of an effluent gas stream resulting from exposure to ionizing radiation from a radionuclide.

The ECD (see Figure 1 for a schematic) is a selective detector that responds to electronegative analyte molecules capable of "capturing electrons"—more specifically, halogenated, organometallic and nitro-containing compounds. The radionuclide is ^{63}Ni and around 10 millicuries, and is typically embedded in a foil within the detector cell that emits beta particles:

$$^{63}Ni \rightarrow \beta^- \quad [1]$$

These negatively charged particles collide with make-up gas molecules and ionize them, and the subsequently produced electrons go on to ionize additional make-up gas molecules. Nitrogen is typically used as make-up gas in modern ECD detectors, due to its low ionization potential (low excitation energy).

The free electrons produced are accelerated toward a cathode within the detector, and a standing current is obtained:

$$\beta^- + N_2 \rightarrow 2e^- + N_2^+ \quad [2]$$

When an electronegative analyte is eluted, the analyte molecules capture some of the "background" electrons, and this results in a reduction of the standing (background) current:

$$A + e^- \rightarrow A^- \quad [3]$$

MORE ONLINE:

FIND THIS, AND OTHER WEBCASTS, AT
www.CHROMacademy.com/Essentials
(free until August 20).

One might wonder why the negatively charged analyte ions do not also migrate towards the cathode and maintain the same level of standing current. The answer lies in the fact that the process of neutralization of the charged analyte with nitrogen cations happens very rapidly, at a much shorter time scale than the recombination of the initially liberated electrons with nitrogen cations, and, therefore, the number of charged species reaching the anode or cathode is reduced. The size of the reduction in the standing current is proportional to the analyte concentration.

The carrier gases used for ECD operation should be pure and dry. Oxygen and water are both electronegative, and as such contribute to a noisy baseline if they are present in the carrier or makeup gases, even in trace amounts.

When optimized, the detector can achieve sensitivity in the picogram (10^{-12} g) range, but because the change in standing current is relatively low, the detector linear range is limited to around three or four orders of magnitude, depending upon the electronegativity of the analyte.

Improved performance and linearity can be obtained by operating the detector in a "pulsed" mode. A square wave pulse is applied at a frequency (typically a width of 1 ms at intervals of 20–50 µs) that maintains a constant current in the detector cell; to maintain the current in the presence of an analyte, the pulse frequency has to be increased. The signal is generated in proportion to the frequency of the applied pulse.

The cleanliness of the detector needs to be maintained at all times, which often means care with sample preparation. Chromatographic peaks

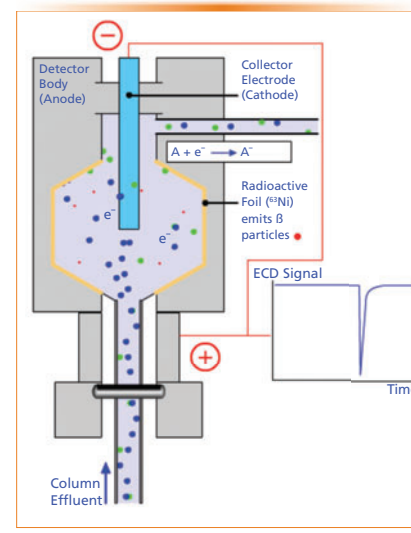

FIGURE 1: Schematic of a typical ECD detector. Red species are β particles; green species are nitrogen make-up gas molecules; blue species are analyte molecules.

obtained from a dirty ECD detector show a distinctive negative dip at the start or end of the peak, and counter-intuitively the response of the detector can often increase as detector performance deteriorates (although signal to noise will deteriorate).

Collision or reaction cells can be added to the instrument to avoid the interference of polyatomic isobaric species with target analytes, by dissociating potentially interfering molecular species, or creating reactions products with the target analytes that have a unique mass. Ammonia is often used to generate these reaction products. Alternatively, high resolution (accurate mass) analyzers can be used in order to discriminate between target analyte elements and their nominally isobaric interferents, due to their ability to spectrometrically discriminate between very small mass differences.

References

(1) J.E. Lovelock, *J. Chromatogr.* **1,** 35 (1958).

2019 CANNABIS SCIENCE CONFERENCE

Join us!

SEPT. 4 – 6 • OREGON CONVENTION CENTER

JOIN US at the World's Largest and Most Technical Scientific Cannabis Event!

TRACKS: ANALYTICAL CANNABIS • CULTIVATION SCIENCE • MEDICAL CANNABIS • HEMP SCIENCE

Visit CannabisScienceConference.com for more information and tickets

Contact Andrea@CannabisScienceConference.com for Sponsorship Opportunities!

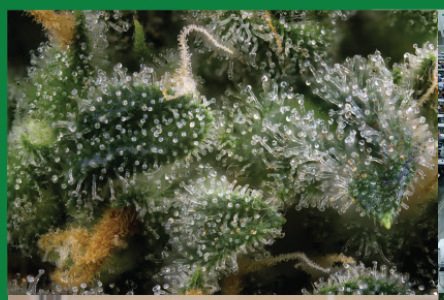

CannabisScienceConference.com

SHIMADZU
Excellence in Science

New Series of GC-MS and GC-MS/MS Instruments

Combines Exceptional Accuracy and Sensitivity with Easy Maintenance and Operation

Utilizing the most advanced gas chromatograph available, and incorporating a variety of technological advances, Shimadzu's **new NX series of single-quad and triple-quad GCMS instruments** offers the highest performance levels available. And, with outstanding functionality, a variety of Smart features, easy maintenance, and intuitive software, these systems provide more efficient workflows, greater uptime, and reduced costs for higher productivity and better ROI for any laboratory.

Learn more about Shimadzu's NX Series Mass Spectrometers
Call (800) 477-1227 or visit us online at **www.ssi.shimadzu.com**
Shimadzu Scientific Instruments Inc., 7102 Riverwood Dr., Columbia, MD 21046, USA

Buy Any Two ACE® Excel or HALO® UHPLC Columns from MAC-MOD

and Get a FitBit® Charge 3 or a $250 MAC-MOD Gift Card

The MAC-MOD gift card can be applied to any future MAC-MOD order.
Promotional offer expires September 30, 2019.

	HALO® 2.0 µm Fused-Core® UHPLC Columns									
	HILIC	Penta-HILIC	ES-CN	PFP	AQ-C18	Biphenyl	Phenyl-Hexyl	RP-Amide	C8	C18
2.1 x 250	91812-901	91812-905	91812-904	91812-909	91812-922	91812-911	91812-906	91812-907	91812-908	91812-902
2.1 x 150	91812-701	91812-705	91812-704	91812-709	91812-722	91812-711	91812-706	91812-707	91812-708	91812-702
2.1 x 100	91812-601	91812-605	91812-604	91812-609	91812-622	91812-611	91812-606	91812-607	91812-608	91812-602
2.1 x 75	91812-501	91812-505	91812-504	91812-509	91812-522	91812-511	91812-506	91812-507	91812-508	91812-502
2.1 x 50	91812-401	91812-405	91812-404	91812-409	91812-422	91812-411	91812-406	91812-407	91812-408	91812-402
2.1 x 30	91812-301	91812-305	91812-304	91812-309	91812-322	91812-311	91812-306	91812-307	91812-308	91812-302
2.1 x 20	91812-201	91812-205	91812-204	91812-209	91812-222	91812-211	91812-206	91812-207	91812-208	91812-202
3.0 x 250	91813-901	91813-905	91813-904	91813-909	91813-922	91813-911	91813-906	91813-907	91813-908	91813-902
3.0 x 150	91813-701	91813-705	91813-704	91813-709	91813-722	91813-711	91813-706	91813-707	91813-708	91813-702
3.0 x 100	91813-601	91813-605	91813-604	91813-609	91813-622	91813-611	91813-606	91813-607	91813-608	91813-602
3.0 x 75	91813-501	91813-505	91813-504	91813-509	91813-522	91813-511	91813-506	91813-507	91813-508	91813-502
3.0 x 50	91813-401	91813-405	91813-404	91813-409	91813-422	91813-411	91813-406	91813-407	91813-408	91813-402
3.0 x 30	91813-301	91813-305	91813-304	91813-309	91813-322	91813-311	91813-306	91813-307	91813-308	91813-302
3.0 x 20	91813-201	91813-205	91813-204	91813-209	91813-222	91813-211	91813-206	91813-207	91813-208	91813-202

SHOP NOW:

1 (800) 441-7508 ▪ info@mac-mod.com ▪ mac-mod.com/shop.php

For FitBit® Charge 3 Use Code: MMFitbit ▪ For MAC-MOD Gift Card Use Code: MM250GC

macmod

ACE® Excel 1.7 µm UHPLC Columns

	NH_2	HILIC-A	HILIC-B	HILIC-N	CN-ES	C18-PFP	C18-AR	C18-Amide	C18	SuperC18
2.1 x 100	EXL17141002U	HILA171002U	HILB171002U	HILN171002U	EXL17131002U	EXL17101002U	EXL1791002U	EXL17121002U	EXL1711002U	EXL17111002U
2.1 x 75	EXL17147502U	HILA177502U	HILB177502U	HILN177502U	EXL17137502U	EXL17107502U	EXL1797502U	EXL17127502U	EXL1717502U	EXL17117502U
2.1 x 50	EXL17140502U	HILA170502U	HILB170502U	HILN170502U	EXL17130502U	EXL17100502U	EXL1790503U	EXL17120502U	EXL1710502U	EXL17110502U
2.1 x 30	EXL17140302U	HILA170302U	HILB170302U	HILN170302U	EXL17130302U	EXL17100302U	EXL1790302U	EXL17120302U	EXL1710302U	EXL17110302U
2.1 x 20	EXL17140202U	HILA170202U	HILB170202U	HILN170202U	EXL17130202U	EXL17100202U	EXL1790202U	EXL17120202U	EXL1710202U	EXL17110202U
3.0 x 100	EXL17141003U	HILA171003U	HILB171003U	HILN171003U	EXL17131003U	EXL17101003U	EXL1791003U	EXL17121003U	EXL1711003U	EXL17111003U
3.0 x 75	EXL17147503U	HILA177503U	HILB177503U	HILN177503U	EXL17137503U	EXL17107503U	EXL1797503U	EXL17127503U	EXL1717503U	EXL17117503U
3.0 x 50	EXL17140503U	HILA170503U	HILB170503U	HILN170503U	EXL17130503U	EXL17100503U	EXL1790503U	EXL17120503U	EXL1710503U	EXL17110503U
3.0 x 30	EXL17140303U	HILA170303U	HILB170303U	HILN170303U	EXL17130303U	EXL17100303U	EXL1790303U	EXL17120303U	EXL1710303U	EXL17110303U
3.0 x 20	EXL17140203U	HILA170203U	HILB170203U	HILN170203U	EXL17130203U	EXL17100203U	EXL1790203U	EXL17120203U	EXL1710203U	EXL17110203U

ACE® Excel 2.0 µm UHPLC Columns

	CN	CN-ES	C18-PFP	AQ	Phenyl	C18-AR	C18-Amide	C4	C8	C18	SuperC18
2.1 x 150	EXL1041502U	EXL10131502U	EXL10101502U	EXL1061502U	EXL1051502U	EXL1091502U	EXL10121502U	EXL1031502U	EXL1021502U	EXL1011502U	EXL10111502U
2.1 x 125	EXL1041202U	EXL10131202U	EXL10101202U	EXL1061202U	EXL1051202U	EXL1091202U	EXL10121202U	EXL1031202U	EXL1021202U	EXL1011202U	EXL10111202U
2.1 x 100	EXL1041002U	EXL10131002U	EXL10101002U	EXL1061002U	EXL1051002U	EXL1091002U	EXL10121002U	EXL1031002U	EXL1021002U	EXL1011002U	EXL10111002U
2.1 x 75	EXL1047502U	EXL10137502U	EXL10107502U	EXL1067502U	EXL1057502U	EXL1097502U	EXL10127502U	EXL1037502U	EXL1027502U	EXL1017502U	EXL10117502U
2.1 x 50	EXL1040502U	EXL10130502U	EXL10100502U	EXL1060502U	EXL1050502U	EXL1090502U	EXL10120502U	EXL1030502U	EXL1020502U	EXL1010502U	EXL10110502U
2.1 x 30	EXL1040302U	EXL10130302U	EXL10100302U	EXL1060302U	EXL1050302U	EXL1090302U	EXL10120302U	EXL1030302U	EXL1020302U	EXL1010302U	EXL10110302U
2.1 x 20	EXL1040202U	EXL10130202U	EXL10100202U	EXL1060202U	EXL1050202U	EXL1090202U	EXL10120202U	EXL1030202U	EXL1020202U	EXL1010202U	EXL10110202U
3.0 x 150	EXL1041503U	EXL10131503U	EXL10101503U	EXL1061503U	EXL1051503U	EXL1091503U	EXL10121503U	EXL1031503U	EXL1021503U	EXL1011503U	EXL10111503U
3.0 x 125	EXL1041203U	EXL10131203U	EXL10101203U	EXL1061203U	EXL1051203U	EXL1091203U	EXL10121203U	EXL1031203U	EXL1021203U	EXL1011203U	EXL10111203U
3.0 x 100	EXL1041003U	EXL10131003U	EXL10101003U	EXL1061003U	EXL1051003U	EXL1091003U	EXL10121003U	EXL1031003U	EXL1021003U	EXL1011003U	EXL10111003U
3.0 x 75	EXL1047503U	EXL10137503U	EXL10107503U	EXL1067503U	EXL1057503U	EXL1097503U	EXL10127503U	EXL1037503U	EXL1027503U	EXL1017503U	EXL10117503U
3.0 x 50	EXL1040503U	EXL10130503U	EXL10100503U	EXL1060503U	EXL1050503U	EXL1090503U	EXL10120503U	EXL1030503U	EXL1020503U	EXL1010503U	EXL10110503U
3.0 x 30	EXL1040303U	EXL10130303U	EXL10100303U	EXL1060303U	EXL1050303U	EXL1090303U	EXL10120303U	EXL1030303U	EXL1020303U	EXL1010303U	EXL10110303U
3.0 x 20	EXL1040203U	EXL10130203U	EXL10100203U	EXL1060203U	EXL1050203U	EXL1090203U	EXL10120203U	EXL1030203U	EXL1020203U	EXL1010203U	EXL10110203U
4.6 x 150	EXL1041546U	EXL10131546U	EXL10101546U	EXL1061546U	EXL1051546U	EXL1091546U	EXL10121546U	EXL1031546U	EXL1021546U	EXL1011546U	EXL10111546U
4.6 x 125	EXL1041246U	EXL10131246U	EXL10101246U	EXL1061246U	EXL1051246U	EXL1091246U	EXL10121246U	EXL1031246U	EXL1021246U	EXL1011246U	EXL10111246U
4.6 x 100	EXL1041046U	EXL10131046U	EXL10101046U	EXL1061046U	EXL1051046U	EXL1091046U	EXL10121046U	EXL1031046U	EXL1021046U	EXL1011046U	EXL10111046U
4.6 x 75	EXL1047546U	EXL10137546U	EXL10107546U	EXL1067546U	EXL1057546U	EXL1097546U	EXL10127546U	EXL1037546U	EXL1027546U	EXL1017546U	EXL10117546U
4.6 x 50	EXL1040546U	EXL10130546U	EXL10100546U	EXL1060546U	EXL1050546U	EXL1090546U	EXL10120546U	EXL1030546U	EXL1020546U	EXL1010546U	EXL10110546U
4.6 x 30	EXL1040346U	EXL10130346U	EXL10100346U	EXL1060346U	EXL1050346U	EXL1090346U	EXL10120346U	EXL1030346U	EXL1020346U	EXL1010346U	EXL10110346U
4.6 x 20	EXL1040246U	EXL10130246U	EXL10100246U	EXL1060246U	EXL1050246U	EXL1090246U	EXL10120246U	EXL1030246U	EXL1020246U	EXL1010246U	EXL10110246U

macmod
SMARTER CHROMATOGRAPHY

The Essential Bonded Phases of UHPLC

Providing smarter chromatography solutions, state-of-the-art analytical software, and products for **all your separation needs**

GREATER RETENTION

ACE Excel **NH_2*** 1000 bar pH 2-7				ACE Excel **C4** 1000 bar pH 2-8	
HALO **HILIC*** 1000 bar pH 1-8				HALO **C8** 1000 bar pH 2-9	
HALO **Penta-HILIC*** 1000 bar pH 2-9			ACE Excel **Phenyl** 1000 bar pH 2-8	ACE Excel **C8** 1000 bar pH 2-8	
ACE **HILIC-A*** 1000 bar pH 2-7	ACE Excel **CN** 1000 bar pH 2-8		HALO **Biphenyl** 1000 bar pH 2-9	HALO **C18** 1000 bar pH 2-9	
ACE **HILIC-B*** 1000 bar pH 2-7	HALO **ES-CN** 1000 bar pH 1-8	HALO **PFP** 1000 bar pH 2-9	ACE Excel **AQ** 1000 bar pH 2-8	HALO **Phenyl-Hexyl** 1000 bar pH 2-9	HALO **RP-Amide** 1000 bar pH 2-9	ACE Excel **C18** 1000 bar pH 2-8
ACE **HILIC-N*** 1000 bar pH 2-7	ACE Excel **CN-ES** 1000 bar pH 2-8	ACE Excel **C18-PFP** 1000 bar pH 2-8	HALO **AQ-C18** 1000 bar pH 2-9	ACE Excel **C18-AR** 1000 bar pH 2-8	ACE Excel **C18-Amide** 1000 bar pH 2-8	ACE Excel **SuperC18**[1] 1000 bar pH 1.5-11.5

Temperature Maxima (low pH, 60 °C; mid pH, 40 °C)

MORE POLAR

*No difference in retention 💧=100% Aqueous Compatible [1]Note: ACE SuperC18 can be used from pH 7.5 to pH 11.5 at 40 °C or lower with volatile mobile phase additives

	Bonded Phase	Brand	Phase	Particle Size (µm)	100% Aqueous Compatible	Endcapped	Carbon Load (%)	Surface Area (m^2/g)
AMINO	**NH_2**	ACE	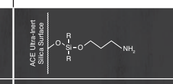	1.7	No	No	4.0	300
HILIC	**HILIC**	HALO		2.0	No	NA	N/A	120
HILIC	**Penta-HILIC**	HALO	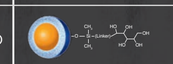	2.0	No	No	2.8	120
HILIC	**HILIC-A**	ACE	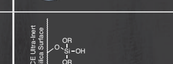	1.7	No	No	N/A	300
HILIC	**HILIC-B**	ACE	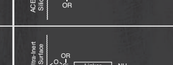	1.7	No	No	4.0	300
HILIC	**HILIC-N**	ACE	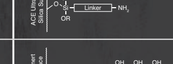	1.7	No	No	7.0	300
CN	**CN**	ACE	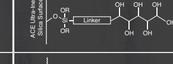	2.0	No	Yes	5.5	300
CN	**ES-CN**	HALO	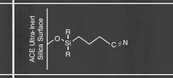	2.0	No	Yes	3.4	120
CN	**CN-ES**	ACE	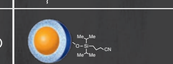	1.7, 2.0	Yes	Yes	12.6	300
PFP	**PFP**	HALO	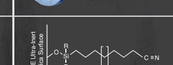	2.0	No	Yes	5.3	120
PFP	**C18-PFP**	ACE		1.7, 2.0	Yes	Yes	14.3	300
AQ	**AQ**	ACE	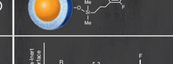	2.0	Yes	Yes	14.0	300
AQ	**AQ-C18**	HALO	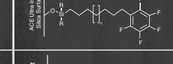	2.0	Yes	Yes	6.5	120
PHENYL	**Phenyl**	ACE	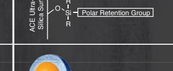	2.0	No	Yes	9.5	300
PHENYL	**Biphenyl**	HALO	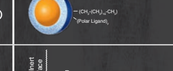	2.0	Yes	Yes	7.0	135
PHENYL	**Phenyl-Hexyl**	HALO	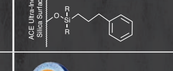	2.0	Yes	Yes	6.3	120
PHENYL	**C18-AR**	ACE	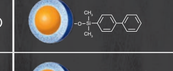	1.7, 2.0	Yes	Yes	15.5	300
+POLAR EMBEDDED	**RP-Amide**	HALO	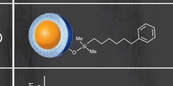	2.0	Yes	Yes	7.3	120
+POLAR EMBEDDED	**C18-Amide**	ACE	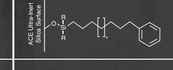	1.7, 2.0	Yes	Yes	17.0	300
ALKYL	**C4**	ACE	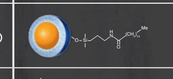	2.0	No	Yes	5.5	300
ALKYL	**C8**	HALO	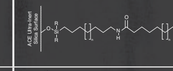	2.0	No	Yes	4.8	120
ALKYL	**C8**	ACE	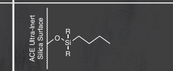	2.0	No	Yes	9.0	300
ALKYL	**C18**	HALO	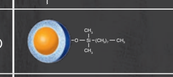	2.0	No	Yes	7.2	120
ALKYL	**C18**	ACE	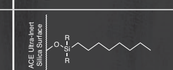	1.7, 2.0	No	Yes	15.5	300
ALKYL	**SuperC18**	ACE	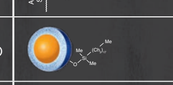	1.7, 2.0	No	Encapsulated	14.8	400